A. C. Partridge

FLOTATION AND ADSORPTION CHARACTERISTICS OF THE

HEMATITE - DODECYLAMINE - STARCH SYSTEM

Simultaneous adsorption of ^{3}H-dodecylamine and ^{14}C-starch onto hematite was investigated by two-channel liquid scintillation counting. Floatability of the resultant hematite was determined using a new type of laboratory test cell.

Amine adsorption followed a Freundlich type isotherm, $\Gamma = KC^n$, n varying with pH and starch concentration. Adsorption increased with pH, especially at pH 8 - 10, and was enhanced by starch at low pH. Starch decreased amine adsorption at high pH.

Starch adsorption increased with concentration and rose with amine concentration to 10^{-4} molar. Higher amine concentrations lowered starch adsorption.

Floatability increased with amine concentration up to 10^{-3} molar and fell at 10^{-2} molar amine. Maximum flotation was achieved in slightly alkaline solution. Starch was most effective as a depressant at high and low pH but the maximum floatability value was little affected. Starch produced a shift of the maximum floatability peak to higher pH levels.

An explanation, based on amine-starch complexing, is proposed.

HEMATITE-DODECYLAMINE-STARCH:

FLOTATION AND ADSORPTION

FLOTATION AND ADSORPTION CHARACTERISTICS

OF THE

HEMATITE – DODECYLAMINE – STARCH SYSTEM

Anthony C. Partridge

A thesis submitted to the Faculty of

Graduate Studies and Research in partial

fulfillment of the requirements for the

Degree of Master of Science

Department of Metallurgical Engineering
McGill University
Montreal, Canada   July 1970

A. C. Partridge

FLOTATION AND ADSORPTION CHARACTERISTICS OF THE

HEMATITE - DODECYLAMINE - STARCH SYSTEM

Simultaneous adsorption of ^{3}H-dodecylamine and ^{14}C-starch onto hematite was investigated by two-channel liquid scintillation counting. Floatability of the resultant hematite was determined using a new type of laboratory test cell.

Amine adsorption followed a Freundlich type isotherm, $\Gamma = KC^n$, n varying with pH and starch concentration. Adsorption increased with pH, especially at pH 8 - 10, and was enhanced by starch at low pH. Starch decreased amine adsorption at high pH.

Starch adsorption increased with concentration and rose with amine concentration to 10^{-4} molar. Higher amine concentrations lowered starch adsorption.

Floatability increased with amine concentration up to 10^{-3} molar and fell at 10^{-2} molar amine. Maximum flotation was achieved in slightly alkaline solution. Starch was most effective as a depressant at high and low pH but the maximum floatability value was little affected. Starch produced a shift of the maximum floatability peak to higher pH levels.

An explanation, based on amine-starch complexing, is proposed.

ACKNOWLEDGEMENTS

The author wishes to express his appreciation for the
direction and guidance given by Dr. G. W. Smith during the course
of this study.

He is also indebted to the J. W. McConnell Foundation for
personal support in the form of a fellowship and to the National
Research Council and the Mines Branch, Department of Energy, Mines
and Resources, for grants covering the practical costs of the
research.

The Iron Ore Company of Canada is to be thanked for donating
the iron ore from which the hematite was obtained.

TABLE OF CONTENTS

LIST OF FIGURES

I. INTRODUCTION

Fifty years ago an iron ore could have been defined as any iron-bearing mineral deposit suitable for direct charge to a blast furnace. Depletion of high grade deposits and, more especially, the increasing quantity and quality demands of consumers have radically changed that situation. Today, beneficiation is employed to improve the grade and physical characteristics of more than 90% of North American production[1].

The special importance of this trend to the Canadian economy is evident from a consideration of the rapid growth of the industry in this country from 14.5 million long tons in 1955 to 44 million in 1968[2, 3]. (Strikes reduced the 1969 figure to 37 million long tons[4]). The premium on beneficiation is unusually high in this country due to the long distances much of the ore must be transported, approximately 80% of the production being exported[5].

Although the list of iron-bearing minerals is a long one, only four are of major importance as sources of the metal[6], namely:

	Magnetite	Fe_3O_4	($\doteq$ 72% Fe)
	Hematite	Fe_2O_3	($\sim$ 70% Fe)
	Limonite	$Fe_2O_3 \cdot xH_2O$	(x $\sim$ 1.5, $\sim$ 60% Fe)
and	Siderite	$FeCO_3$	($\sim$ 48% Fe)

Of these, hematite is by far the most significant.

Common methods of up-grading hematitic ores include gravity separation (Humphrey's spirals and dense media), high intensity magnetic separation and electrostatic separation[7, 8]. Reduction roasting to magnetite or to iron followed by magnetic separation has proved successful in some cases[9]. The experimental leaching of siliceous gangue by concentrated sodium hydroxide solution has also been reported[10].

Conventional processes all give concentrates of acceptable grade (> 60% Fe) but recovery is generally low and falls off rapidly with decreasing particle size. The results achieved at the Wabush mill, Labrador, are typical. Spiralling followed by electrostatic cleaning yields a product containing 66.3% Fe but recovery is less than 40%[11]. As high grade hematite deposits are steadily depleted and fine-grained taconites become of greater significance, the loss of fines will become unacceptable. Furthermore, the increasing practice of ore pelletization[12] and the advent of direct reduction techniques in powder-metallurgy[13] both require a feed consisting partly or wholly of fine (-325 mesh) material. Consequently, attention is being focussed on concentration by flotation - a process used over many years for finely disseminated minerals of higher intrinsic value.

II. THEORETICAL REVIEW

FLOTATION

Froth flotation is a process in which finely divided solids are separated one from another according to differences in surface affinities for a gas phase and a liquid phase in which the particles are suspended. Separation is effected by forming a thorough mixture of the phases such that solid species with sufficiently hydrophobic surface properties can become attached to rising gas bubbles. These particles will concentrate in the surface layers and may be removed in a froth.

The surface properties of a mineral depend, ultimately, upon the nature of the bonds between the atoms comprising the substrate. Five types of bonds are generally recognized: <u>Covalent</u>, in which shared electrons are symmetrically disposed between bound nuclei; <u>Ionic</u>, in which electron transfer gives rise to electrostatic binding forces; <u>Metallic</u>, ions packing according to geometrical considerations in a mobile 'sea' of electrons; <u>Molecular</u> (Van der Waals' or Physical), binding being due to mutually induced dipoles; and <u>Polar</u>, an intermediate stage between covalent and ionic binding in which shared electrons are displaced towards one of the bound nuclei resulting in electrostatic attraction. Most minerals are polar in nature and, when freshly cleaved, tend to attract polar liquids such as water. That is, they are hydrophyllic. Consequently, in order to achieve flotation a hydrophobic

II. THEORETICAL REVIEW

FLOTATION

Froth flotation is a process in which finely divided solids are separated one from another according to differences in surface affinities for a gas phase and a liquid phase in which the particles are suspended. Separation is effected by forming a thorough mixture of the phases such that solid species with sufficiently hydrophobic surface properties can become attached to rising gas bubbles. These particles will concentrate in the surface layers and may be removed in a froth.

The surface properties of a mineral depend, ultimately, upon the nature of the bonds between the atoms comprising the substrate. Five types of bonds are generally recognized: Covalent, in which shared electrons are symmetrically disposed between bound nuclei; Ionic, in which electron transfer gives rise to electrostatic binding forces; Metallic, ions packing according to geometrical considerations in a mobile 'sea' of electrons; Molecular (Van der Waals' or Physical), binding being due to mutually induced dipoles; and Polar, an intermediate stage between covalent and ionic binding in which shared electrons are displaced towards one of the bound nuclei resulting in electrostatic attraction. Most minerals are polar in nature and, when freshly cleaved, tend to attract polar liquids such as water. That is, they are hydrophyllic. Consequently, in order to achieve flotation a hydrophobic

nature must be induced by the addition of reagents which will modify the mineral surface by adsorption.

Minerals may be divided into two broad classes, 'metallics' including sulphides and 'non-metallics' such as oxides. The difference lies in the ionic character of the polar bond - that is, in the extent of electron displacement and consequent electrostatic field strength. This is relatively low for the metallics but high for the non-metallics which, consequently, strongly attract a water layer. Derjaguin et al.[14] have investigated this layer, which is from 0.3 to 40 nm thick, and have shown it to constitute a distinct phase having different properties and, contrary to common opinion, being separated by a distinct boundary from the bulk water phase[15]. This hydration sheath has been shown to persist even after apparent displacement of water by the adhesion of a gas bubble and clearly hinders chemical reactions at the surface. Reactivities of metallic surfaces, which are less strongly hydrated, are relatively unaffected.

THE ELECTRICAL DOUBLE LAYER

In order to explain adsorption onto surfaces 'protected' by a hydration sheath it is necessary to introduce the concept of the Electrical Double Layer.

Depending upon the ions present in solution and upon their respective concentrations, ions at the surface of a solid immersed in water will experience two opposing forces. Bonding within the crystal

tends to hold such ions in their places at the edge of the lattice and polar attraction from the liquid will tend to draw them into solution. Transfer of ionic species will occur between the phases to reduce the imbalance of forces but the consequent charge separation gives rise to an electrostatic restoring force so that an equilibrium distribution is set up. The system will be at its lowest energy level when the separation of charges is a minimum so it is to be expected that the ions in solution will tend to accumulate immediately adjacent to the solid surface. Such a configuration was envisaged by Helmholtz who postulated an electrical double layer configuration analogous to a parallel plate condenser[16]. His model had the electrostatic charge of the solid located in a tightly bound ionic monolayer in the surface and a closely held layer of mobile ions of opposite charge in solution. Gouy[17] and Chapman[18] proposed modifications which took into account thermal agitation of the mobile ions, giving rise to an exponential decrease in their concentration with distance from the surface. The theoretical capacity values for these systems, however, were found to be considerably greater than those determined experimentally. In 1924, Stern[19] proposed an important correction which, with a minor modification due to Grahame[20], gives the modern view of the double layer shown in Figure 1.

The inner layer is pictured as being an extension of the crystal lattice. That is, it consists of ions (termed 'potential determining ions', p.d.i.) bound in an ordered array as part of the solid structure. Ions forming this layer may have originated in either phase but, at

FIGURE 1

NATURE AND CHARGE DISTRIBUTION

OF THE ELECTRICAL DOUBLE LAYER

			IONS IN	$+$
			LATTICE	$-$
			UN-HYDRATED	$\overset{..}{+}$
			GEGEN ION	
			HYDRATED	$\oplus$
			GEGEN ION	
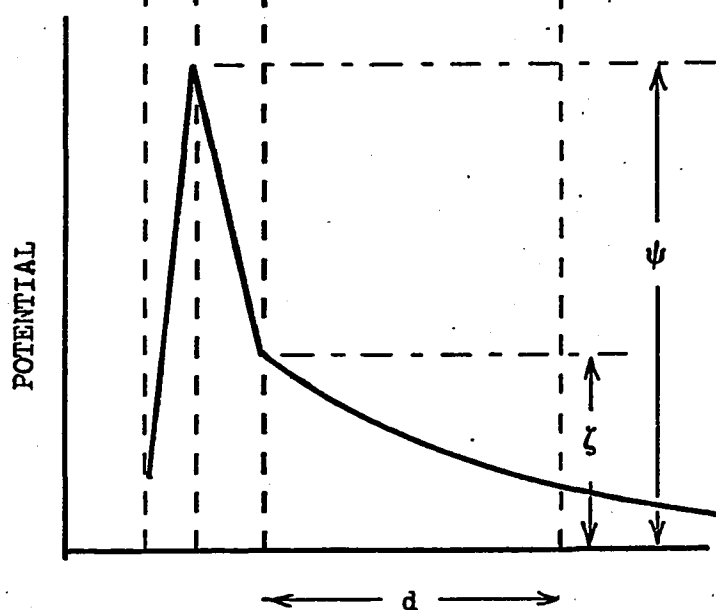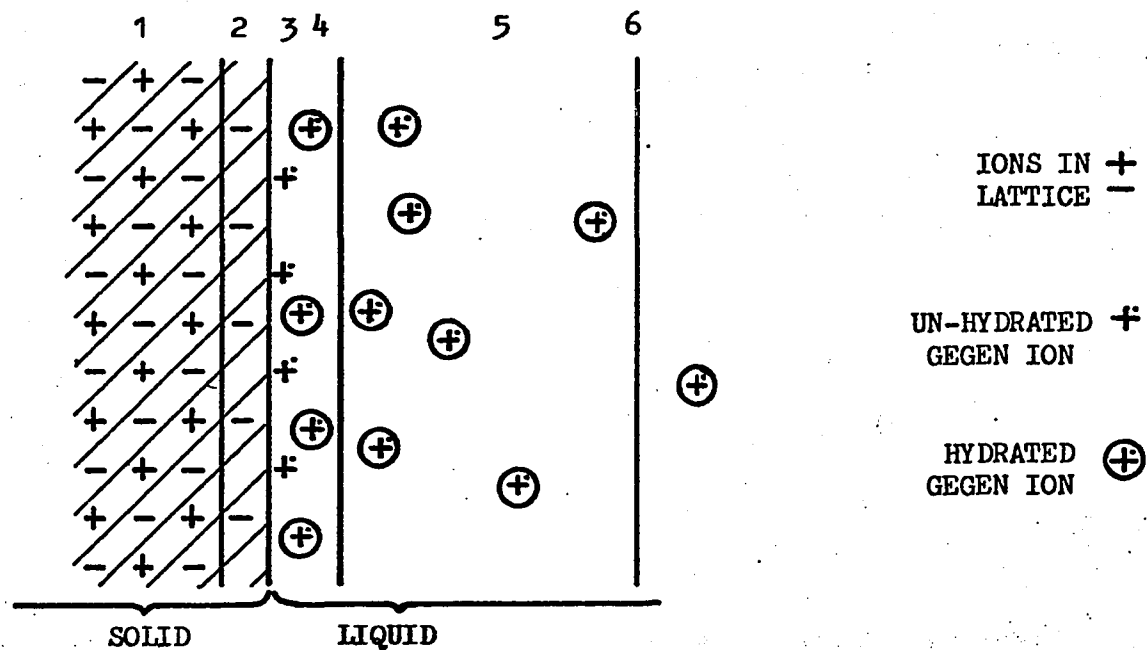
(1) UNALTERED CRYSTAL LATTICE

(2) ALTERED LATTICE - POTENTIAL DETERMINING IONS

(3) GRAHAME'S 'INNER HELMHOLTZ LAYER' ⎫
                                        ⎬ STERN LAYER
(4) GRAHAME'S 'OUTER HELMHOLTZ LAYER' ⎭

(5) DIFFUSE (GOUY) LAYER

(6) CENTRE OF CHARGE OF GOUY LAYER

equilibrium, are of a type common to both. The outer layer consists of two regions in which ions of opposite charge to the surface ('gegen' ions) are concentrated. Immediately adjacent to the solid surface the gegen ions are held firmly in a layer considered to be no thicker than one hydrated ion. This region, in which the ions occupy regular sites with respect to the solid lattice, is termed the Stern layer. Grahame has suggested that some ions in the region may become de-hydrated and specifically adsorbed. He named the de-hydrated and hydrated ionic regions the inner- and outer-Helmholtz planes respectively. Beyond the outer Helmholtz plane the gegen ions are mobile, their concentration decreasing exponentially until it equals that in the bulk solution. This region is known as the 'diffuse' or 'Gouy' layer. The distribution is similar to the ionic atmosphere about a reference ion in solution for which the average radius is the reciprocal of the Debye-Hückel function, κ :-

$$ d = \frac{1}{\kappa} = \sqrt{\frac{DkT}{4\pi e^2 \sum_i n_{i_o} z_i^2}} $$

where d is the effective radius, κ is the Debye-Hückel function, e is the charge on an electron, n_{i_o} is the concentration of the ith component in the bulk solution, z_i is the valence with sign of the ith component, D is the dielectric constant on the liquid, k is Boltzmann's constant and T is the absolute temperature[21].

Slight allowance has to be made for the relatively large size

of a mineral particle, the effective planar surface giving rise to a more extensive diffuse layer than that about a point charge. The important conclusion that the thickness is inversely proportional to the square root of the ionic concentration of the bulk solution is unaltered. Calculation shows[22] that for a typical flotation system of millimolar concentration this thickness is approximately 10 nm.

Two electrical potentials are used to describe the nature of the charge field. The potential at the solid surface, due only to potential determining ions, is termed the surface potential, ψ_o. The thermodynamic (or zeta) potential, ζ, is the experimentally determined potential at the shear plane between gegen ions bound to the solid and those free to move with the solvent. It is generally assumed that when the solution moves relative to the solid all the ions in the Gouy layer move with it and all those in the Stern layer remain with the solid. That is, the ζ potential is the potential at the Stern layer - Gouy layer interface, as indicated in the diagram. However, some evidence has been produced[23-25] which indicates that factors such as surface roughness exert an influence on the location of the shear plane.

For simple mineral oxides the potential determining ions are usually the hydrogen and hydroxyl ions[26]. Changes of pH consequently lead to changes of ψ_o and, therefore, ζ. Changes in the concentration of gegen ions, on the other hand, can only alter ζ which can become of opposite sign to ψ_o. 'Indifferent ions' (which do not enter into the Stern layer) also affect ζ by causing 'condensation' of the Gouy

layer into the Stern layer in accord with the Debye-Hückel equation.
A thorough quantitative treatment is given by Smith[27]. Parks and
de Bruyn[28] summarized the probable mechanism which gives rise to the
surface potential of hematite.

Broken bonds at the limits (grain surfaces) of the theoretically
infinite crystal lattice are satisfied by OH^- ions and protons from
solution, completing the coordination shells of surface cations and
anions. The net result is that the surface is covered by a hydroxyl
layer with the cations buried below the surface. This hydroxyl layer
has been detected by Glemser and Rieck[29] in infra-red spectra. The
surface potential is thought to arise from the amphoteric dissociation
of this surface 'hydroxide' layer:-

$$MOH \text{ (s.)} \rightleftharpoons MO^- \text{ (s.)} + H^+ \text{ (aq.)} \qquad \ldots 1$$

or
$$MOH \text{ (s.)} + H_2O \rightleftharpoons MOH_2^+ \text{ (s.)} + OH^- \text{ (aq.)} \qquad \ldots 2$$
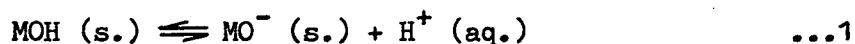
Thus in alkaline solutions the surface becomes negatively
charged due to removal of a proton while in acidic conditions hydroxyl
ions are removed giving the surface a net positive charge. The
concentration of potential determining ions (in this case, the pH)
at which their surface charge densities are equal is termed the iso-
electric point, i.e.p. At the i.e.p., surface potential and zeta
potential are zero. Zeta potential may also be reduced to zero by
concentration of gegen ions inside the shear plane. This condition
is termed the zero point of charge, z.p.c.

ADSORPTION

Adsorption is the process in which atoms, molecules or ions of an 'adsorbate' become concentrated at the surface of another phase, an 'adsorbent'. The phenomenon is conventionally considered as being either chemical or physical although the difference between them is not clear-cut. Generally, chemisorption is regarded as being characterized by heats of adsorption in excess of 15 Kcal/mole and physical adsorption by values below 3 Kcal/mole[30]. The limits, however, are somewhat arbitrary. Mokrousov, for instance, suggests the lower limit for chemisorption to be an order of magnitude higher[31].

Joy and Robinson[32] subdivide the groups as follows:-

(a) Chemisorption: involving the complete or partial transfer of an electron or orbital overlap; adsorbate is a reactive ion or molecule forming:

(i) a true chemical compound capable of existing in a bulk state;

(ii) a surface compound for which analogous species are known to exist as a crystal, or in solution, with the same molecular configuration;

(iii) a surface compound for which no analogous compounds have been isolated.

(b) Physical adsorption: no true bond formation; adsorbate may be an ion or an un-ionized molecule. Cases include:

(i) un-ionized molecule held in vicinity of surface by
dispersion forces;

(ii) ion held in outer structure of double layer by
electrostatic forces;

(iii) ion held close to the surface by a combination of
electrostatic and dispersion forces;

(iv) molecule or ion retained by relatively weak bonding,
e.g. hydrogen bonding. (This type of adsorption could
equally well be classified as a weak chemisorption.)

Chemisorption is characterized by a temperature dependent reaction
rate and high specificity. The adsorbate enters the crystal lattice
through chemical reaction at the inner double layer. The degree of
chemisorption depends on the size and charge of the adsorbate ion, the
same factors that control isomorphous substitution in minerals[33].
That is, ions of the correct dimensions (approximately) and of higher
valency are favoured. In addition, of course, the newly formed compound
must not be soluble.

Physical adsorption, on the other hand, takes place in the outer
double layer. Any ions may be adsorbed, irrespective of their nature,
dimensions or size of charge, since only the overall electrical balance
is important. Consequently, physical adsorption is not specific with
respect to the solid, thus accounting for the difficulty in the flotation
of mineral oxides. Important features of physical adsorption are its
lack of selectivity and its ready reversibility.

ADSORPTION ISOTHERMS

The relationship between adsorption density, Γ (expressed in terms of quantity of adsorbate/quantity of adsorbent), and the bulk solution concentration at constant temperature is termed an adsorption isotherm. Most early work was carried out on gas-solid systems and the important equations were originally derived to describe such systems. However they can be used, with slight modifications, to describe adsorption from dilute solutions.

The first significant treatment was published by Langmuir in 1918[34]. He considered adsorption to be a dynamic phenomenon which could occur in no more than a monolayer. He also assumed that all surface sites were equally probable and that no interaction occured between adsorbed molecules. Balancing adsorption and desorption rates led to the expression:

$$V = \frac{a\,b\,P}{1 + b\,P} \qquad \ldots 3$$

where V is the volume of adsorbed gas and P is the gas pressure. The constants a and b are related to the adsorbate quantity required for a complete monolayer and to the heat of adsorption, respectively. For adsorption from dilute solutions, the equation may be written:

$$\Gamma = \frac{a\,b\,C}{1 + b\,C} \qquad \ldots 4$$

or

$$\frac{C}{\Gamma} = \frac{1}{a\,b} + \frac{C}{a} \qquad \ldots 5$$

where C is the concentration of adsorbate in solution and Γ denotes the amount of adsorbate per unit of adsorbent (e.g. μmoles/g, etc.). Equation 5 shows that data conforming to the Langmuir isotherm give a straight line, with intercept $1/ab$ and gradient $1/a$, when C/Γ is plotted against C.

Due to the restrictive assumptions made in the derivation of the Langmuir isotherm it is only of limited application. Thus its use to describe physical adsorption is frequently precluded by multilayer formation, adsorbate mobility on the surface and significant forces between adsorbate molecules. Chemisorption systems, on the other hand, often give good fit[35, 36].

Multilayer formation was first attributed to attraction due to induced polarization effects but Brunauer, Emmett and Teller[37] showed that these forces, which decrease exponentially with distance from the adsorbent, are negligible, even for the second layer. They concluded that multilayer build-up is due to Van der Waals' forces. It then follows that the energy of adsorption in each layer subsequent to the first will be identical, and equal to the heat of condensation of the adsorbate. Balancing adsorption and desorption rates as did Langmuir, but considering many layers, they obtained an expression which may be written:

$$\frac{C}{\Gamma (C_o - C)} = \frac{1}{a\,b} + \frac{b - 1}{a\,b} \cdot \frac{C}{C_o} \qquad \ldots 6$$

Here, C_o is the saturation concentration of the adsorbate. The other symbols are as defined previously. For systems conforming to the B.E.T. conditions, a plot of $C/\Gamma.(C_o - C))$ against C/C_o yields a straight line of gradient $(b - 1)/ab$ and intercept $1/ab$.

An empirical isotherm equation of the form

$$\Gamma = a\, C^n \qquad\qquad ...7$$

was used extensively by Freundlich[38] and is named after him. Data conforming to this equation yield a straight line in a plot of log Γ versus log C. Although empirical, the Freundlich equation can be obtained as the envelope of superimposed Langmuir equations with different values for the constant b[39]. This can be interpreted as implying monolayer coverage on a surface with sites of varying activity.

FLOTATION REAGENTS

Reagents added to the flotation medium to modify the surface characteristics of the minerals are commonly considered under three headings:

(a) Collectors are organic compounds which, by concentration at a mineral surface, lower the stability of the hydration layer. Disruption of the hydration sheath and attachment to air bubbles are thus readily achieved. Non-polar oils were first used but were rapidly replaced with the far more specific heteropolar reagents and are today used only in the flotation of non-polar, non-sulphide minerals. The heteropolar

collectors are characterized by a polar group which can ionize in solution and a non-polar hydrocarbon group which gives rise to the required hydrophobicity. Their mode of action is envisaged as attachment of the ionic 'head' to an oppositely charged mineral surface leaving exposed the hydrophobic organic 'tail'. They can be made highly specific by appropriate selection of the polar group which may become bound to the mineral by chemical as well as electrostatic forces.

(b) <u>Frothers</u> concentrate chiefly at the liquid-gas interface and, by lowering the surface tension, provide a stable froth in which floated minerals are held and removed.

(c) <u>Modifiers</u> include Activators, which make appropriate mineral surfaces amenable to collector action; Depressants, with the opposite purpose from activators; and pH modifiers, the action of which may alter the characteristics of minerals and/or reagents.

AMINE-STARCH-HEMATITE SYSTEM

Major-Marothy has made an extensive study of the flotation systems available for hematite concentration[40]. He concluded that cationic flotation of gangue minerals was economically the most promising scheme. Optimum results were obtained using a collector consisting, essentially, of dehydroabietylamine acetate at pH 6 - 9. Alkyl amines were shown to give similar results but at pH 10 - 11. Dodecylamine has been used in this study, as it was more readily available. Several workers have made comparative studies of hematite depressants[41-46]. Colloidal

substances, notably starch, have proved most effective. Causticized starch was adopted for this study.

(a) <u>Dodecylamine</u>

Amines are organic compounds which may be regarded as derivatives of ammonia (NH_3), in which hydrogen atoms are replaced by aliphatic, aromatic or heterocyclic radicals. Derivatives with one, two or three replaced hydrogens are termed primary, secondary or tertiary amines respectively. Dodecylamine, $CH_3(CH_2)_{11}NH_2$, is a primary amine, one hydrogen being replaced with a straight hydrocarbon chain of twelve carbon atoms. Long chain amines are only slightly soluble in water and are employed in flotation in the form of a salt, usually of hydrochloric or acetic acid, e.g.:-

$$C_{12}H_{25}NH_2 + CH_3COOH \longrightarrow C_{12}H_{25}NH_2CH_3COOH \qquad \ldots 8$$
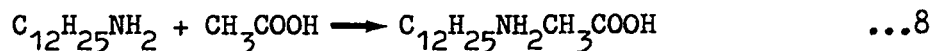
These salts readily ionize in water:-

$$C_{12}H_{25}NH_2CH_3COOH \rightleftharpoons C_{12}H_{25}NH_3^+ + CH_3COO^- \qquad \ldots 9$$
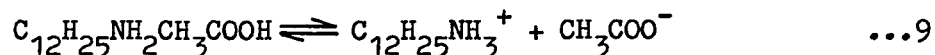
and the polar group greatly increases the solubility of the reagent.

Kellogg and Vásquez-Rosas[47] first calculated the ratio of the species RNH_3^+, RNH_2 (soln.) and RNH_2 (ppt.) in test solutions, 'R' representing the dodecyl- radical. Considering the equilibria:

$$RNH_2 + H_2O \overset{K_1}{\rightleftharpoons} RNH_3^+ + OH^- \qquad \ldots 10$$

and $\qquad\qquad RNH_3^+ \overset{K_2}{\rightleftharpoons} RNH_2 + H^+ \qquad\qquad \ldots 11$
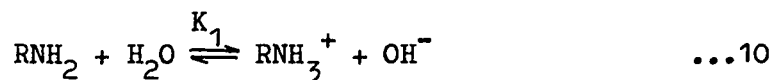
we have

$$K_1 = \frac{[OH^-][RNH_3^+]}{[RNH_2][H_2O]}$$

$$= 4.3 \times 10^{-4} \ ^{(48)} \qquad \qquad \ldots 12$$

and

$$K_2 = \frac{[RNH_2][H^+]}{[RNH_3^+]} \qquad \qquad \ldots 13$$

But

$$K_{H_2O} = \frac{[OH^-][H^+]}{[H_2O]}$$

$$= 1.02 \times 10^{-14} \text{ at } 25^\circ C \ ^{(49)} \qquad \qquad \ldots 14$$

therefore

$$\frac{K_{H_2O}}{K_1} = \frac{[OH^-][H^+]}{[H_2O]} \cdot \frac{[RNH_2][H_2O]}{[OH^-][RNH_3^+]}$$

$$= \frac{[H^+][RNH_2]}{[RNH_3^+]}$$

$$= K_2 \qquad \qquad \ldots 15$$

Hence

$$K_2 = 2.4 \times 10^{-11} \qquad \qquad \ldots 16$$

Putting X = fraction of amine as RNH_2 and C = stoichiometric concentration of the amine acetate, RNH_3Ac we have, from equation 11:

$$K_2 = \frac{CX[H^+]}{C(1-X)} \qquad \qquad \ldots 17$$

Hence

$$X = (2.4 \times 10^{-11}) / (2.4 \times 10^{-11} + [H^+]) \qquad \ldots 18$$

But RNH_2 is relatively insoluble, the most recent data[50] being

$$[RNH_2]_{soln.}^{max.} = 2 \times 10^{-5} \text{ mole/l} \qquad \ldots 19$$

If this value is exceeded the concentration of RNH_3^+ is given by

$$[RNH_3^+] = \frac{[RNH_2][H^+]}{K_2}$$

$$= \frac{2 \times 10^{-5}[H^+]}{2.4 \times 10^{-11}} \qquad \ldots 20$$

and precipitated amine is calculated from

$$RNH_{2(ppt.)} = \text{Stoichiometric concentration}$$

$$- ([RNH_3^+]_{soln.} + [RNH_2]_{soln.}) \qquad \ldots 21$$

Values of RNH_3^+, RNH_2 (soln.) and RNH_2 (ppt.) for the pH and concentration ranges used in this study are given in Table 1 and shown in Figure 2 (p. 20).

(b) <u>Starch</u>

Starch is one of a family of natural polymeric carbohydrates known as the polysaccharides. The members of this group are made up from repeated glucose units:-

$$[\quad\text{CH}_2\text{OH structure}\quad]_n$$
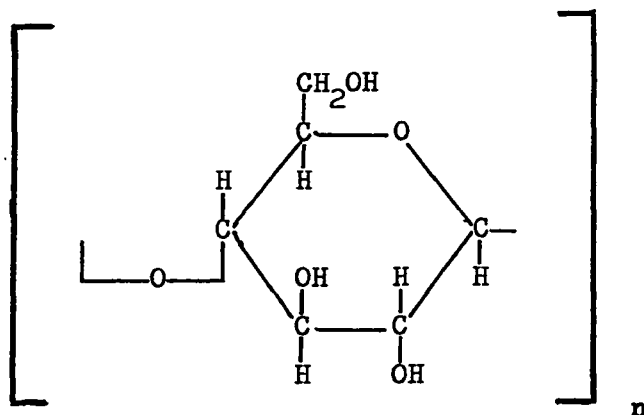
Two starch fractions, amylose and amylopectin, are recognized. Amylopectin is relatively insoluble in water and gives a pale reddish colour with iodine whereas amylose is water soluble and gives a deep blue colour. Physical measurements have shown that the molecular weights differ considerably, amylose being in the range 10^5 to 10^6 and amylopectin as high as 10^8.[51] Chemical analyses show a structural difference[52], glucose units being joined chiefly by 1, 4 linkages in amylose whereas 1, 6 linkages are common in amylopectin. Amylopectin, thus has a highly branched structure in contrast with the linear amylose configuration. The arrangement of the branch chains in amylopectin is still a matter of conjecture[53]. The unbranched amylose chains, on the other hand, give a good X-ray diffraction pattern which shows the chain to be helical[54]. Each turn contains 6 - 8 glucose units, hydrogen bonding occuring between adjacent turns. The helix has been shown capable of expansion to permit the inclusion of molecules of other species in a form of complex[55].

(c) Hematite

Hematite, α-Fe_2O_3, has a corundum-type structure, six oxygen

FIGURE 2

CONCENTRATIONS OF RNH_2 (DISSOLVED), RNH_3^+ (DISSOLVED)

AND RNH_2 (PRECIPITATED) FOR DODECYLAMINE SOLUTIONS

AS A FUNCTION OF pH AND TOTAL CONCENTRATION
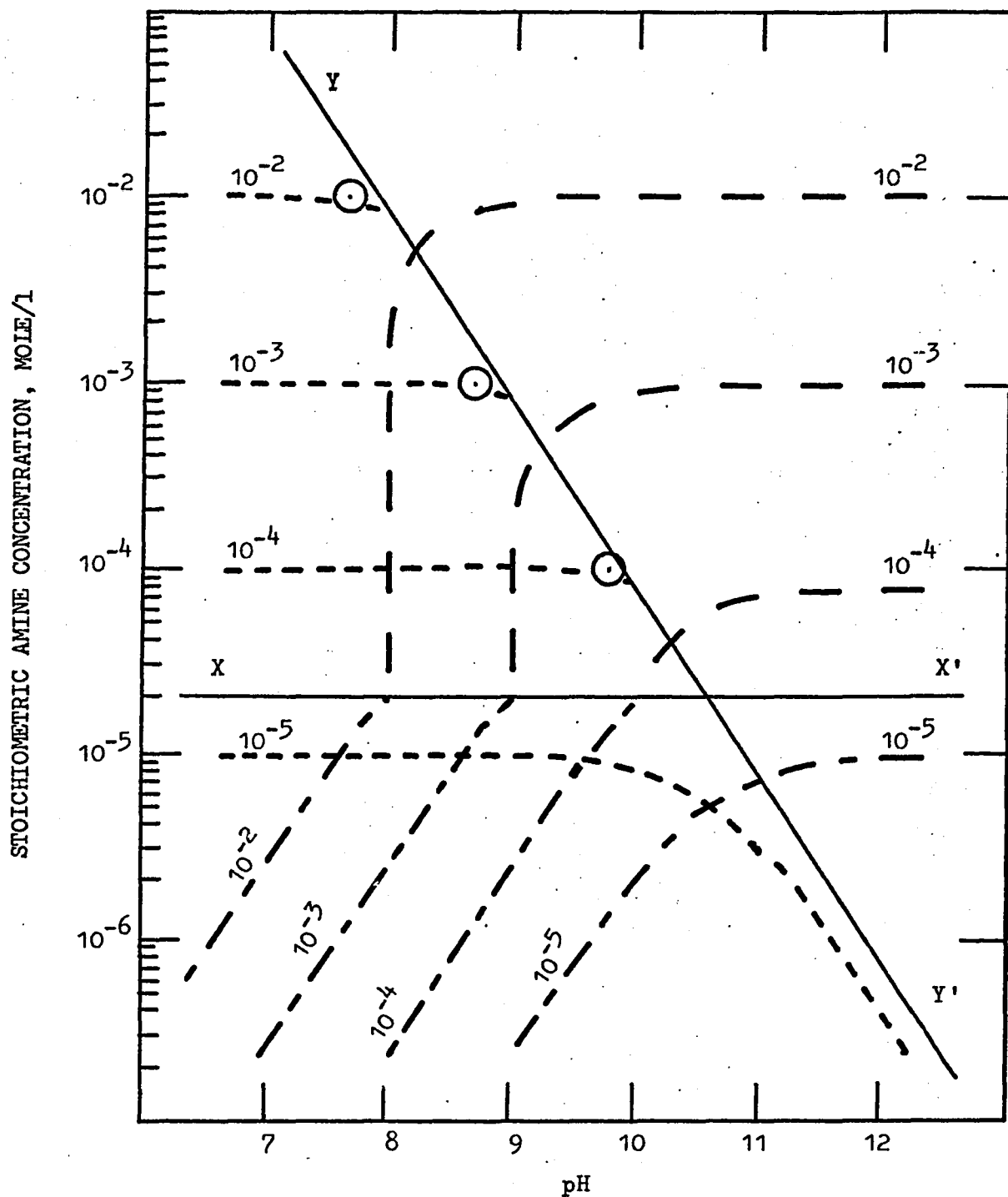
FIGURES ON CURVES INDICATE MOLARITY OF PARENT SOLUTION

X - X' MAXIMUM RNH$_2$ soln.   Y - Y' SOLUBILITY LIMIT

RNH$_2$ ppt.   RNH$_3^+$ RNH$_2$ soln.   EXPERIMENTAL

atoms forming an octahedral group around each Fe atom and each O atom being coordinated with four Fe atoms[56].

Few of the mineral's properties are of significance in this study and only one, the zero point of charge, will be considered here. The nature of the surface charge has been shown earlier to be dependent on the equilibrium position of the relationship:

$$Fe(OH)_2^+ \text{ (s.)} \rightleftharpoons FeO_2^- \text{ (s.)} + 2H^+ \qquad \text{...21}$$
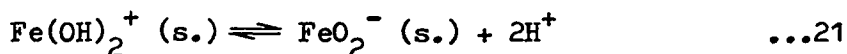
Consequently, it is to be expected that the z.p.c. will coincide with the pH at which the concentrations of the two species $Fe(OH)_2^+$ and FeO_2^- are equal. Parks and de Bruyn have calculated this point as being pH 8.5[57, 58]. This value agrees well with experimental values, although some results have been reported as low as pH 5.4 – probably due to siliceous impurities[59, 60]. Hematite thus exhibits a negative surface potential at pH $\gtrsim$ 8 and a positive charge at lower pH.

III. STATEMENT OF INTENT

Several workers have considered various aspects of hematite flotation systems involving amine collectors and colloidal depressants[40-44, 61] but each study has usually been restricted to a limited range of conditions. Correlation between these diverse results is difficult due to the variety of hematite sources[43], techniques, specific reagents and preparation methods. It was the intention of this research to provide a background for these studies by determining the characteristics of a particular system over a wide range of conditions.

The method of attack was to determine adsorption and flotation data for the hematite-dodecylamine-starch system over the range of conditions listed below. Radioactively-tagged reagents were used to give the required sensitivity and to facilitate the determination of each reagent in the presence of the other.

All combinations of zero, 10^{-5}, 10^{-4}, 10^{-3} and 10^{-2} molar amine with zero, 100, 400 and 1000 mg/l starch were investigated and each combination was tested at six pH levels, approximately pH 2, 4, 6, 8, 10 and 12.

IV. MATERIALS AND APPARATUS

1. MATERIALS

(a) Hematite

Ore, crushed to -10 mesh and containing approximately 30% hematite, 20% magnetic iron oxides and 50% quartz, was supplied by the Iron Ore Company of Canada from the Carol Lake deposit, Labrador.

As inspection under low magnification showed very little intergrowth except in the coarsest particles, primary stages of separation were carried out before size reduction in order to facilitate subsequent handling. Several different techniques were employed, as no one method could yield a product of the desired purity.

The bulk of the dielectric material was first removed in a Dings electrostatic separator, Coronatron Model 12DX4WC, operating at 27 kV and 150 r.p.m. Middlings were recycled once and the combined concentrates scalped at 20 mesh to remove much of the misplaced material. After dry size reduction in a Bico pulverizer, Model UD32, to 95% -48 mesh and further treatment in the electrostatic separator, running at 50 r.p.m., a product largely free from silicates was obtained. Magnetic iron oxides, chiefly magnetite, were next removed in a Jeffrey Magnetic Separator, type 125, and the product transferred to a laboratory ball mill for wet grinding to the required size range (-325 +400 mesh).

Sizing by wet screening and mechanical dry screening were attempted but proved unsatisfactory due, respectively, to blinding and balling on the finer mesh. Manual brushing of the material (dried at 60°C) through electrically vibrated screens was adopted to overcome these difficulties. Material finer than 400 mesh (approximately 34% of the ground product) was discarded and that greater than 325 mesh (~64%) was recycled. The intermediate fraction was treated by mechanical dispersion in water and slow introduction into the top of an elutriation column (Figure 3). By control of the water flow rate, both siliceous impurities and undersize hematite were removed in the overflow while hematite of the desired size was collected at the bottom.

Laminar free-settling conditions were assumed, since the solids concentration in the column and particle size were within the accepted limits[62]. Settling velocities were calculated from Stokes' equation[63]:-

$$V = \frac{1}{18} \cdot \frac{g \; d^2 \; (\sigma - \rho)}{\eta} \qquad \qquad ...22$$

where V = terminal velocity of the falling particle (cm/s)

 g = gravitational acceleration (981 cm/s^2)

 d = equivalent spherical diameter of the particle (cm)

 σ = specific gravity of the particle

 ρ = specific gravity of the fluid

and η = fluid viscosity (1 centi-poise for water at 20°C)

Substituting appropriate values for 400 mesh (37 micron) hematite thus gave the maximum acceptable vertical water velocity (3.13 mm/s).

FIGURE 3

HEMATITE PREPARATION - THE ELUTRIATION COLUMN

FINE GLASS SYPHON

FEED SUSPENSION

OVERFLOW
(REJECTS)

COLUMN I.D. 21.8 mm

S: SCREWCLAMP

F: FLOWMETER

WATER FROM
CONSTANT HEAD
RESERVOIR

3 m

EFFECTIVE LENGTH
1 m

SCALE APPROX.
1 : 6

S

F

UNDERFLOW (PRODUCT)
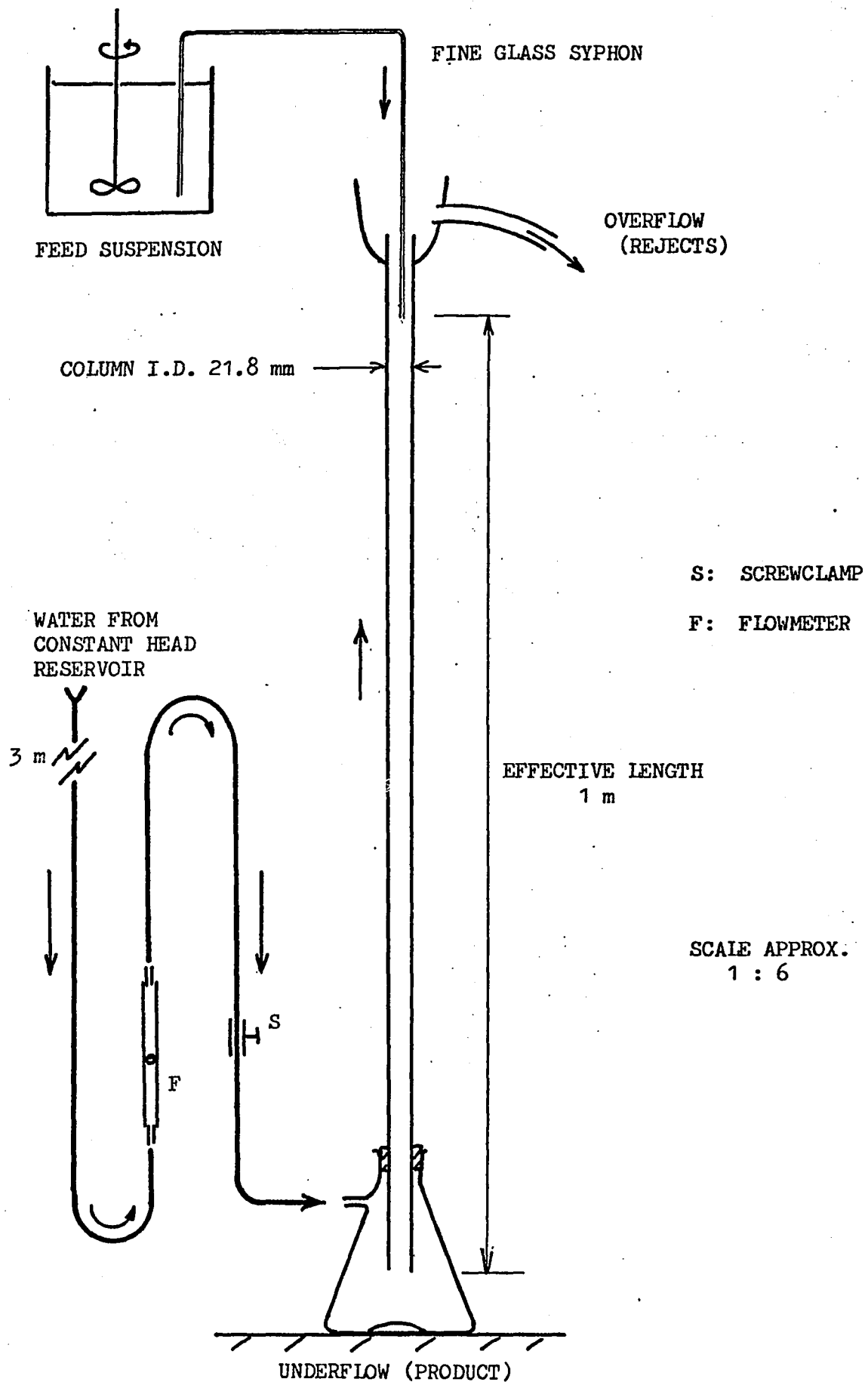
Similarly, in order to remove -325 mesh quartz the lowest permissible velocity is the terminal velocity of that material (1.74 mm/s). These values correspond, for the column used, to volumetric flow rates of 1.17 cc/s and 0.65 cc/s respectively. Flow was therefore maintained at approximately 1.0 cc/s by means of a screw clamp and a Gilmont No. 3 spherical float flow meter.

Final upgrading was carried out in two stages, magnetics being removed in a Davis tube (Dings model 'TT') and low density impurities on a Haultain Superpanner. Less than 1% was removed in each of these steps.

The surface was then cleaned by agitation for ten minutes as a dense suspension in 1:10 hydrochloric acid at $60^{\circ}C$ followed by repeated washing with double distilled water until equilibrium was reached, as indicated by pH measurements of the water before and after washing. This procedure was similar to that of Iwasaki et al.[64], Oko[65] and Smith[66]. The cleaned product was stored under moderate vacuum (~100 Torr) as protection against atmospheric contamination after drying to constant weight at $50^{\circ}C$.

X-ray diffraction analysis confirmed the material to be α-hematite and indicated no other crystalline substances. X-ray fluorescence analysis revealed only the presence of iron. Quantitative analysis for iron using an atomic absorption spectrograph gave a value of 69.7% Fe, agreeing closely with the theoretical 69.94% Fe for hematite. The material was 99.8% soluble in a hot 1% solution of

stannous chloride in concentrated hydrochloric acid. Details of the
analyses are given in Appendix 1.

(b) Dodecylamine Acetate

Dodecylamine was supplied by the Aldrich Chemical Co.
(Catalogue No. D22,220) and a one-gram sample sent to the Radiochemical
Centre, Amersham, U.K. for tritiation and subsequent purification.

The melting point of the pure amine is given by Timmermans[67]
as being 26.8°C, but at as high as 40°C a significant quantity of solid
was still evident. Consequently, an initial purification was carried
out by decantation and recrystallization at 28°C.

Batches of the amine acetate were made up by the following
method[68]. Forty grams of amine were dissolved in 250 cc of reagent-
grade benzene, cooled to 15°C and 12 cc (~12.4 g) of glacial acetic
acid added. The acetate, being only slightly soluble in benzene,
crystallized out and was filtered off, washed in pure benzene and dried
under vacuum to constant weight. Yield (45 g) was approximately 85% of
theoretical. The preparation of the radioactive batches differed only
in that the tritiated amine (2 mCi ≃ 1.5 mg) was first dissolved in the
benzene. The second tagged batch was made up from 4.0 g 'cold' amine
and 1.3 cc acetic acid in 25 cc benzene in order to obtain a product of
approximately 10 x the specific activity of the first batch. Measured
activities of the two batches were 47 µCi/g and 354 µCi/g respectively.

The melting point of the product was determined as $68.4 \pm 0.2^{\circ}C$ (cf. the published value[68] of $68.5 - 69^{\circ}C$), the sharp phase change indicating a high purity product.

(c) Starch

Starches from two sources were used. A sample incorporating carbon-14, prepared by photosynthesis of tobacco leaf in a $^{14}CO_2$ atmosphere and subsequent extraction, was obtained from Amersham/Searle Corp., Illinois. Corn starch, marketed as 'Soluble Starch', was purchased from British Drug Houses Ltd. for use as the non-active diluent. It was assumed that any differences between them (notably of amylose/ amylopectin ratio) would be insignificant after the extensive degradation occuring during causticization.

The active starch was stored in a small glass vial, the non-active portion in a desiccator at atmospheric pressure.

(d) Conductivity Water

Distilled water from a 'Precision' brand laboratory still was re-distilled in an all-Pyrex Yoe-type still (Corning Model AG-2). Dissolved carbon dioxide, which reacts with amines in solution to form insoluble carbonates, was displaced by bubbling high-purity nitrogen until the pH, initially about 5.5, became constant at approximately 7.2 . The slight basic impurity indicated by this final value was probably due to

the formation of NaOH with sodium from the glass carboy in which the water was stored. Air entering to replace tapped water was passed through a column of Ascarite to remove carbon dioxide.

(e) Nitrogen

Certified 99.99% nitrogen (Grade L, Canadian Liquid Air Ltd.) was used with no further purification.

(f) Sodium Hydroxide Solution

A saturated aqueous sodium hydroxide solution was made up from low-carbonate pellets and allowed to stand in a closed polythene bottle for two weeks. Any finely divided carbonate was thus allowed to precipitate out[69]. Pure solution was syphoned from the bulk of the concentrate, diluted with conductivity water, and the normality of the diluted solution determined by titration against reagent grade oxalic acid (weighed crystals) using phenolphthalein as indicator. A 1 N solution was prepared by further dilution and stored in a polythene bottle and an N/100 solution also prepared to facilitate subsequent pH control.

(g) Standard Activity Solutions

Solutions of known activity were prepared for both tritium and carbon-14 for subsequent use in calibration.

(a) TRITIUM: Approximately 10 cc of standardized tritiated water were obtained from Packard Instrument Co. and diluted to 200 cc. The resultant water had a specific activity of F x 1.0708 x 10^5 d.p.m./cc (0.48 μCi/cc) where F is a factor to correct for decay after the assay date, 14th March 1969.

(b) CARBON-14: Two solutions were made up from ^{14}C-benzoic acid of known activity supplied by the above source. The benzoic acid was mixed with 50% excess 1 N NaOH and maintained at 60°C overnight. The resultant solutions were each diluted to 250 cc. Specific activities of the two solutions were 17,312.7 and 12,487.8 d.p.m./cc (7.8 nCi/cc and 5.6 nCi/cc).

(h) <u>Other Reagents</u>

All other reagents employed were of the highest purity generally available. They included:-

Acetic acid	C. P. Reagent Grade
Hydrochloric acid	C. P. Reagent Grade

and the components of the scintillator solution:

1, 4 Dioxane	Cert. A. C. S.
P.P.O. (2, 5 diphenyloxazole)	Scintillation Grade
and Naphthalene	Recrystallized from alcohol.

2. AMINE-STARCH SOLUTIONS

Starch in solution is subject to biological degradation and amine solutions also tend to degrade on standing[70]. Consequently the preparation of bulk solutions of known concentrations and specific activities was precluded. Solutions were therefore made up daily as required.

For each of the amine/starch combinations chosen, 500 cc of double-strength solution was prepared containing twice the required amounts of both reagents. A suitable quantity of starch, including a small (<1 mg) portion of tagged material, was weighed into a volumetric flask. Water to make a 4% (w:w) suspension and an equal volume of 1 N sodium hydroxide solution were added and the flask was heated to 100°C in a water bath, held at temperature for fifteen minutes and rapidly cooled to room temperature. The solution, which became colourless and clear on addition of the alkali, did not boil but showed a pale yellow colour on attaining 100°C and became progressively darker during the heating period. The procedure was very similar to that of Iwasaki which gave most effective depressant properties[45, 46]. It was also thought that any difference between the starches from the two sources would be effectively removed during the considerable degradation which has been shown to occur during this operation[45].

In order to avoid subsequent undesirable liberation of free amine due to the high pH, the solution was next acidified by addition

of an approximately equivalent volume of hydrochloric acid and diluted with water to the volume of the flask. The correct volume to yield one litre of the final strength solution was transferred to a 500 cc flask.

To this fraction was added the appropriate volume of a freshly made aqueous solution of the amine acetate, consisting of an arbitrary mixture of high and low activity acetate calculated to yield one litre of final solution of the required concentration and suitable activity. The mixture was then diluted to 500 cc with water.

Fifty millilitre portions of this solution were pipetted in turn into 100 cc beakers, adjusted to the desired pH, washed into 100 cc flasks and diluted to the final concentration. Little change of pH was found to occur on dilution except in near-neutral solutions.

3. APPARATUS

(a) Adsorption

Adsorption was carried out in Pyrex glass vials of 50 cc nominal capacity closed with soft rubber serum caps. When filling, the last portion of solution was injected through the cap by means of a glass syringe and stainless steel hypodermic needle, displacing final traces of air. True volumes of the vials were determined by difference between dry weight and the mean of three weights when filled with water. Mean deviation per vial (i.e. due to filling differences) was found to be

negligible (0.02 cc) but a considerable variation was noted between vials, the appropriate value (after correction for hematite volume) being used in subsequent calculations.

Agitation during the adsorption period was achieved by mounting the vials radially inside a cylinder of 490 mm internal diameter rotated about its horizontal axis at 36 r.p.m. The vials were gripped in slightly undersize holes cut in a foam rubber liner.

(b) Flotation

A number of methods may be regarded as standard practice for small-volume flotation testing but each was rejected as being unsuitable for the current problem. The vacuum technique of Schuhmann and Prakash[71] was considered insensitive unless a very large number of tests were to be made. Correlation between the bubble nucleation characteristic of the process and the collision mechanism regarded as dominant in industrial flotation[72] was also thought to introduce an unnecessary variable.

A simple method has been used with success by Paterson[73] and, recently, by Yoon[74] in their studies of precipitate flotation. Nitrogen was passed through the fritted glass base of a cylindrical funnel containing the test solution and the degree of flotation determined by sampling the solution, floated precipitates being held in the froth layer resulting from the foaming properties of the collectors. However, although amines do form stable froths in all but the most dilute solutions, these froths are usually insufficient to support the

relatively coarse particles encountered in this study. The use of a
supplementary frother, as advocated earlier by M.C. Fuerstenau[75], was
considered an objectionable complication.

The Hallimond tube in the improved form suggested by
D.W. Fuerstenau et al.[76] is commonly employed. However, preliminary
experiments with a version modified for smaller volumes showed that
movement of the particle bed could only be effected by a gas flow rate
which gave rise to excessive turbulence. Configuration of the cell
precludes mechanical agitation and magnetic stirring was ruled out due
to the slight magnetic susceptibility of hematite and to the intended
use of the cell in a subsequent similar study of magnetite.

As no conventional method was found suitable, a new method was
devised. The new cell, shown in Figure 4, is similar in principle to
the Hallimond tube. Mineral particles are initially contained in a
column of the test solution closed at the bottom by a glass frit of fine
(<5 μm) pore size. The bed is maintained in a gently moving suspension
by a mechanical stirrer and a controlled flow of nitrogen is passed
through the porous base. Particles exhibiting hydrophobic surface
properties become attached to the bubbles which rise and are deflected
outwards by the conical baffle before reaching the liquid surface.
Depending upon the properties of the solution, the bubbles may form a
froth or burst, floated particles being retained in both cases, either
in the froth or on the annular floor of the upper section, and can be
collected at the end of the test by washing out through the side tube.

FIGURE 4

THE FLOTATION CELL

DRIVE

BAFFLE

LIQUID
LEVEL

FRIT

N_2

SECTION THROUGH CELL ASSEMBLY

DRIVE
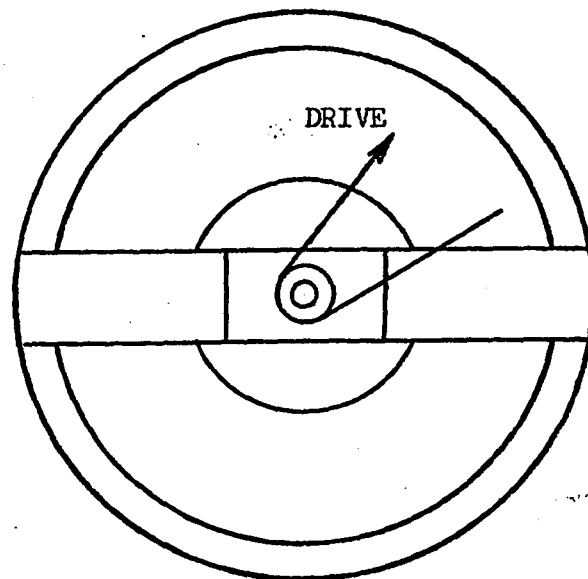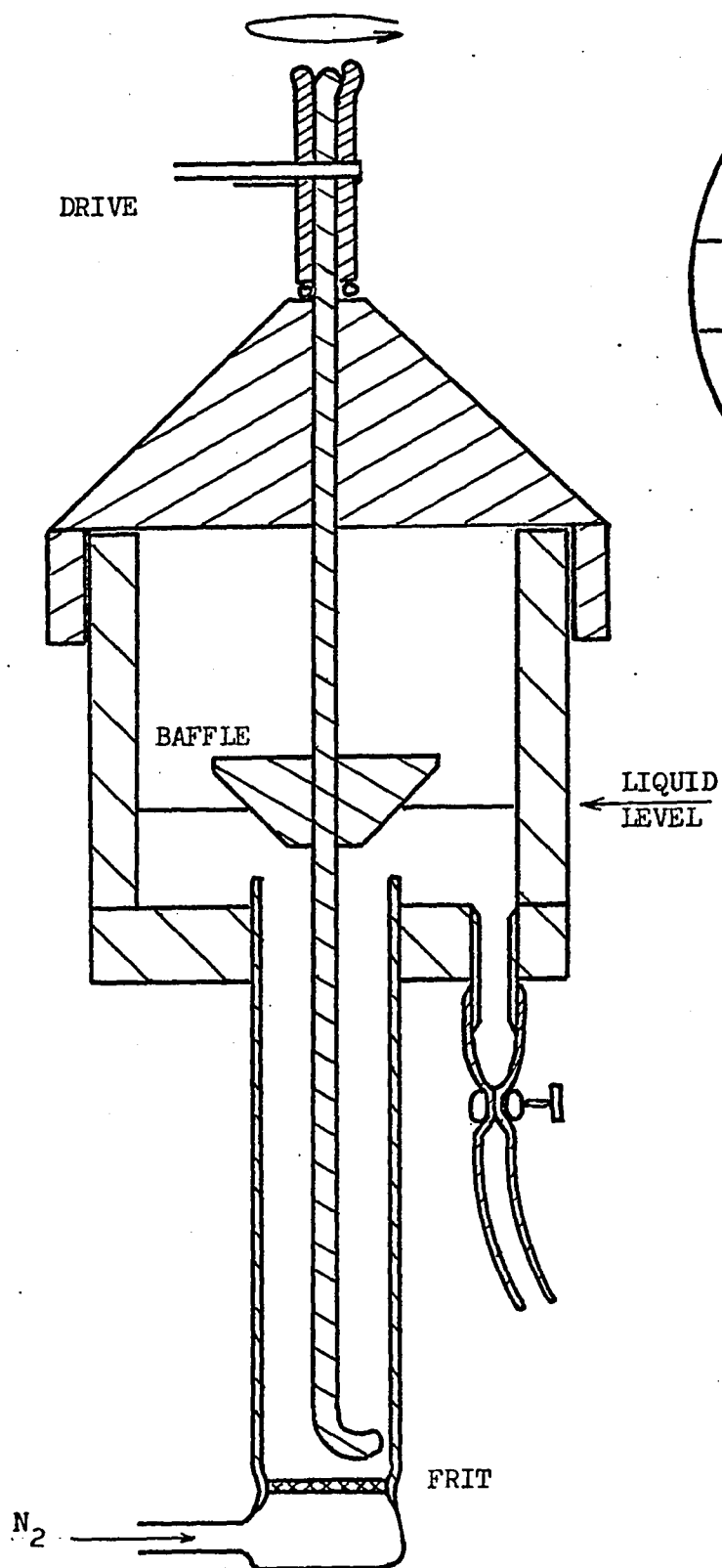
PLAN OF UPPER SECTION

SCALE   1 : 1

PLAN OF LOWER SECTION

A few points which arose during the development of the cell may best be mentioned here. The baffle, which serves the same purpose as the bend in a Hallimond tube in preventing 'fall back' of floated particles, was initially formed with a plane horizontal lower face, it being thought that the rotation imparted by the stirrer on which it was mounted would serve to impel the bubbles outwards. This did not occur, however, and the present conical form was found to be necessary to prevent formation of an air-lock. The second problem arose with an earlier, more complicated stirrer head which gave rise to rotation of the entire liquid column, the fine gas bubbles formed at the bottom then coalescing and rising ineffectually in a sheath about the stirrer rod. Finally, it was also noted that the efficiency of the cell was greatly affected by the height to which the inner tube protruded into the upper space, decreasing markedly as that height was reduced and particles could more readily fall back.

Gas supply to the cell was controlled by the arrangement shown schematically in Figure 5. Cylinder pressure was reduced and adjusted to the desired value by means of the regulator, R, accurate pressure measurement being provided by the mercury manometer, M. Flow rate, as indicated by a No. 1 Gilmont spherical float meter, F, was controlled with a needle valve, N. The cell was connected to the supply by means of a ball-and-socket joint, B. Stopcock S was used to vent the underside of the glass frit to atmosphere, thus providing a sharp cut-off to bubble flow at the end of each run.

FIGURE 5

GAS CONTROL SYSTEM FOR FLOTATION CELL

R   PRESSURE REGULATOR

M   MANOMETER

F   FLOWMETER

N   NEEDLE VALVE

S   3-WAY STOPCOCK

B   BALL JOINT

N

M

R

NITROGEN
CYLINDER

M

N   S

F

B
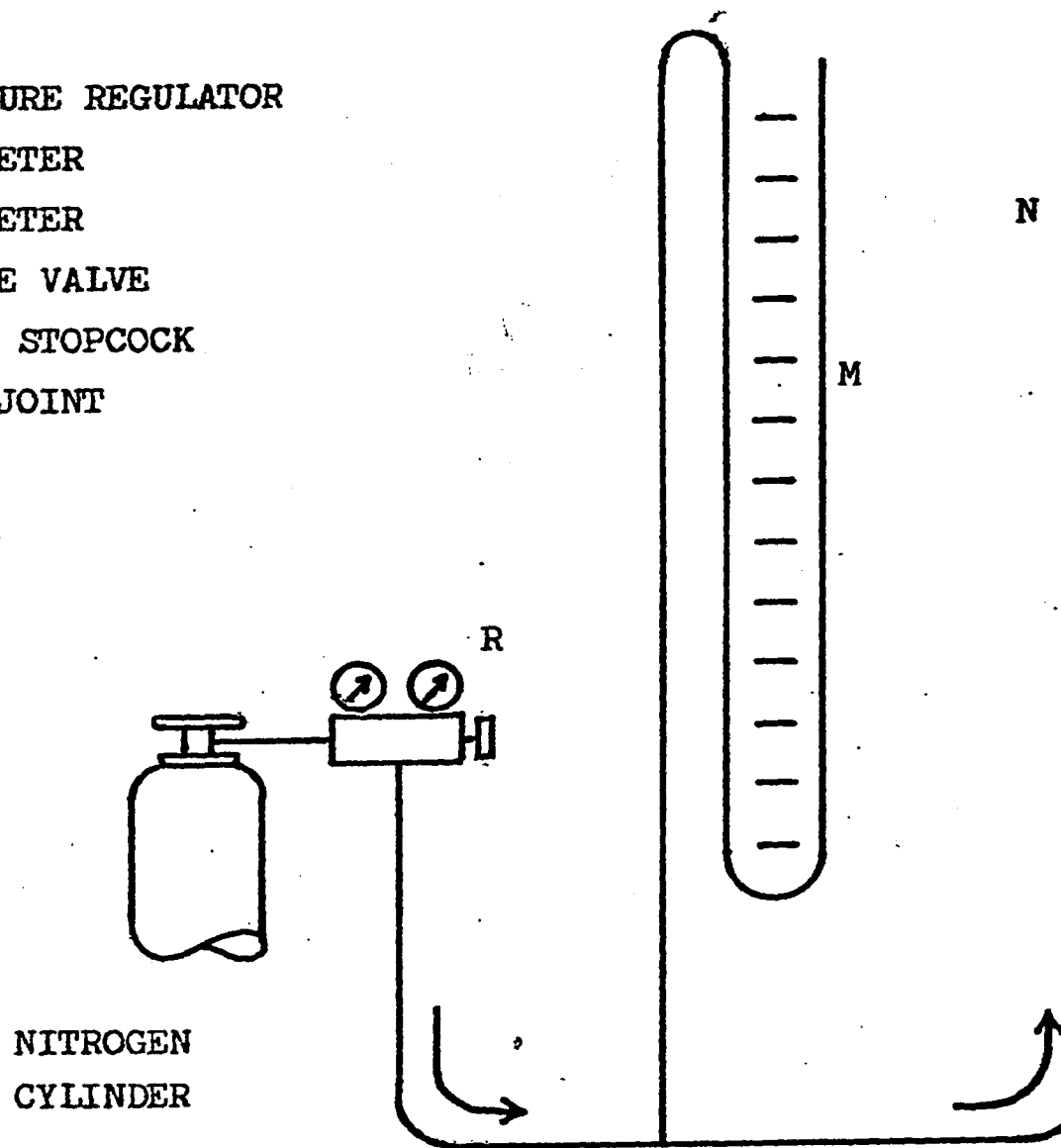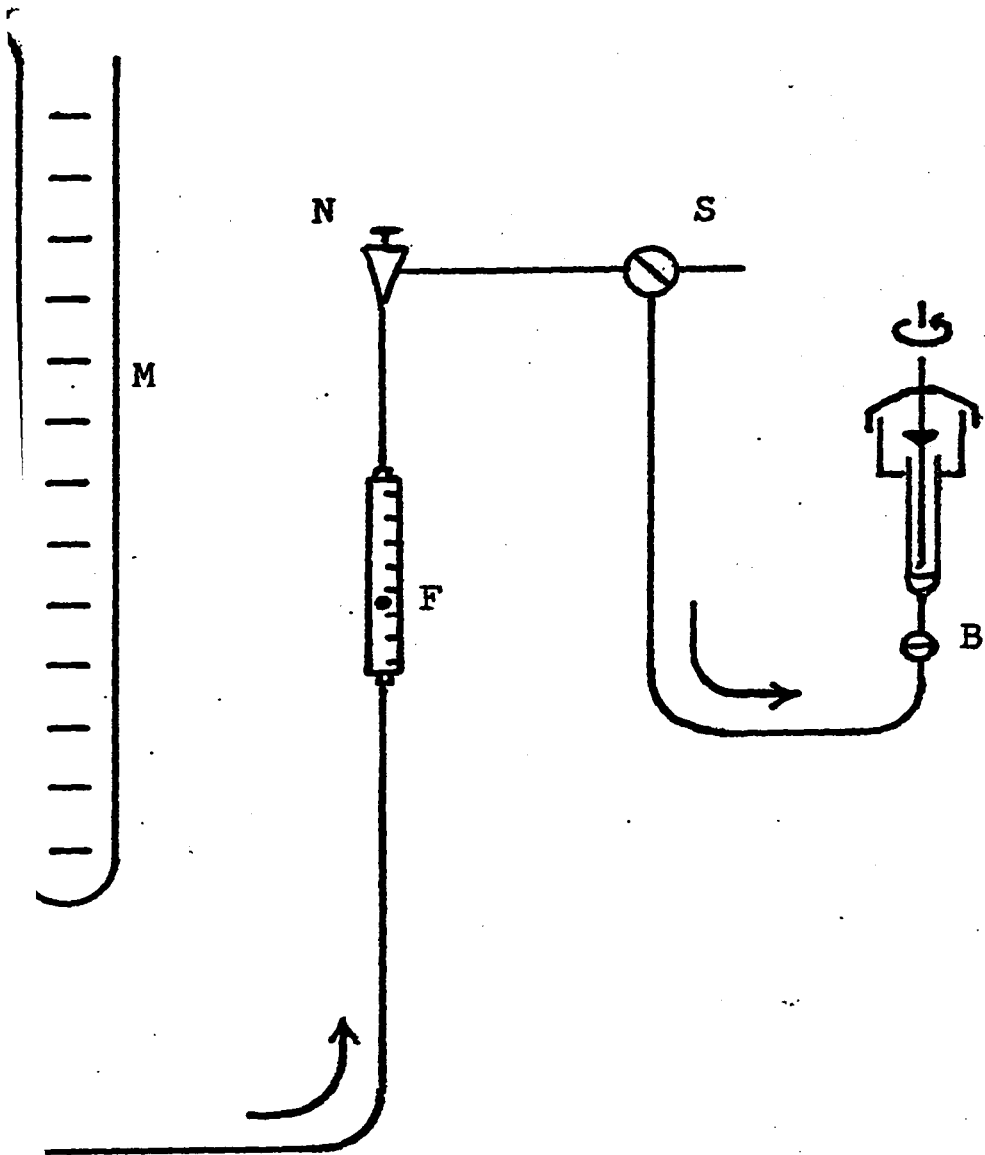
The flowrate was selected as 12 cc/min. at 500 mm Hg gauge pressure, corresponding to a volumetric flowrate through the cell of 20 cc/min. at atmospheric pressure. Flotation time was standardized at 30 s from the appearance of bubbles in the cell.

V. EXPERIMENTAL PROCEDURES

(a) Adsorption

A scoop of approximately 0.6 cc (2 gm loose hematite) capacity
was used to transfer the mineral into the vials, and the sample weight
determined accurately.

A portion of each prepared solution was used to rinse the syringe
and the combination electrode of the Metrohm model E-300B pH meter. The
pH of the solution was determined and recorded as 'initial pH' and the
appropriate vial, containing weighed hematite, filled as described on
p. 32.

After agitation for a pre-determined time, the vials were taken
out of the cylinder, the stoppers removed and the contents allowed to
settle. Centrifuging was rarely necessary as no size degradation occurred,
the particles settling rapidly and completely except in a few cases at
high pH when some adhesion to the glass walls was observed.

By means of an adjustable automatic micro-pipette, three samples
of approximately 1 cc (accurately reproducible) were transferred from
each vial into bottles for subsequent scintillation counting. Triplicate
samples were also taken from the 'parent' (higher concentration) solution,
direct comparison thus eliminating the need for solutions of standard
activity. Adsorption onto the glass vials was assumed to be negligible
due to the very much smaller surface area presented by the smooth glass
wall.

Early tests were carried out in series of constant solution conditions, vials being removed for sampling at pre-selected intervals in order to determine the maximum time required to attain effective equilibrium. Reagent concentrations for these tests were selected as being those likely to approach equilibrium most slowly. It had previously been assumed by Morrow[77] and established by Smith for dehydroabietylamine[78] that dilute amine solutions under favourable adsorption conditions were the slowest to reach equilibrium. Starch adsorption has been shown to be relatively rapid[42]. One test was also made using a combination of the two reagents. From the results, shown in Table 2 and Figure 6, an adsorption time of six hours was chosen for all subsequent tests.

Measurement of final pH was made by immersion of a Fisher micro combination electrode (diameter ~ 5 mm) into the solution in the vial immediately after sampling. The bulk of the solution was pipetted into a conical flask and subsequently used to wash the hematite into the flotation cell.

Vials and other glassware were cleaned between tests by contact with acid dichromate solution for at least twelve hours, rinsed with tap water followed by conductivity water and dried at 120°C.

(b) Flotation

The upper section of the cell, carrying the stirrer, was removed and the sample washed into the inner tube with a jet of the relevant

FIGURE 6

ADSORPTION AS A FUNCTION OF TIME

$\odot$: 10^{-4}M. AMINE

$\triangle$: 10^{-5}M. AMINE WITH 400 mg/1 STARCH

$\odot$: 10^{-5}M. AMINE

4   5   6   7   8

HOURS
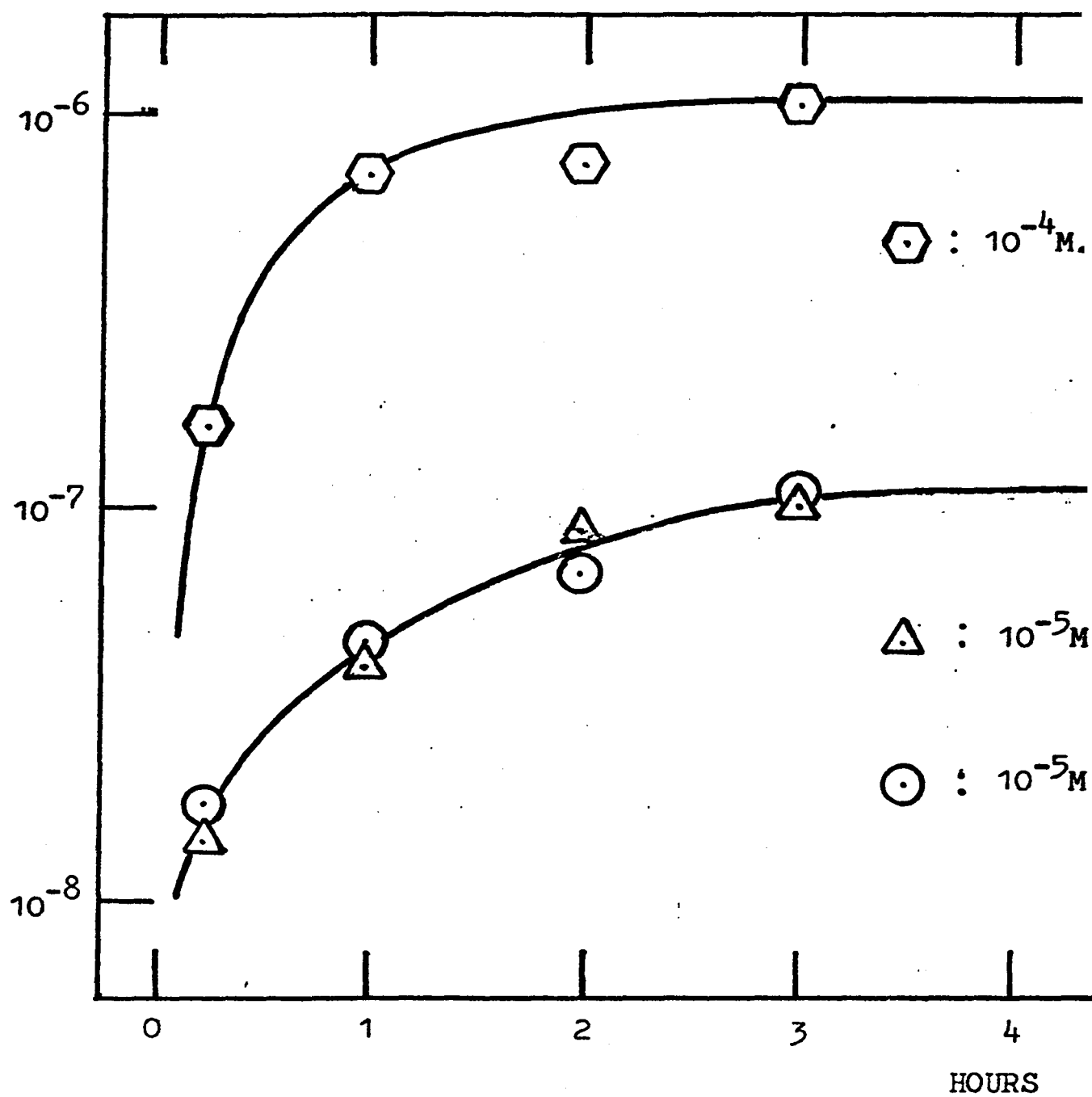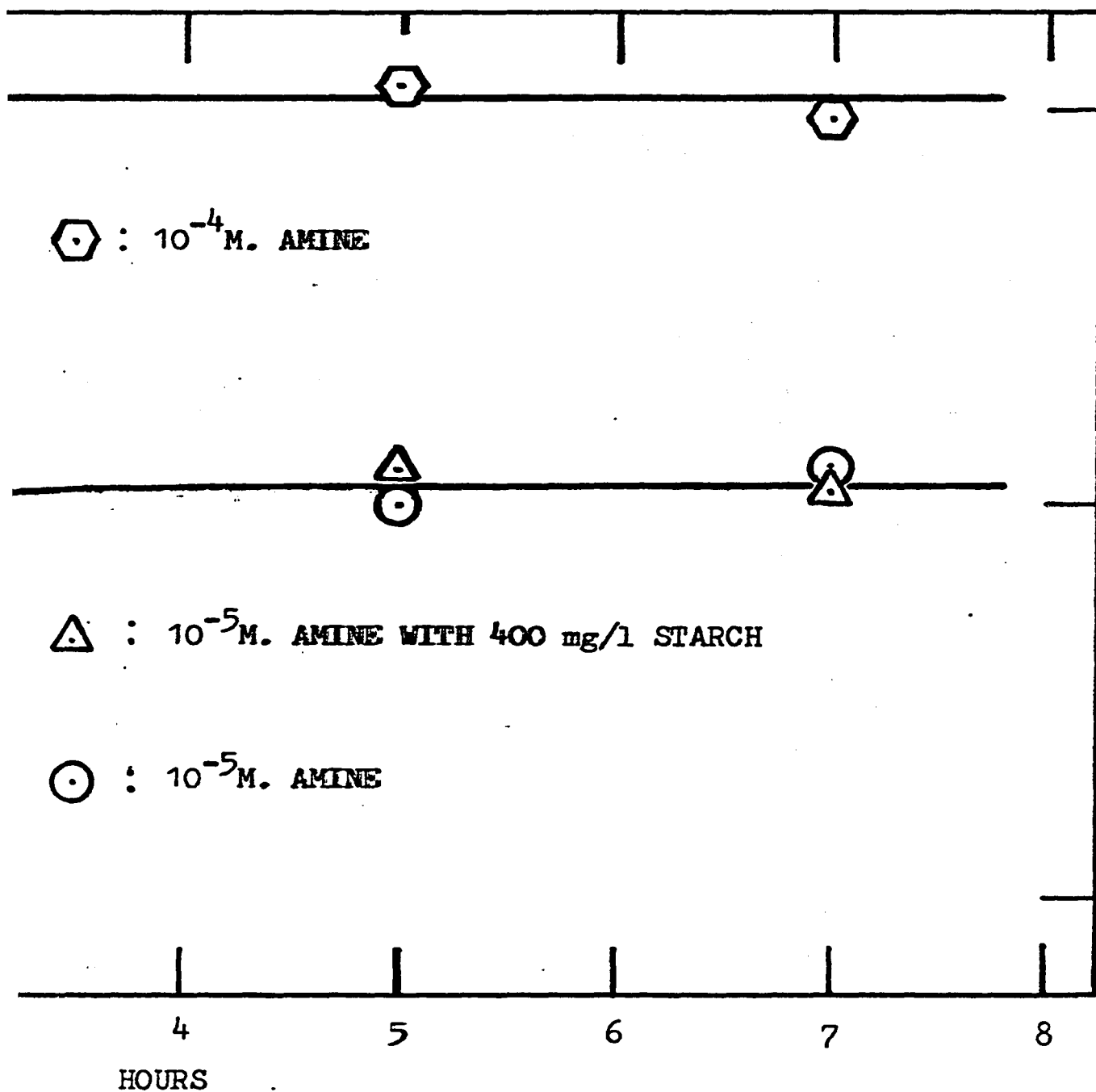
test solution. Effectively all the hematite was transferred from vial to cell in this manner, although complete transfer was not essential since both products (floats and sinks) were weighed to determine the percentage float.

The upper section was replaced, the clamp on the side tube closed, the remaining solution added and the cell connected to the gas train and stirrer motor (Figure 7.a.). The motor was switched on, putting the hematite into suspension (Figure 7.b.) and the gas flow initiated. Bubbles appeared after a delay of 10 - 20 s (Figure 7.c.) and were continued for 30 s, slight corrections of flowrate being made if necessary. At the end of the flotation period the tap was vented to atmosphere, immediately stopping further bubble formation. The motor was switched off and the contents were allowed to come to rest (Figure 7.d.). The two products were washed into separate containers, filtered, rinsed when necessary with dilute hydrochloric acid to remove free amine, dried and weighed.

The cell was rinsed with distilled water between runs of constant reagent concentration and with 10% hydrochloric acid solution at the end of each series. It was immersed in a laboratory detergent solution for day-to-day storage as the Plexiglas portions would have been attacked by the acid dichromate cleaning solution.

(c) Solubility

A series of tests were made to determine the effect of starch

FIGURE 7.a.

THE FLOTATION CELL: PRIOR TO RUN
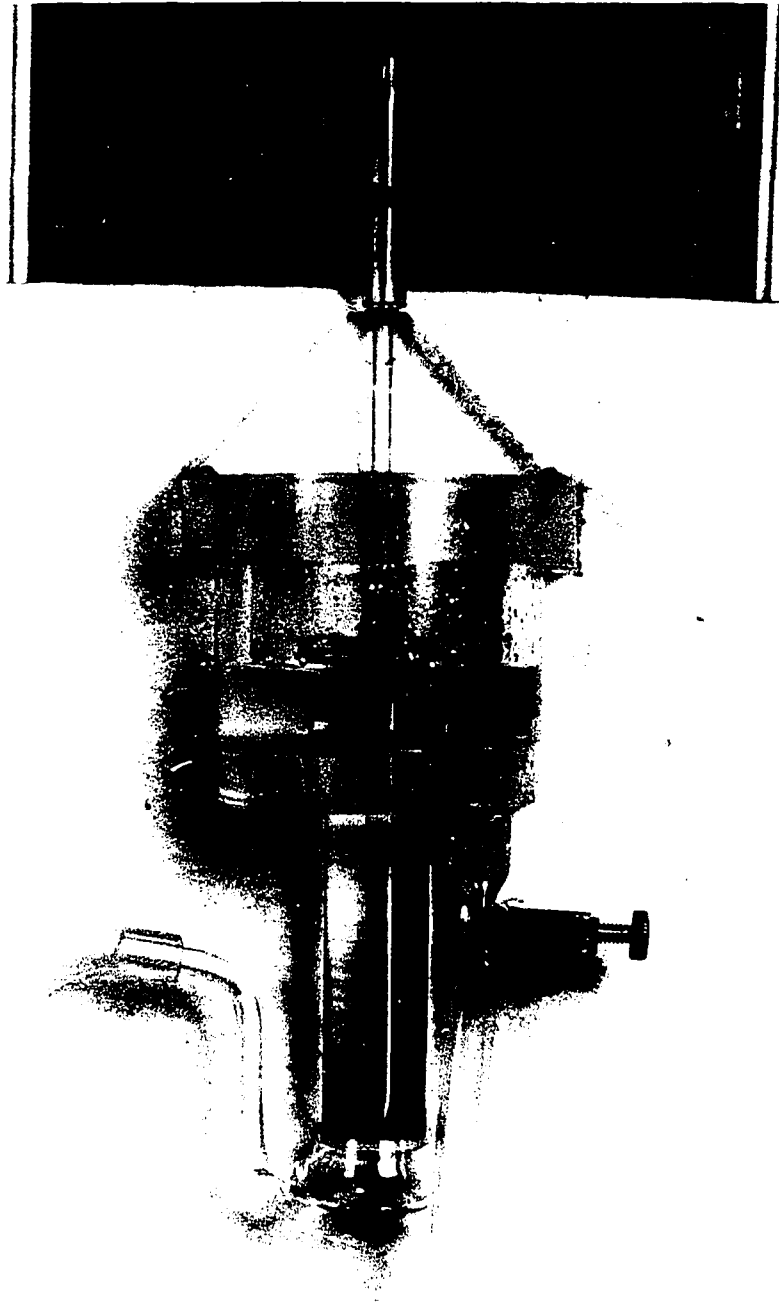
FIGURE 7.b.

THE FLOTATION CELL: AGITATION
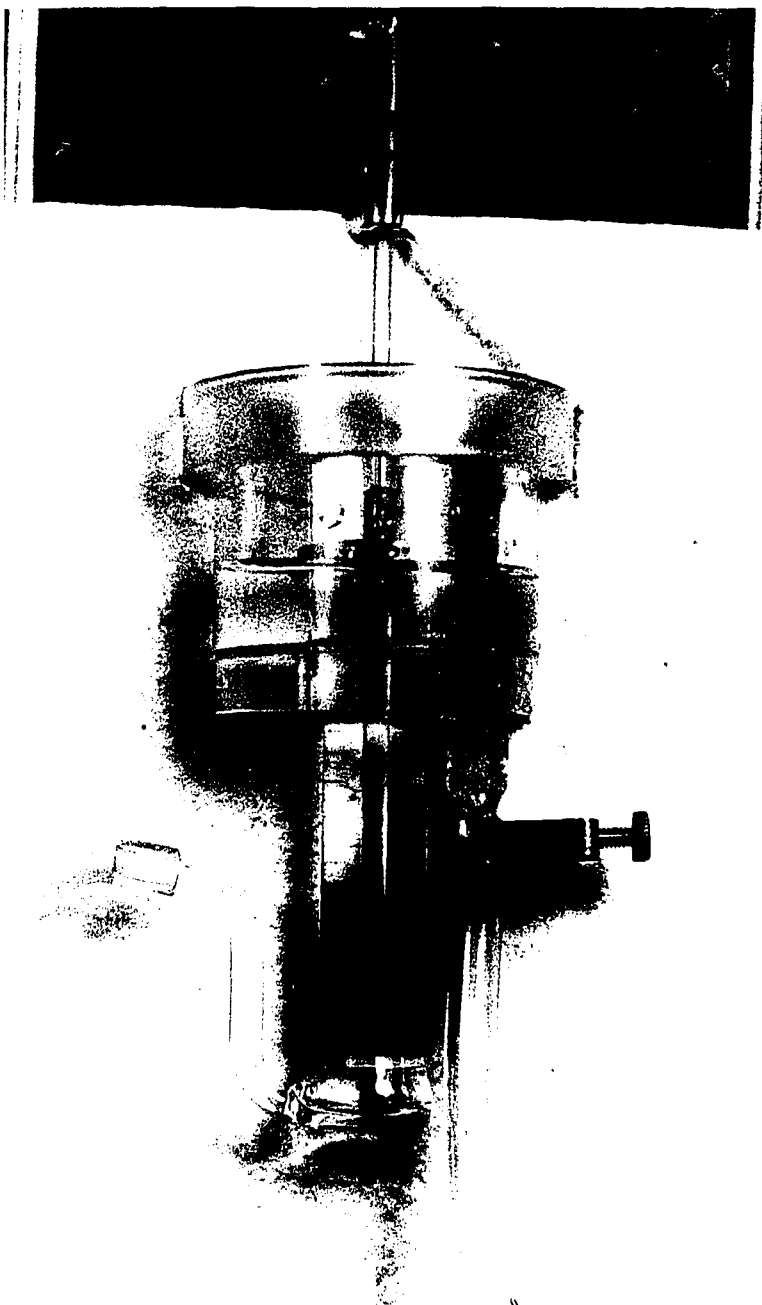
FIGURE 7.c.

THE FLOTATION CELL: AGITATION WITH GAS FLOW
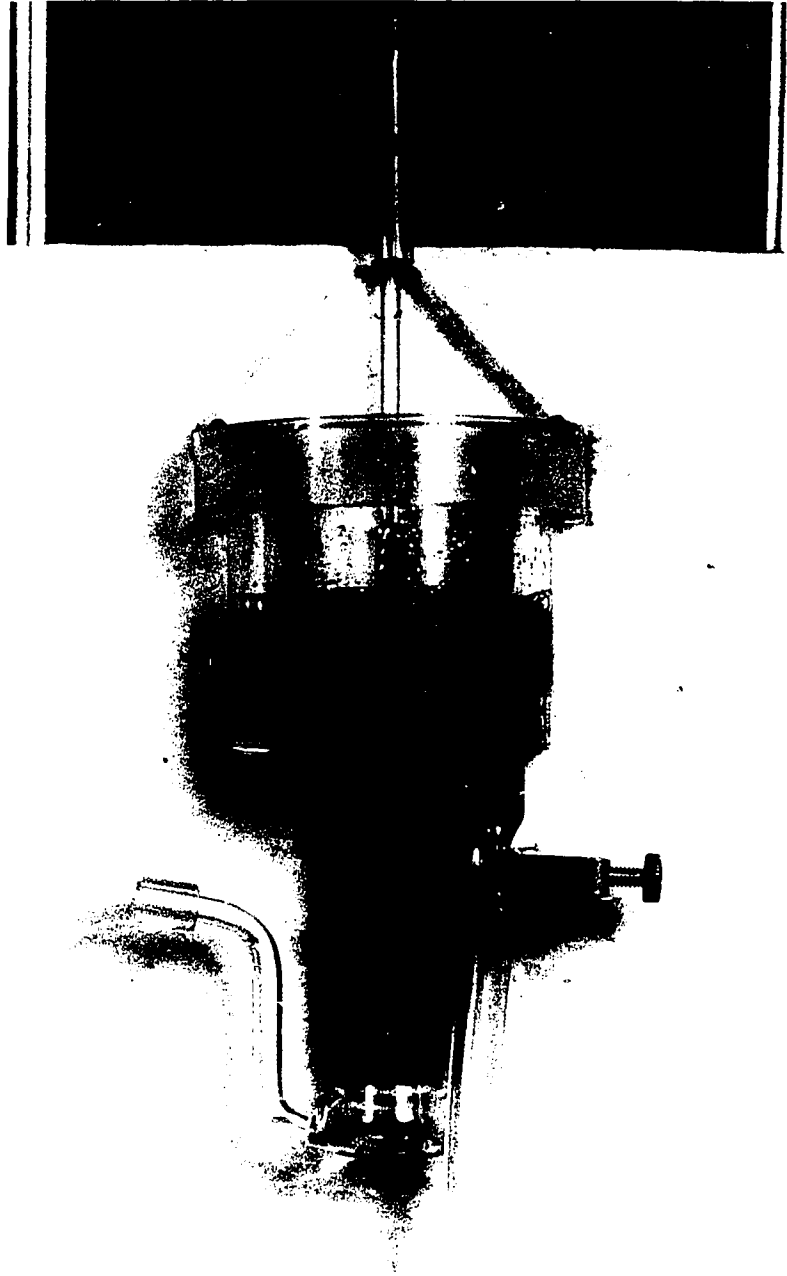
FIGURE 7.d.

THE FLOTATION CELL: END OF RUN
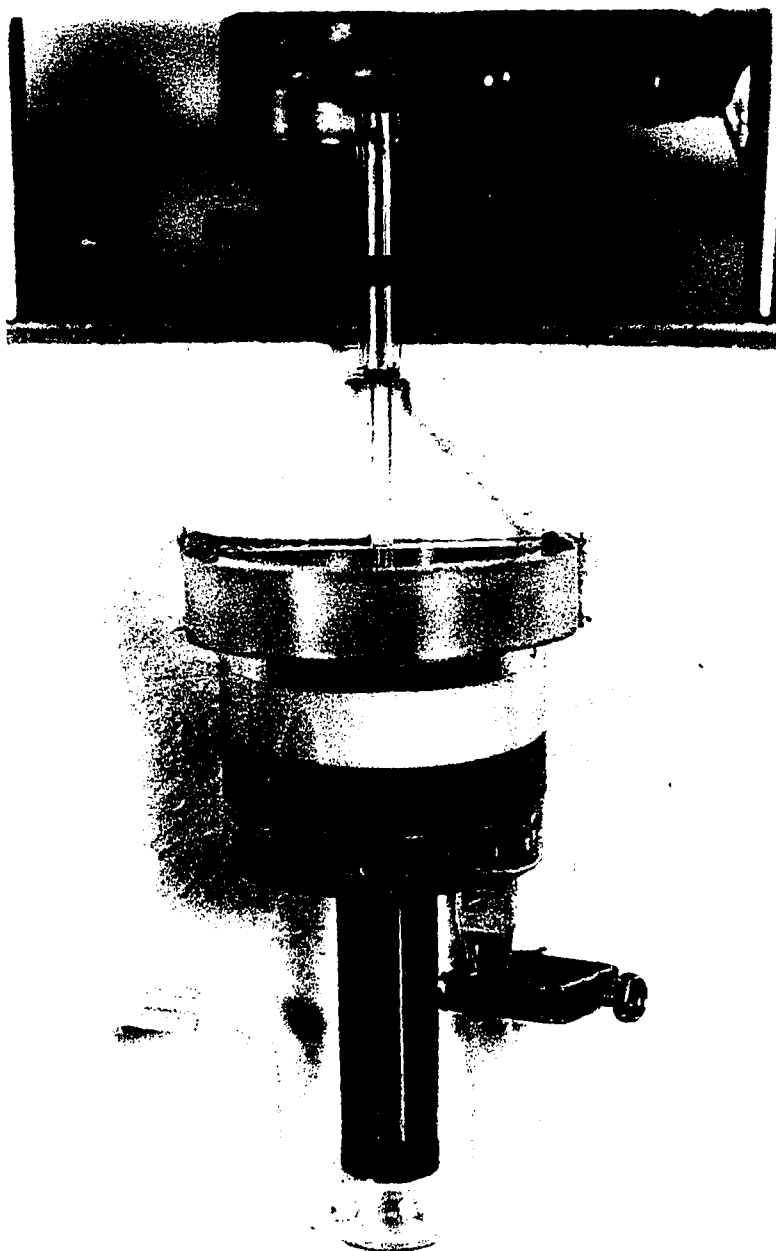
on the solubility of dodecylamine. A 250 cc solution at pH ~ 4 was
prepared for each of the amine-starch combinations used in the previous
tests and placed in a 600 cc beaker. A combination pH electrode and a
burette containing 1 N NaOH were dipped into the solution and a magnetic
stirrer used to provide thorough mixing. A narrow pencil of light from
an electric lamp was projected through the solution and the light path
viewed perpendicularly against a dark background. Sodium hydroxide
solution was slowly added from the burette, the rate of increase of pH
being maintained below 1 pH unit per minute. The pH at which the light
beam became visible due to Tyndall scattering[79] was taken as the limit
of solubility. Each result was checked by reducing the pH with
hydrochloric acid and repetition of the NaOH addition. Volumetric
increase due to the added alkali was less than 1%, considered negligible.

A subjective observation of each solution was also made at pH
levels up to 12.5 .

VI. RESULTS

(a) Flotation

Initial tests were carried out with neither collector nor depressant to determine the natural floatability of the hematite. Sodium hydroxide and acetic acid were used as pH modifiers. Recovery (percentage floated) was less than 7% at pH 12 and decreased slightly with decreasing pH in the alkaline region. Below pH 8, however, the recovery was found to rise and approached 100% at pH 2. When hydrochloric acid was used in place of acetic acid the recovery was found to continue the trend followed in the alkaline region, decreasing to 4% at pH 2. Hydrochloric acid was used throughout all subsequent tests. The 'natural' floatability curves are shown in Figure 8.

The remaining flotation results are plotted in two series; Figures 9 - 12 at constant starch levels and Figures 13 - 16 with constant amine concentrations. In general, the curves of recovery versus pH for any selected reagent conditions increased to a peak in the alkaline region and fell off sharply at high and low pH. The effects of increasing starch concentration and of decreasing amine are similar. In both cases the area under the curve and, usually, the maximum recovery are reduced. The peak also shifts to higher pH values under these conditions.

An exception to these generalizations is the behaviour of the most concentrated amine solution, 10^{-2} molar, which gave lower

FIGURE 8

FLOTATION EFFECTS OF THE pH MODIFIERS

NaOH, HCl AND CH_3COOH

FLOATABILITY - PERCENTAGE vs pH

AMINE: ZERO

STARCH: ZERO

pH MODIFIER:-

△ NaOH

⊙ CH_3COOH

▢ HCl
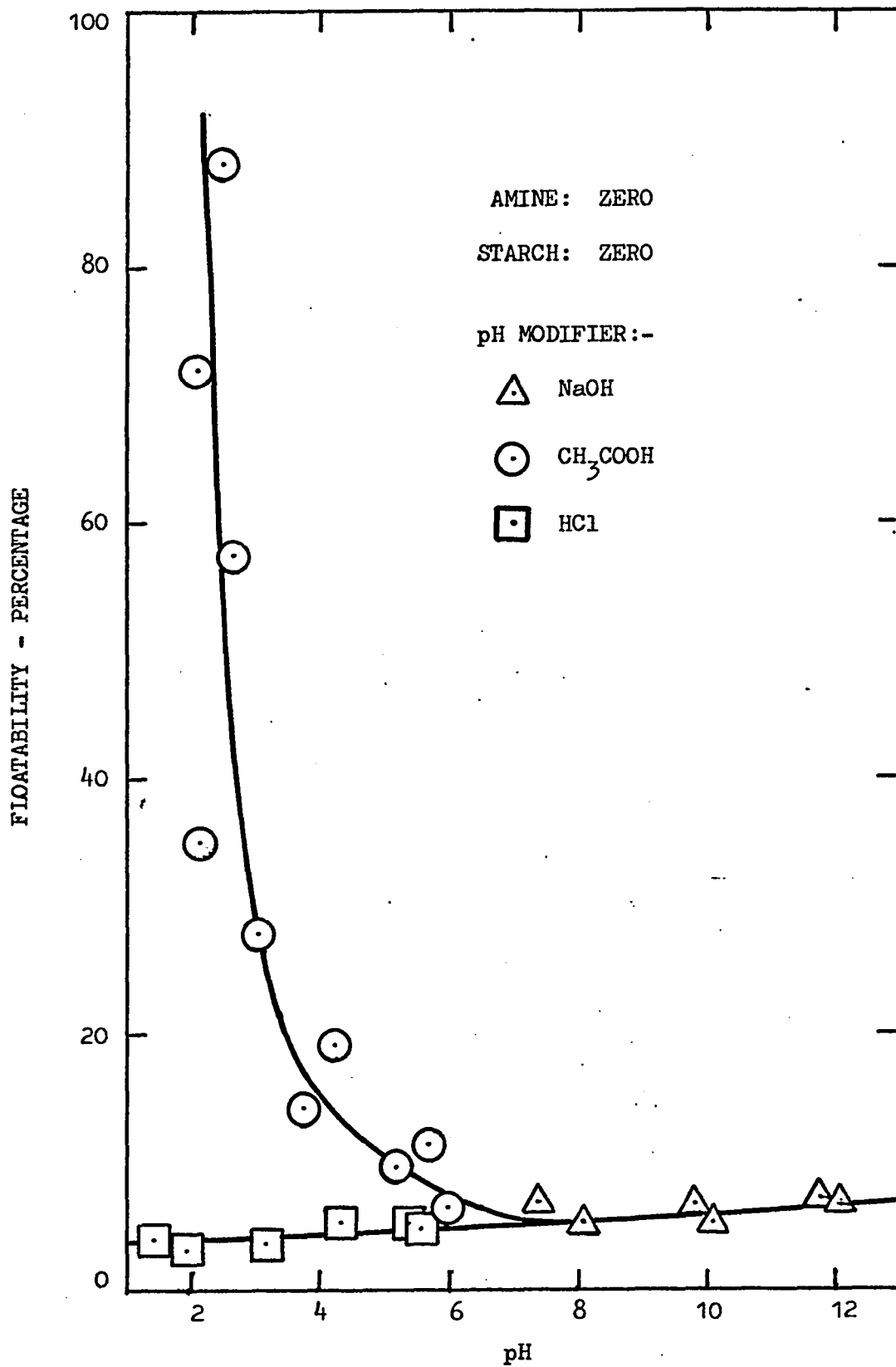
FIGURE 9

FLOATABILITY AS A FUNCTION OF AMINE CONCENTRATION AND pH

STARCH: zero

ZERO STARCH

pH
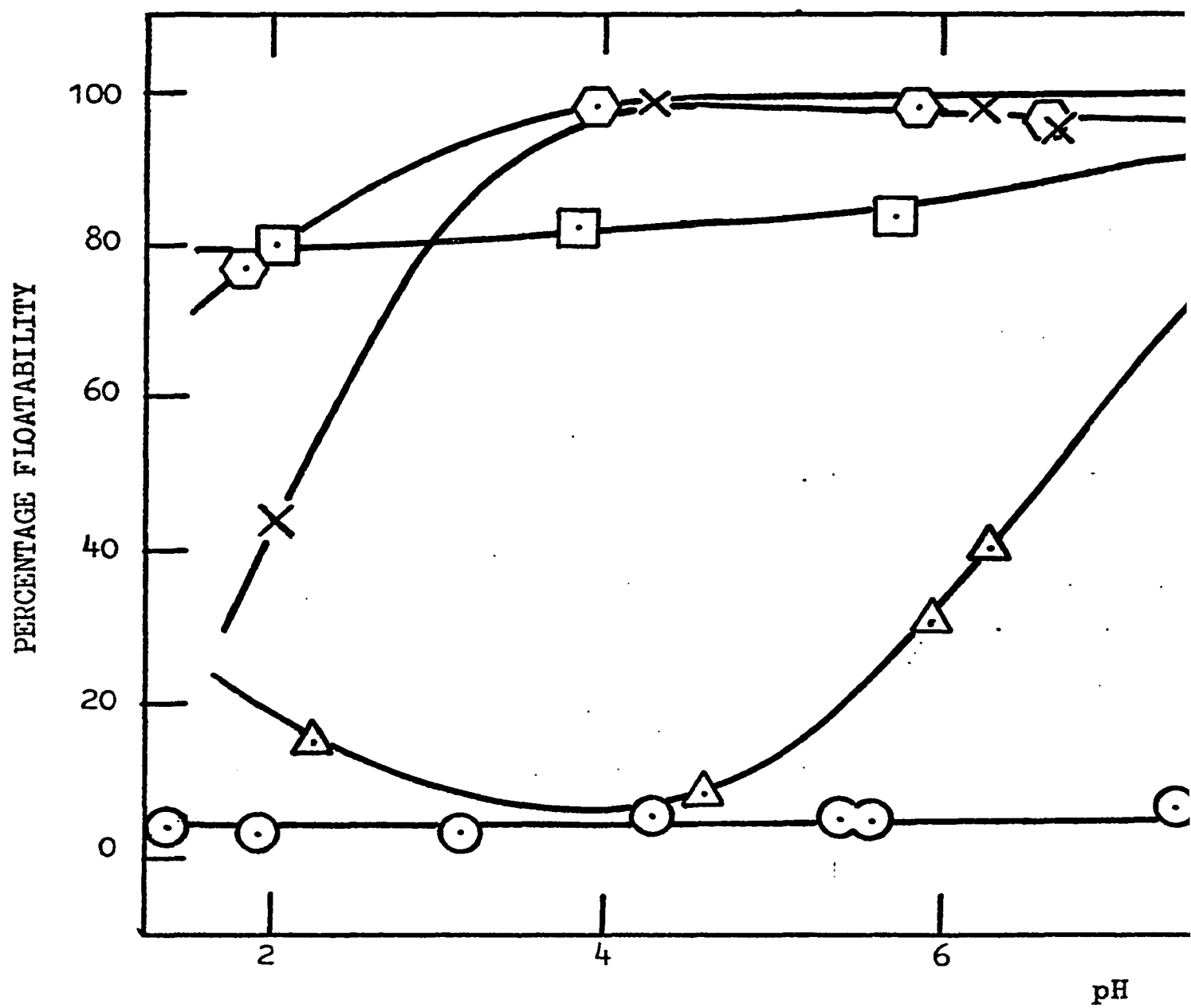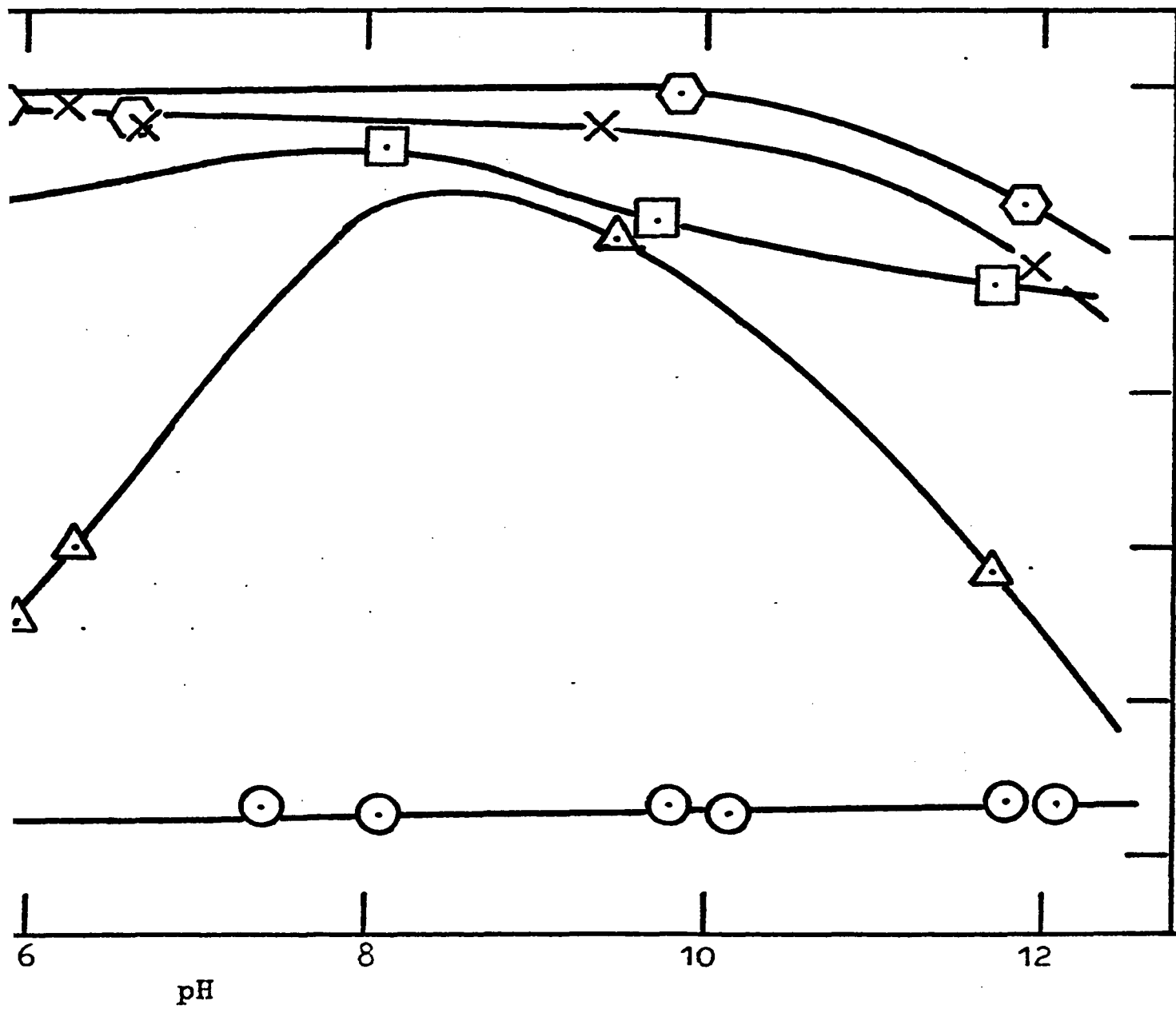
× 10^{-4}M.   ⬡ 10^{-3}M.   ▢ 10^{-2}M.

FIGURE 10

FLOATABILITY AS A FUNCTION OF AMINE CONCENTRATION AND pH

STARCH: 100 mg/l

100 mg/1 SI

PERCENTAGE FLOATABILITY

100

80

60

40

20

0

pH

2

4

6

AMINE: ⊙ zero   △ 10⁻⁵M.   ✕ 10

100 mg/l STARCH

pH
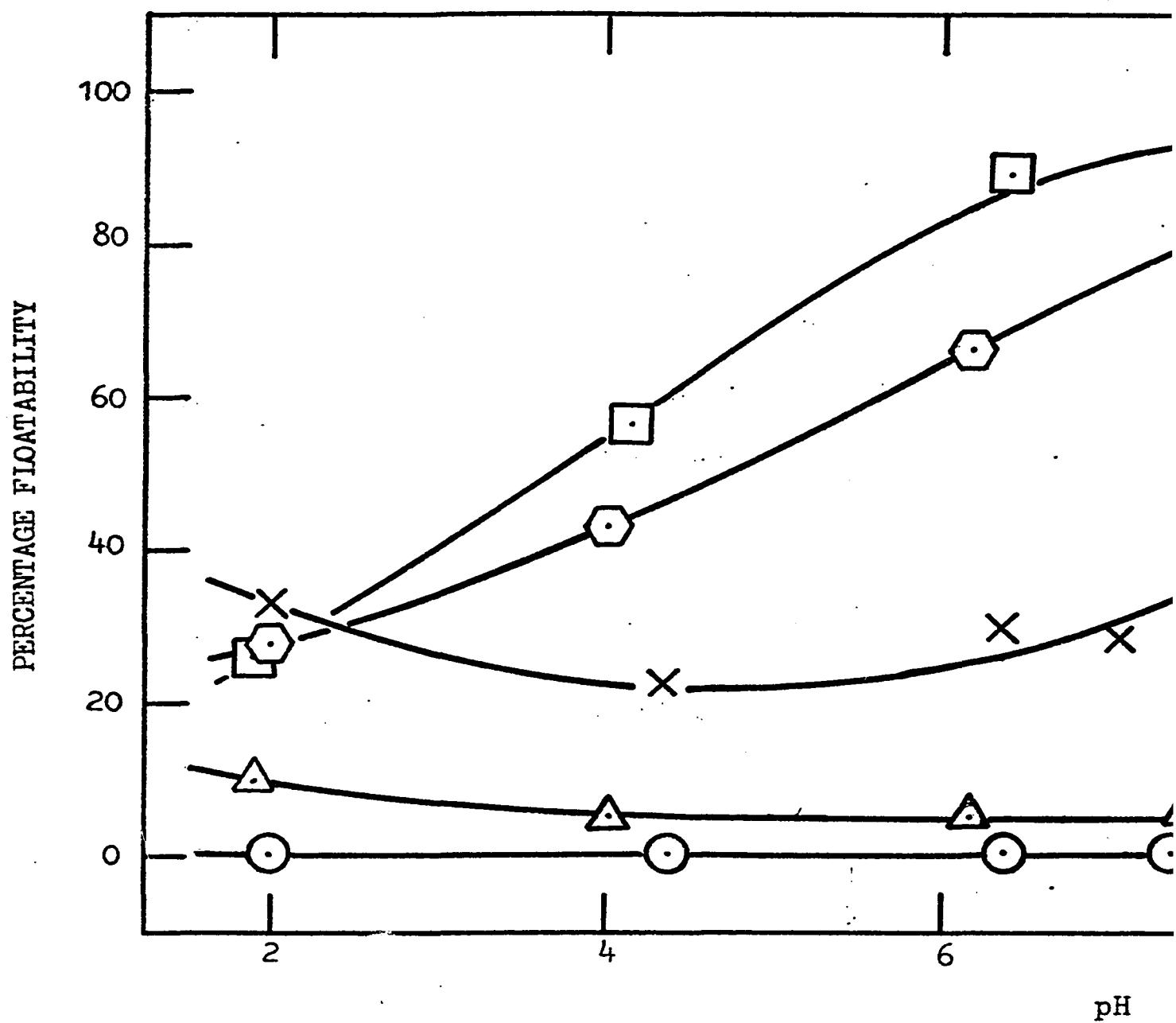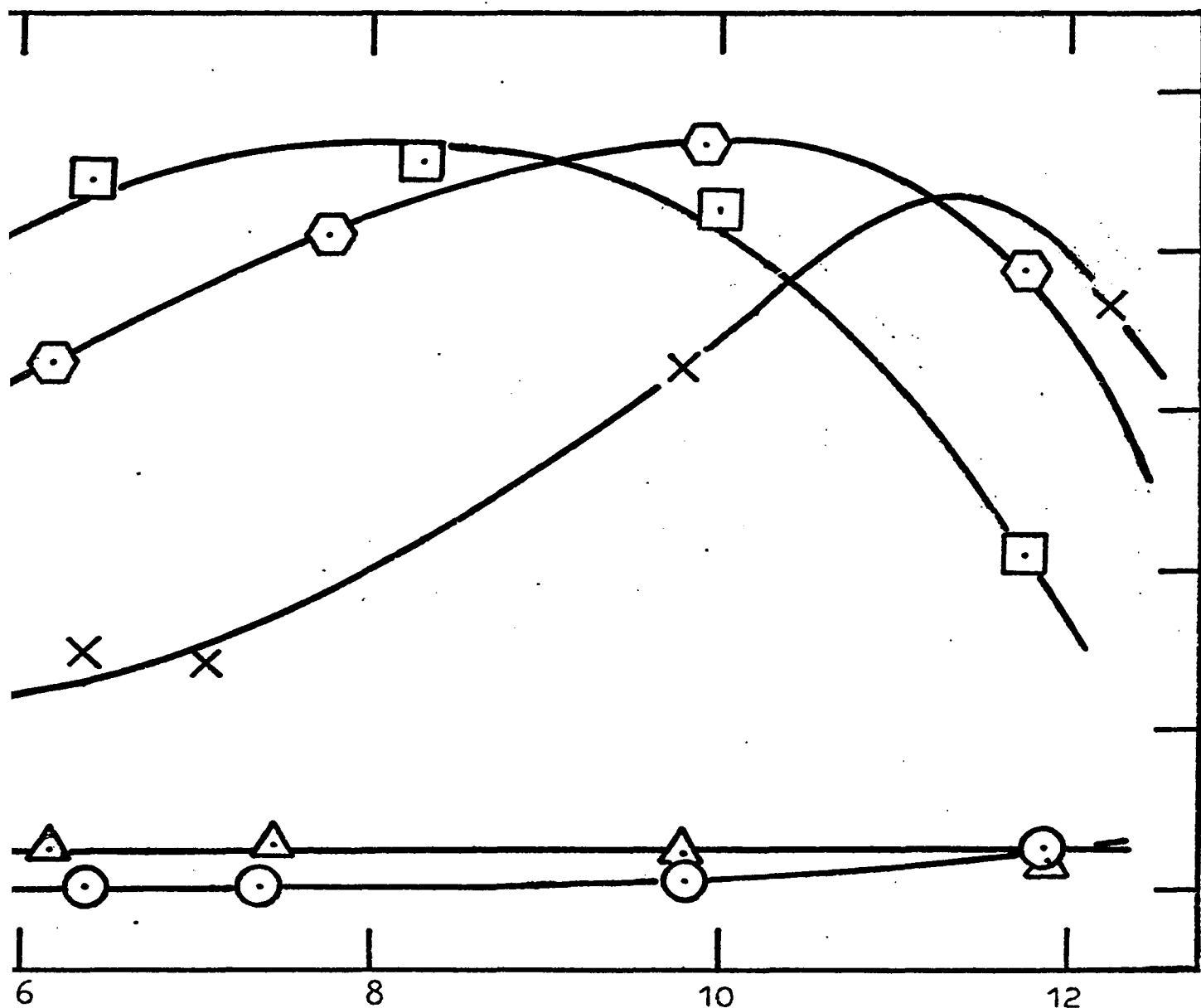
$\times$ 10^{-4}M. $\langle \cdot \rangle$ 10^{-3}M. $\square$ 10^{-2}M.

FIGURE   11

FLOATABILITY   AS   A   FUNCTION   OF   AMINE   CONCENTRATION   AND   pH

STARCH: 400 mg/l

400 mg/1 :

PERCENTAGE FLOATABILITY

100

80

60

40

20

0

2   4   6
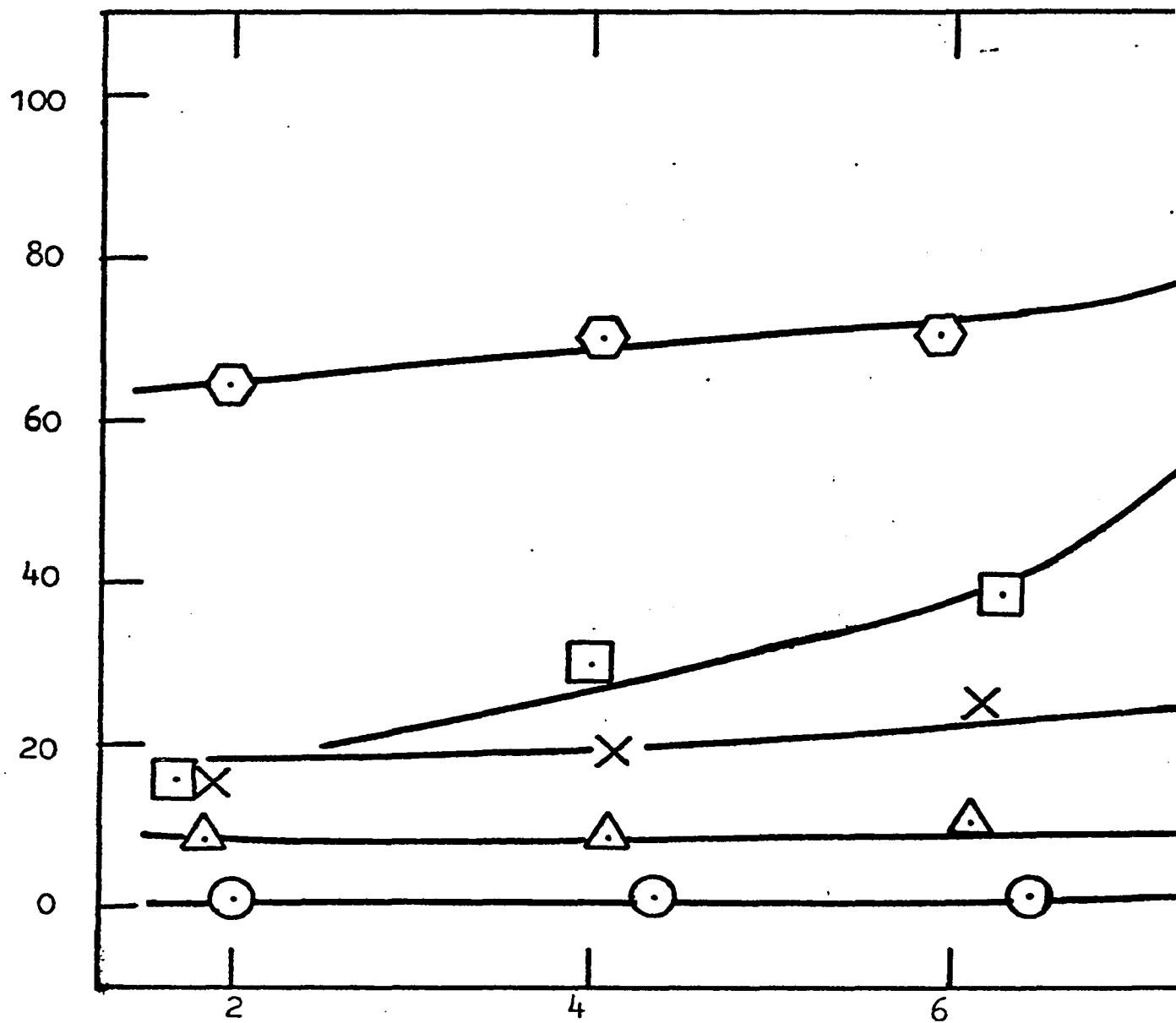
AMINE: ⊙ zero   △ 10⁻⁵M.   ✕

400 mg/1 STARCH
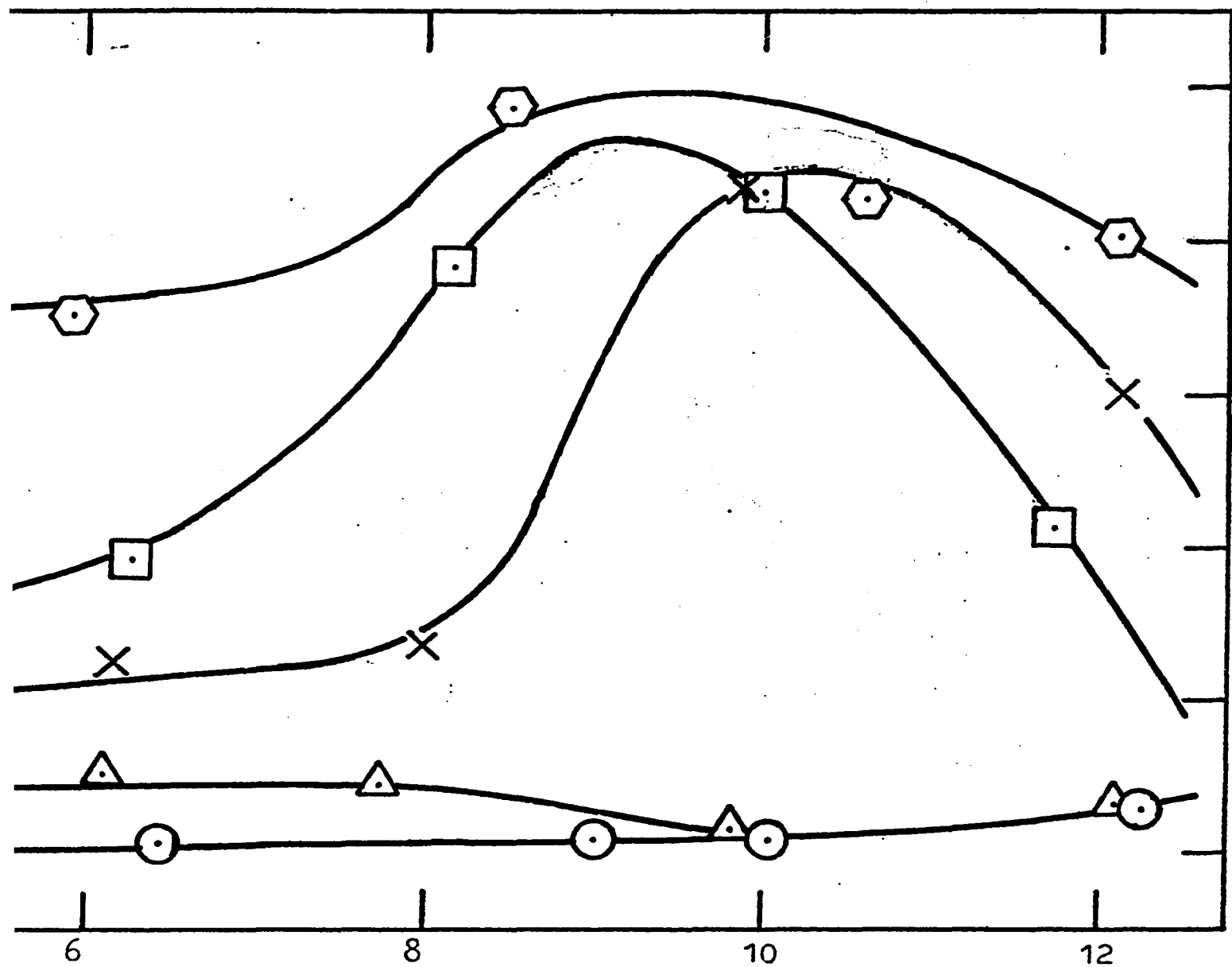
$\bar{5}$M. $\times$ 10^{-4}M.   ⬡ 10^{-3}M.   ☐ 10^{-2}M.

FIGURE   12

FLOATABILITY   AS   A   FUNCTION   OF   AMINE   CONCENTRATION   AND   pH

STARCH: 1000 mg/l

1000 mg/1
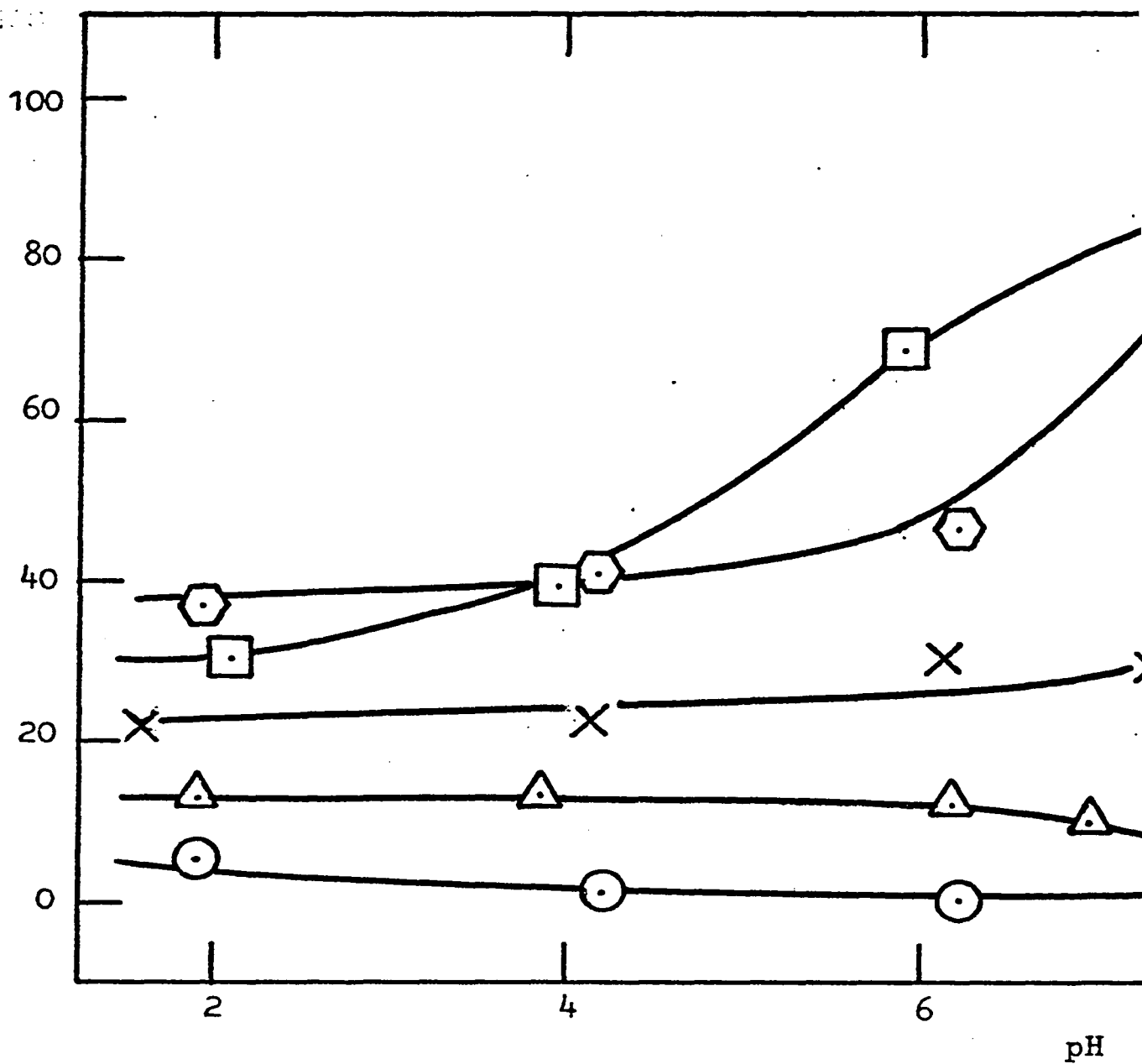
AMINE: ⊙ zero △ 10⁻⁵M. ✕

1000 mg/l STARCH

pH
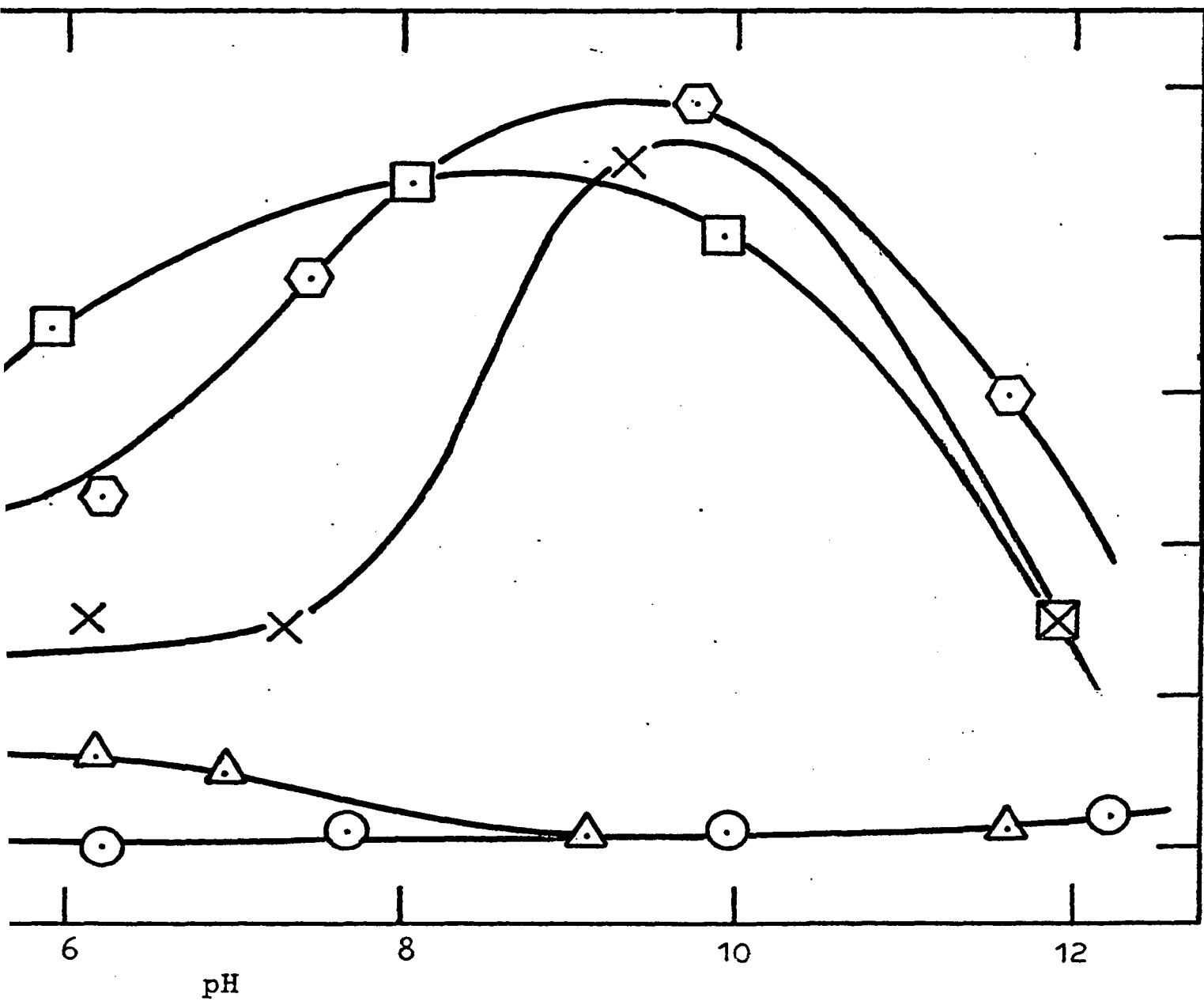
M.   ✕ 10^{-4}M.   ⬡ 10^{-3}M.   ⊡ 10^{-2}M.

FIGURE 13

FLOATABILITY AS A FUNCTION OF STARCH CONCENTRATION AND pH

AMINE: 10^{-5} Mole/l

PERCENTAGE FLOATABILITY

100

80

60

40

20

0

2   4   6   pH

STARCH: ⊙ zero   ⊡ 100 mg/1

AMINE: 10^{-5}M.

pH

☐ 100 mg/l   △ 400 mg/l   ⬡ 1000 mg/l

FIGURE 14

FLOATABILITY AS A FUNCTION OF STARCH CONCENTRATION AND pH
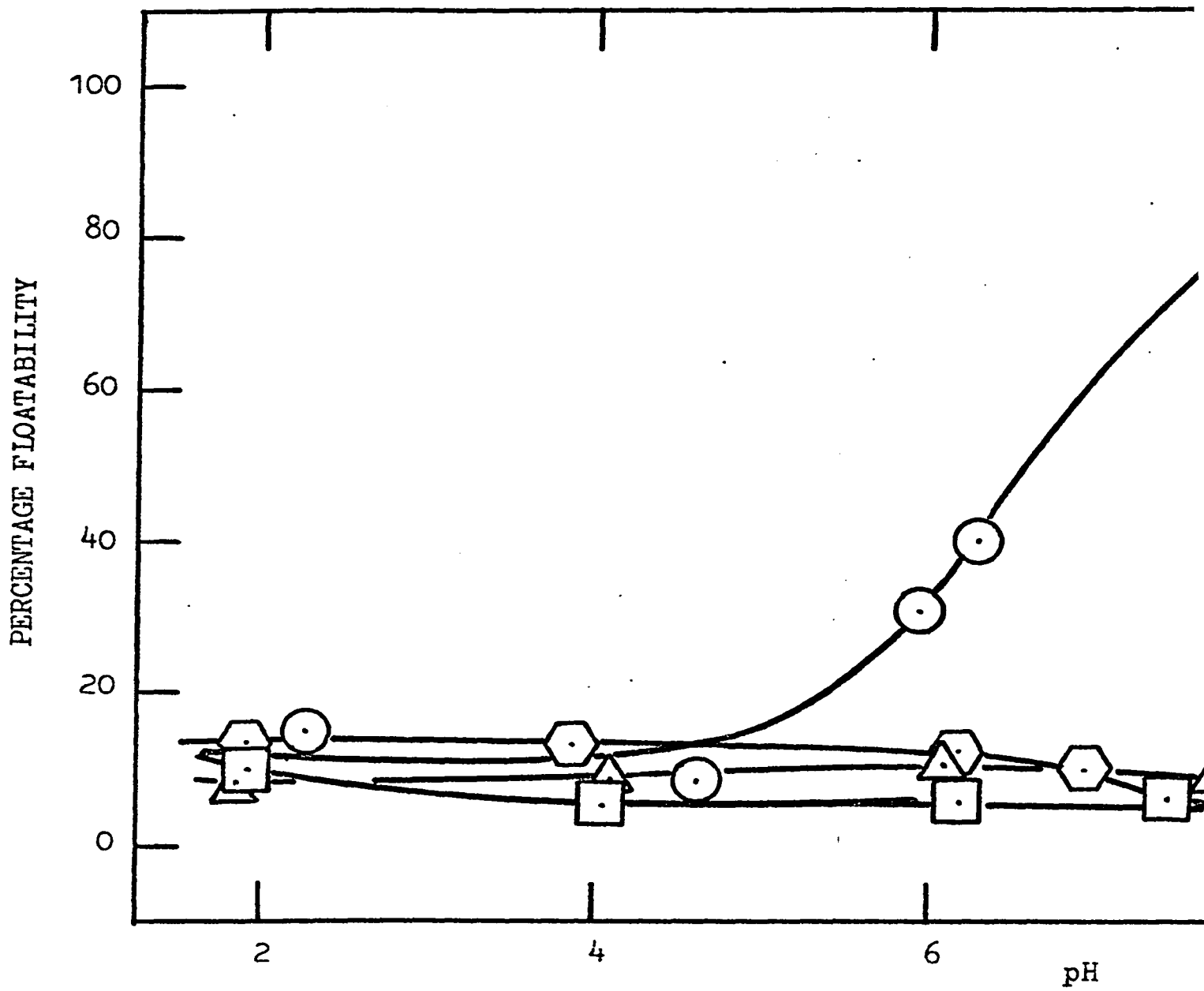
AMINE: 10^{-4} Mole/l
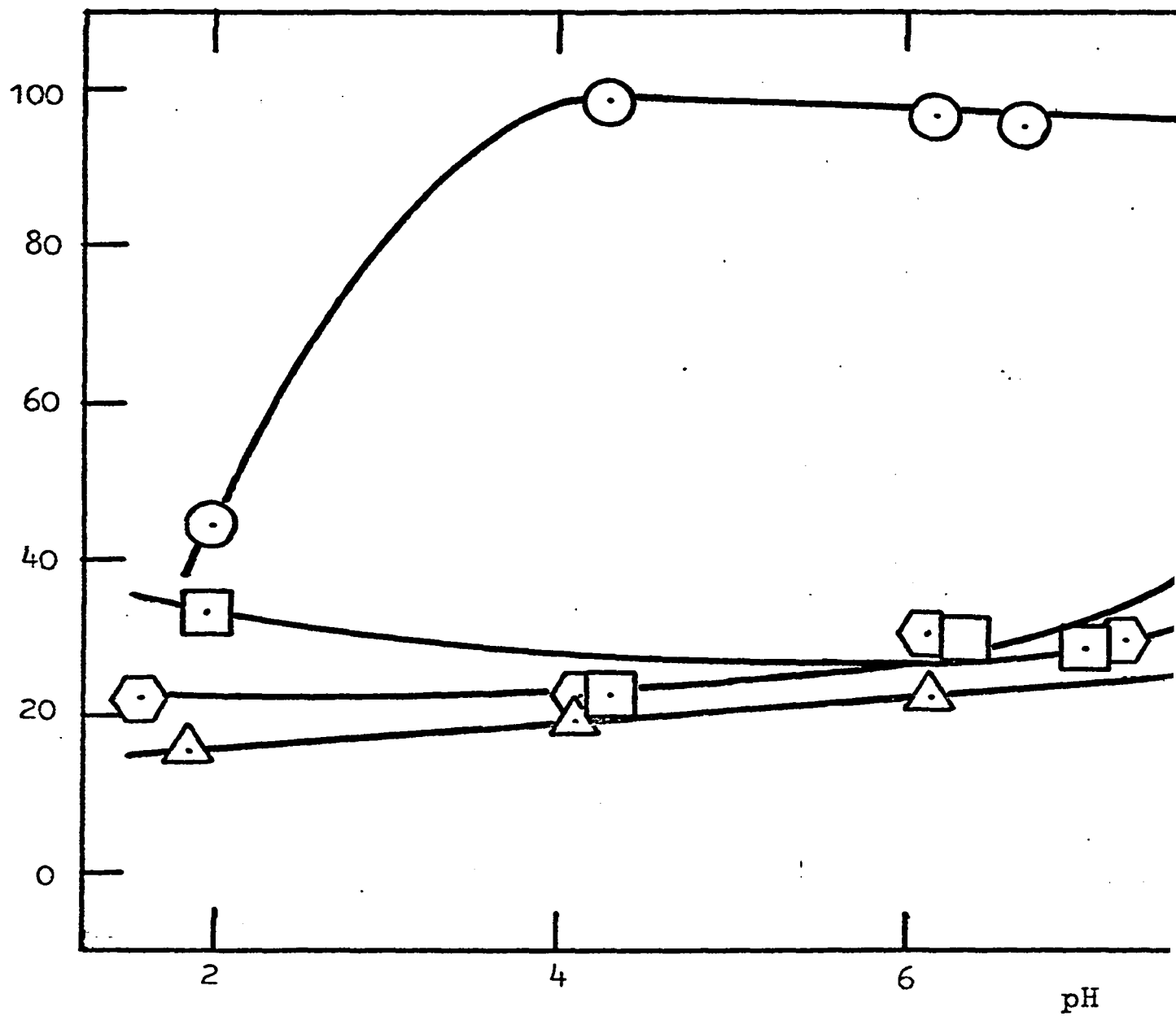
STARCH: ⊙ zero ▢ 100 mg/l

AMINE: 10^{-4}M.

pH

8   10   12
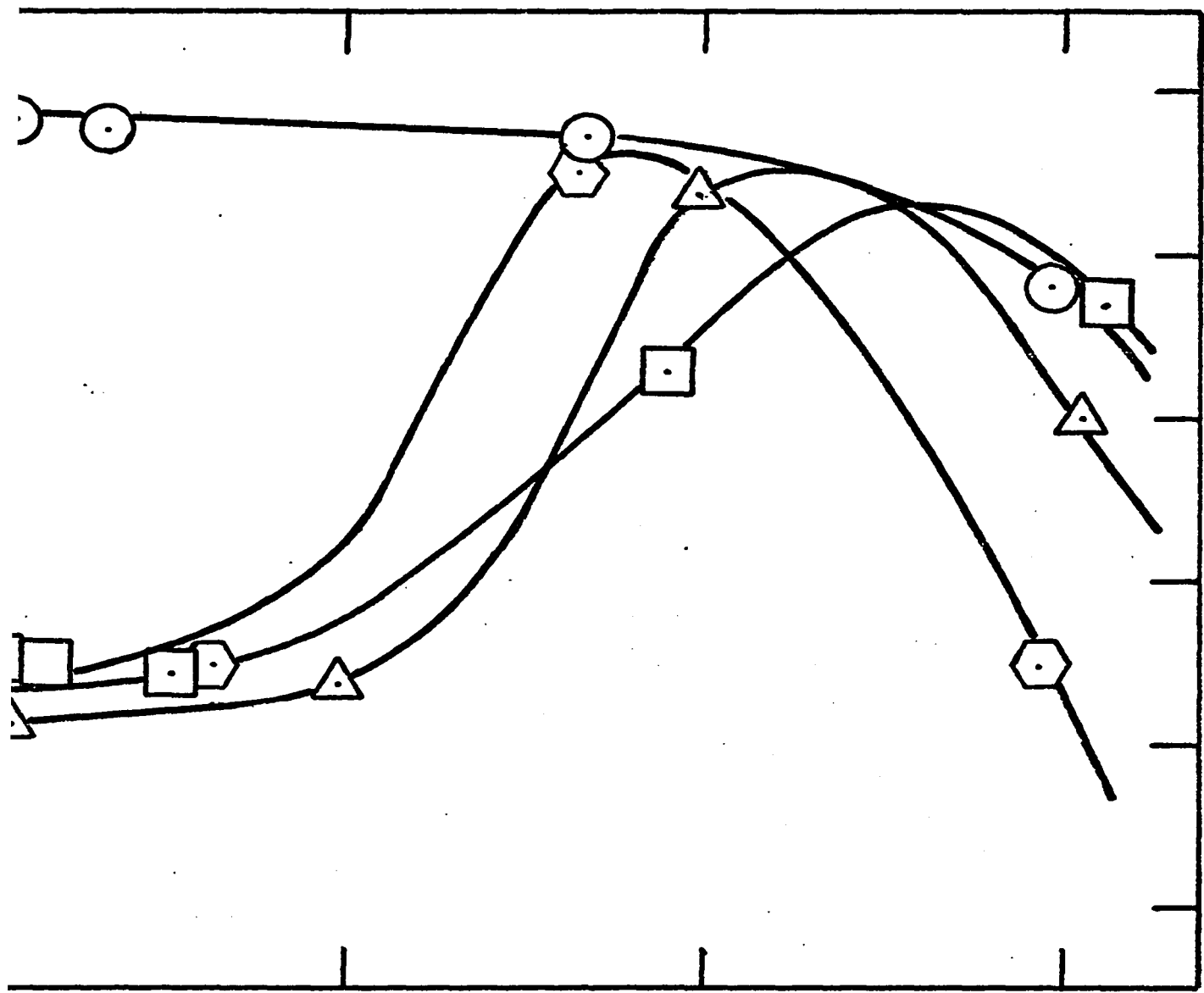
100 mg/l   △ 400 mg/l   ⬡ 1000 mg/l

FIGURE 15

FLOATABILITY AS A FUNCTION OF STARCH CONCENTRATION AND pH

AMINE: 10^{-3} Mole/l

PERCENTAGE FLOATABILITY

STARCH: ⊙ zero ▢ 100 mg/l

pH

AMINE: 10^{-3}M.

pH
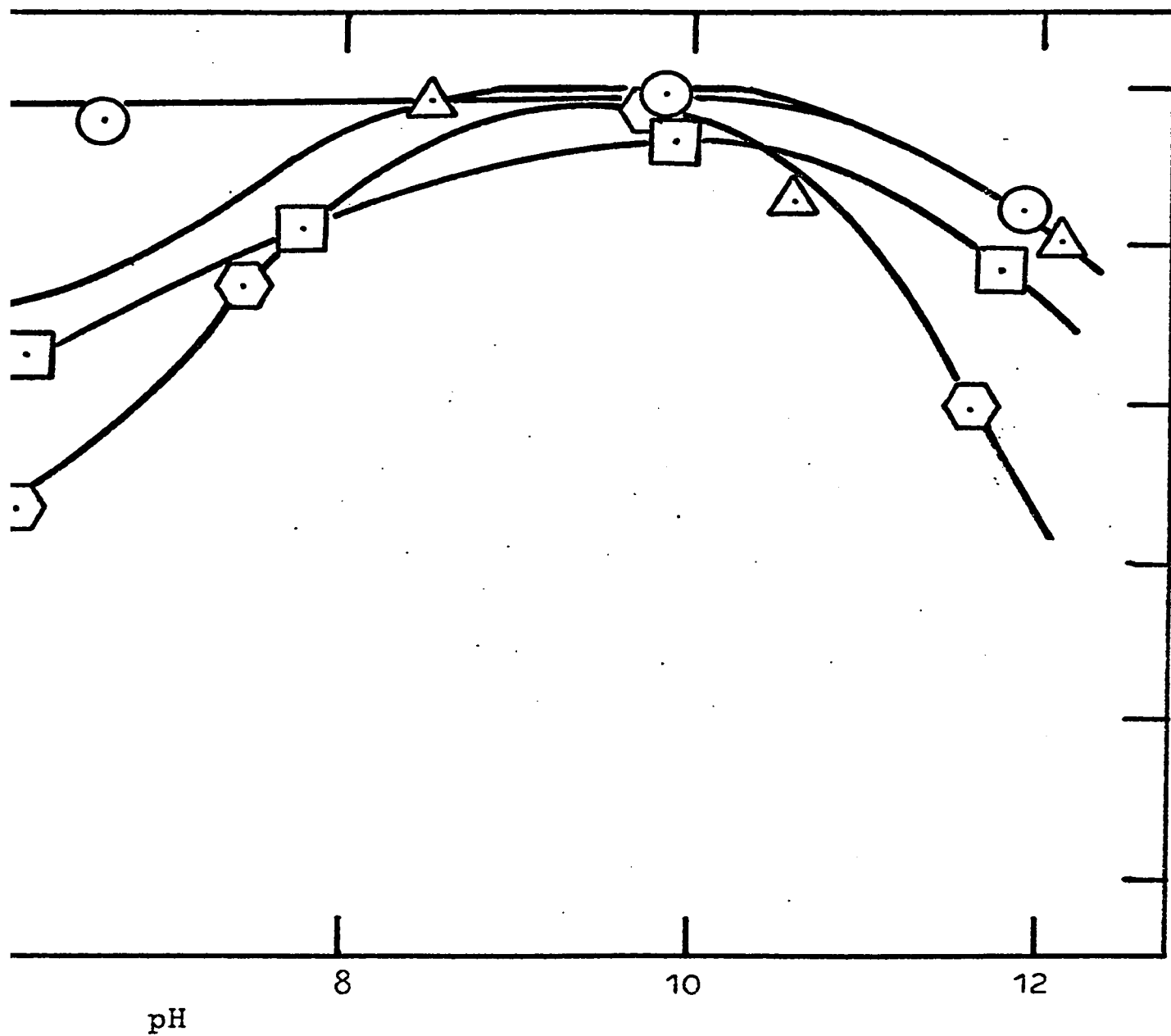
| 100 mg/l | △ 400 mg/l | ⬡ 1000 mg/l |

FIGURE   16

FLOATABILITY   AS   A   FUNCTION   OF   STARCH   CONCENTRATION   AND   pH

AMINE: 10^{-2} Mole/l

AMINE: 10^{-2}M.

pH

8

10

12
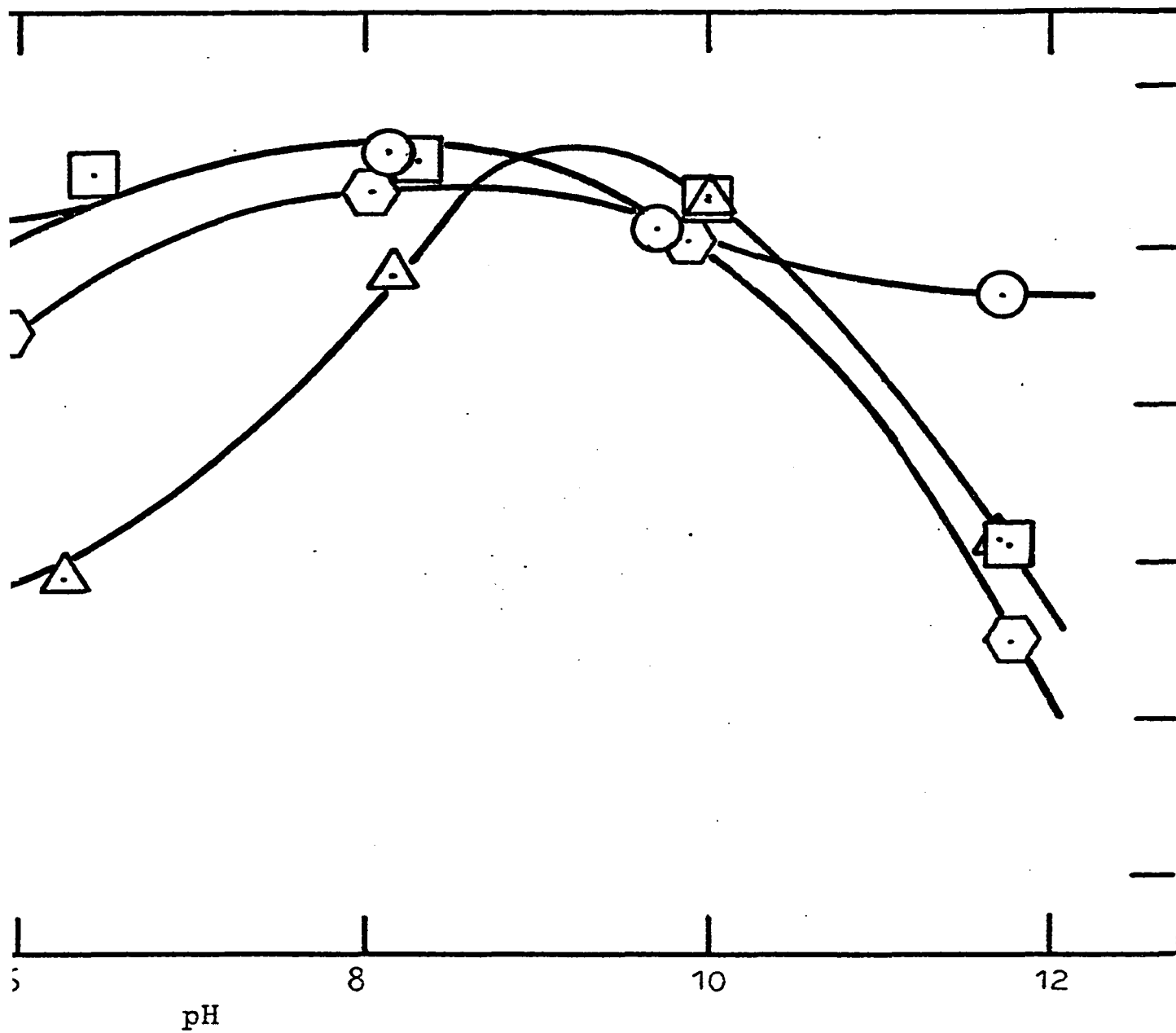
⊡ 100 mg/l △ 400 mg/l ⬡ 1000 mg/l

floatability values than the 10^{-3} molar solution. In the absence of starch, floatability at 10^{-4} molar amine also exceeded that at 10^{-2} (Figure 9).

A secondary rise of floatability was found under conditions of low amine, starch and pH. That is, a recovery minimum was encountered at pH ~4, floatability increasing with decreasing pH below this point for amine concentrations of 10^{-5}M. at zero starch (Figure 9) and both 10^{-4} and 10^{-5}M. amine at 100 mg/l starch (Figure 10). Recovery at 10^{-4}M. amine in the absence of starch was already high in this pH region as an extension of the main peak.

Effective depression was achieved over the entire pH range for 10^{-5}M. amine in the presence of as little as 100 mg/l starch (Figure 10) and, in contrast to all higher amine concentrations, recovery was at a minimum in the alkaline region. The peak recovery always exceeded 85% for the higher amine concentrations at all starch levels, and at zero starch was > 95% for 10^{-3} and 10^{-4}M. amine between pH 4 and 10 (Figure 9).

(b) Adsorption

The adsorption density of the amine (μmole/g hematite) is plotted as a function of pH in Figures 17 - 20. Ignoring the effect of starch, adsorption from initial concentrations of 10^{-5}, 10^{-4} and 10^{-3} molar amine is seen to change little in the acid region but to increase approximately ten-fold for each initial concentration between pH 6 and 10. Another plateau region is found at pH > 10. The curve for the

FIGURE   17

ADSORPTION   OF   AMINE   AS   A   FUNCTION   OF   CONCENTRATION   AND   pH

STARCH: zero

SPECIFIC ADSORPTION: μMole/g

100
30
10
3.0
1.0
0.3
0.1
0.03
0.01

2   4   6

pH

AMINE: △ 10⁻⁵M.   ✕ 10⁻⁴M.   ⟨

STARCH: ZERO

pH
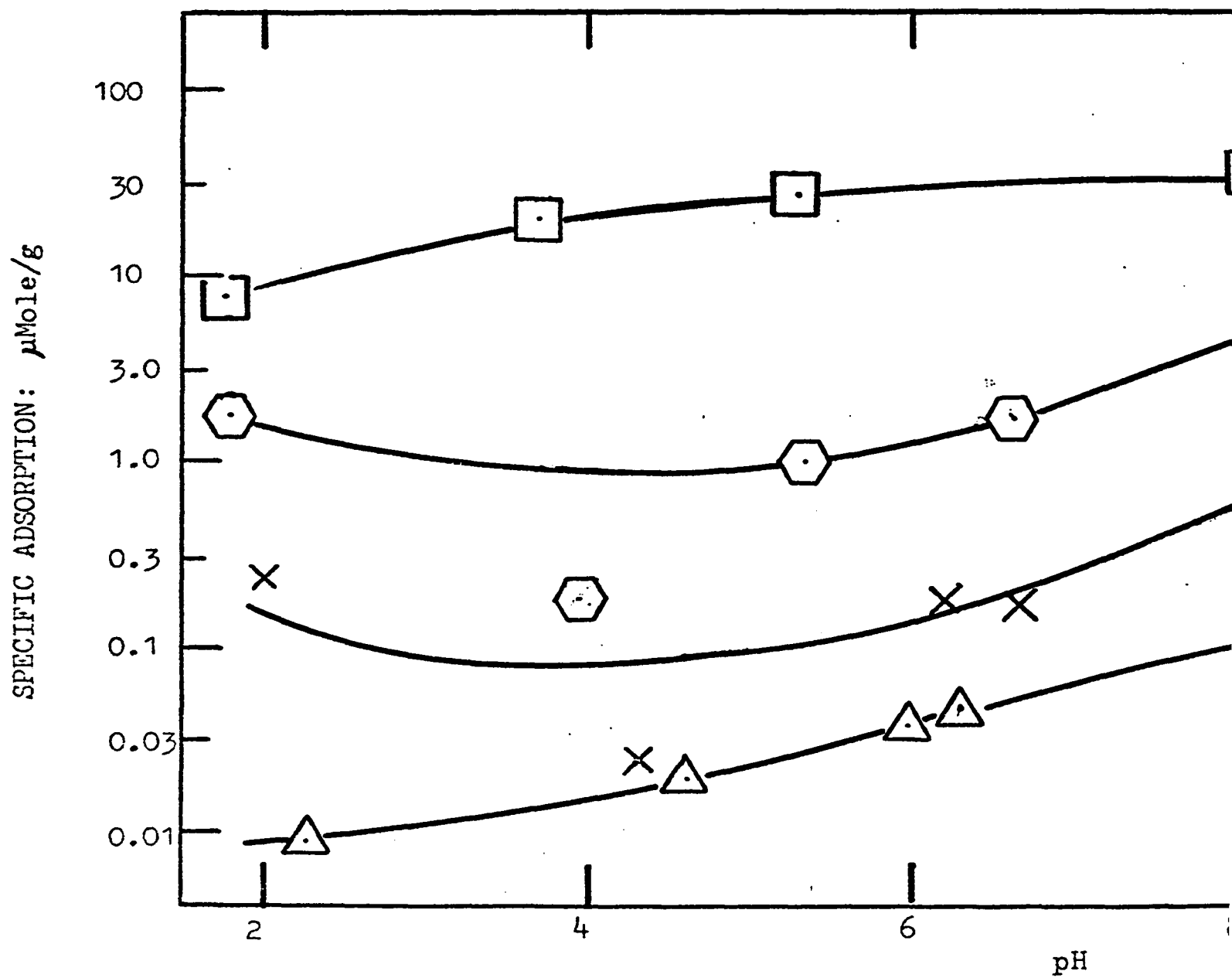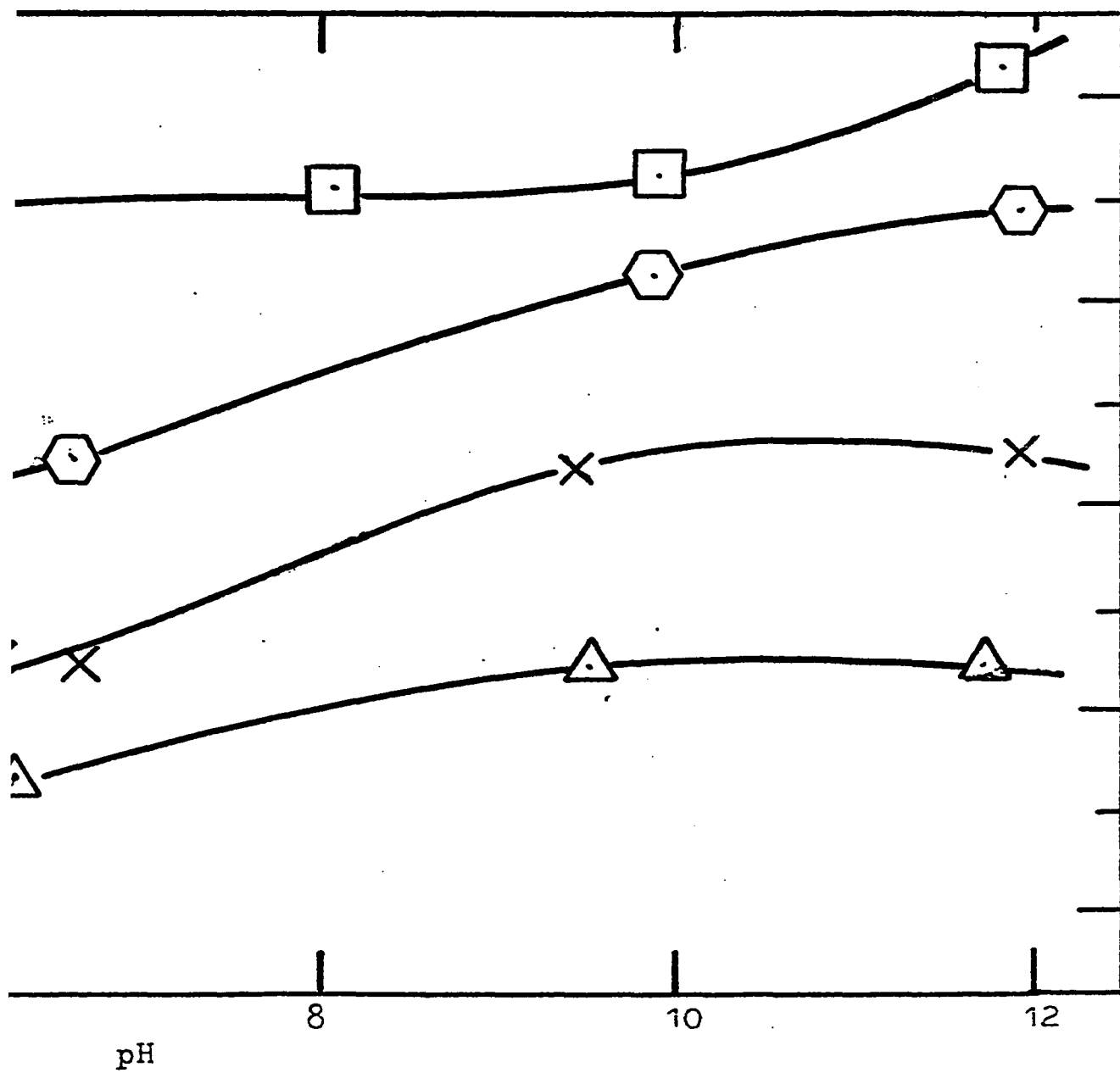
10^{-4}M. ⬡ 10^{-3}M. ☐ 10^{-2}M.

FIGURE   18

ADSORPTION   OF   AMINE   AS   A   FUNCTION   OF   CONCENTRATION   AND   pH

STARCH: 100 mg/1

SPECIFIC ADSORPTION: μMole/g

100
30
10
3.0
1.0
0.3
0.1
0.03
0.01

pH

2   4   6
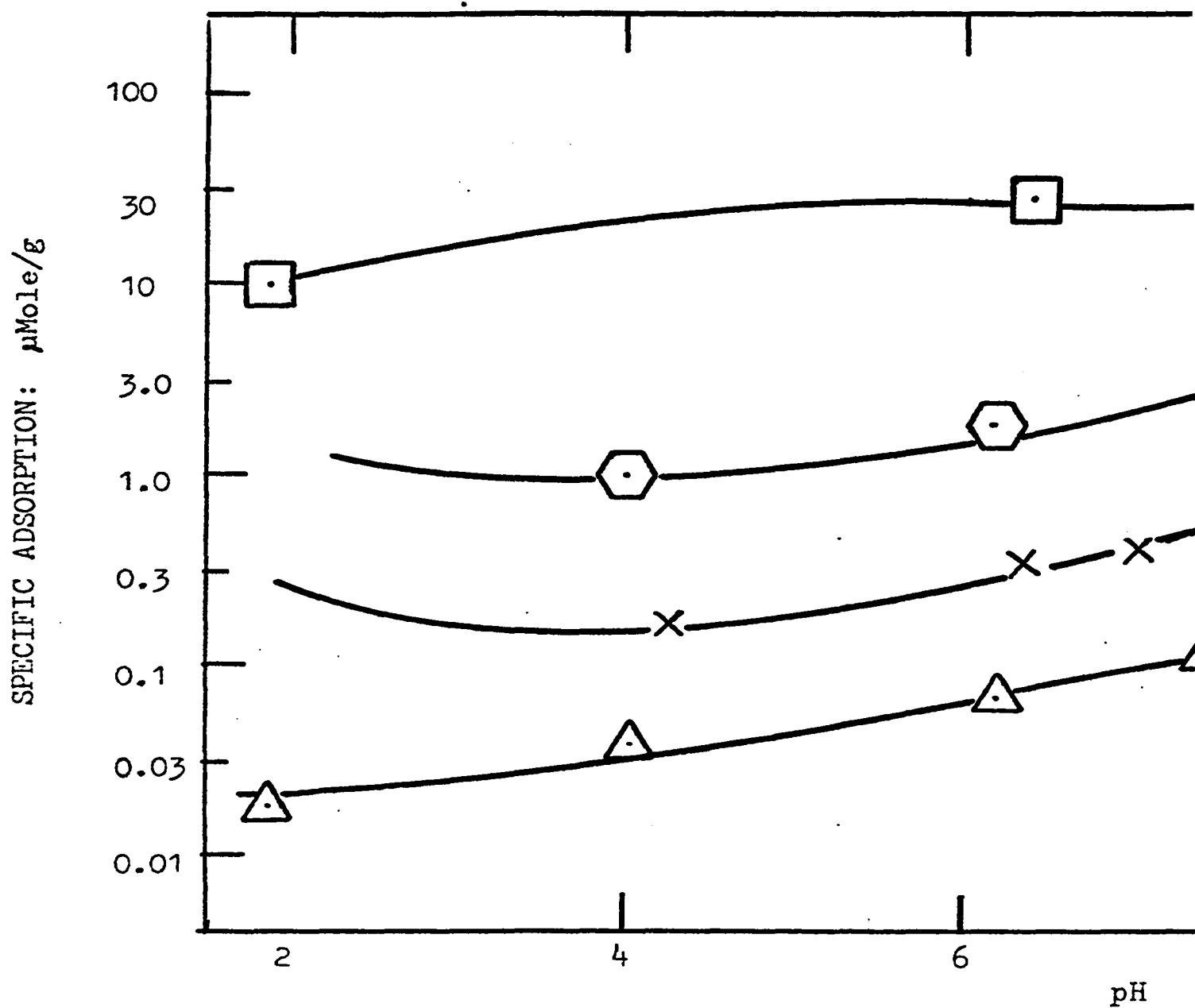
AMINE: △ 10⁻⁵M.   ✕ 10⁻⁴M.

STARCH: 100 mg/l

pH
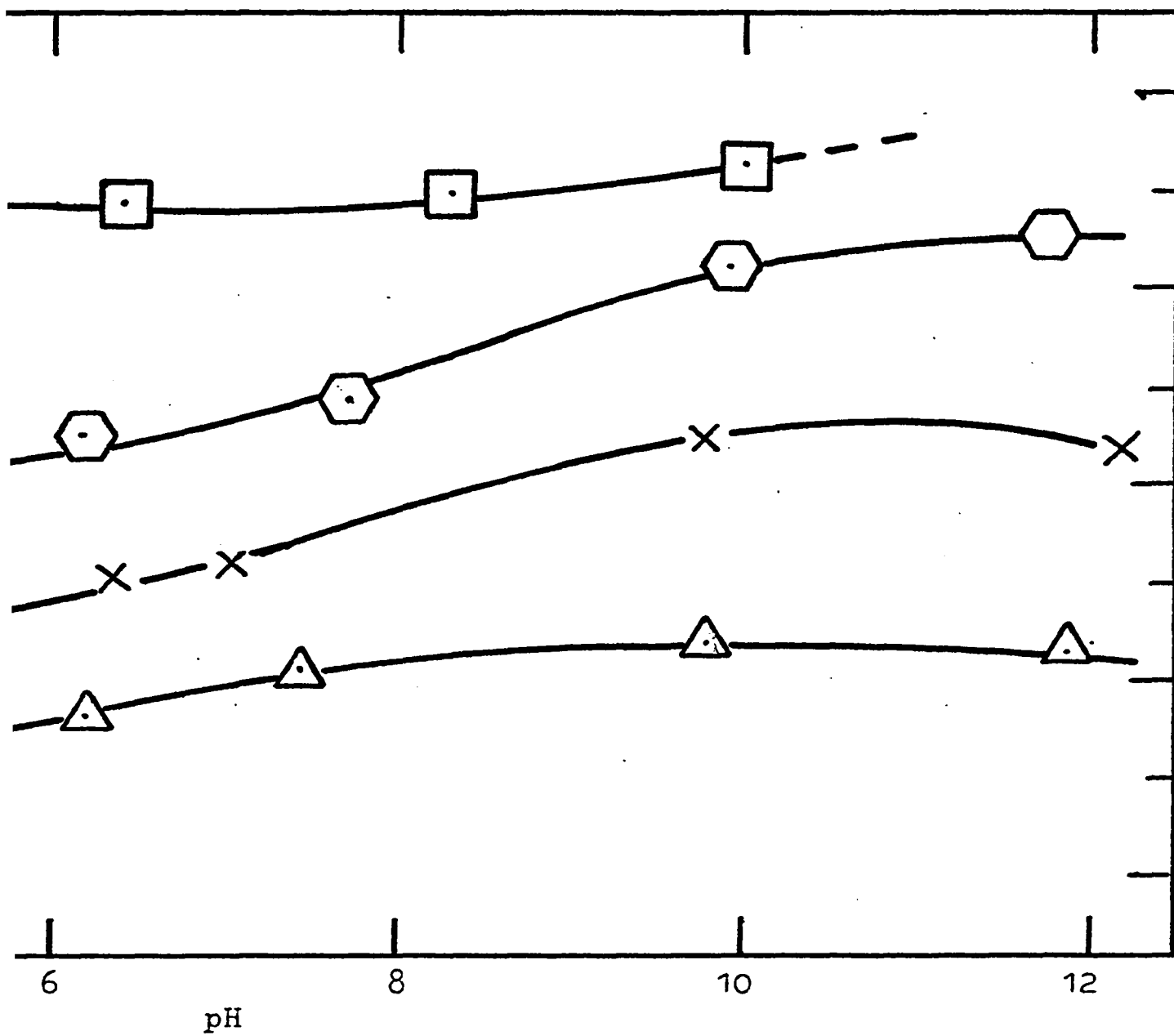
$\times$ 10^{-4}M.   ⬡ 10^{-3}M.   ▢ 10^{-2}M.

FIGURE   19

ADSORPTION   OF   AMINE   AS   A   FUNCTION   OF   CONCENTRATION   AND   pH

STARCH: 400 mg/l

SPECIFIC ADSORPTION: μMole/g

100
30
10
3.0
1.0
0.3
0.1
0.03
0.01

2   4   6

pH
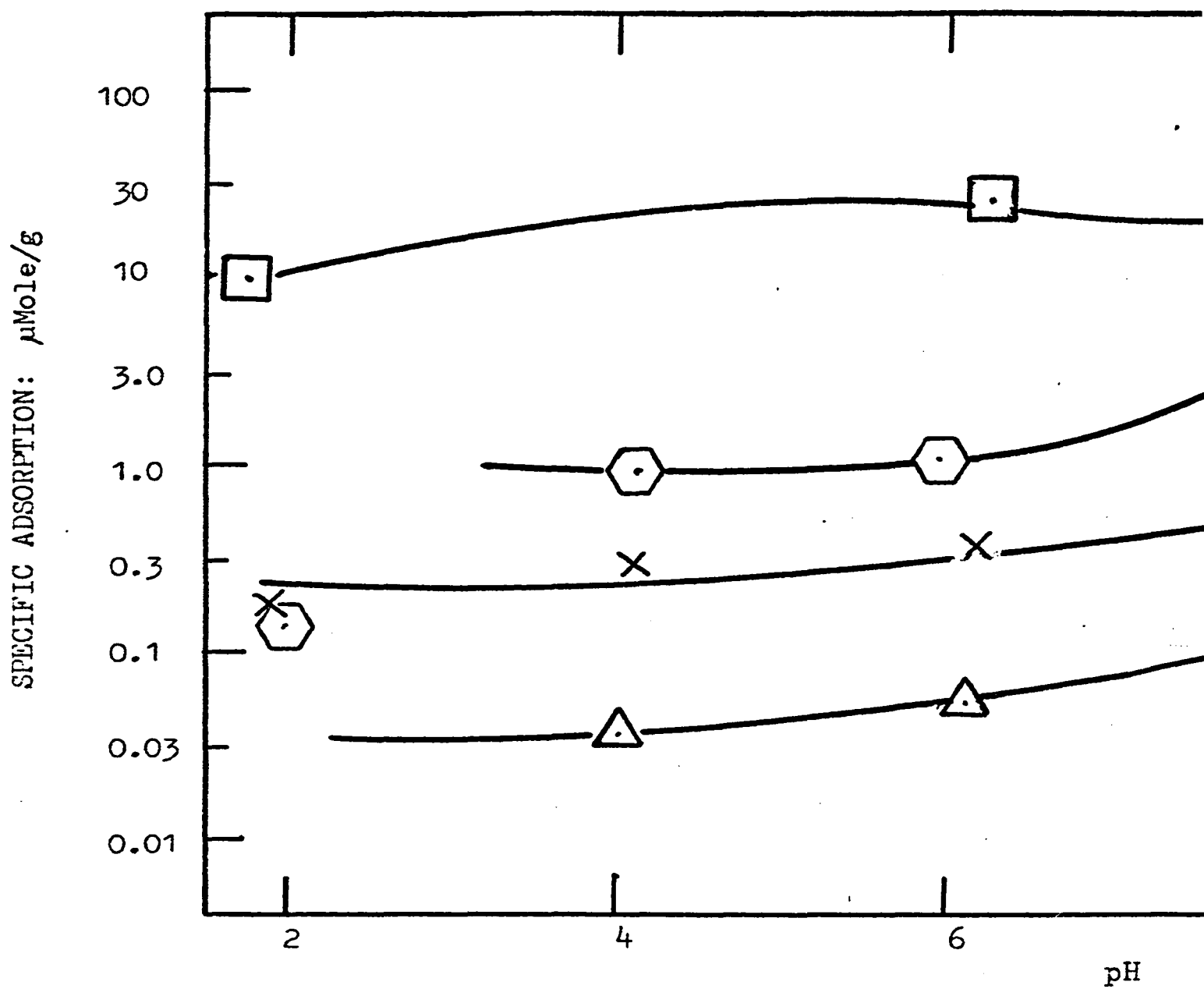
AMINE: △ 10^{-5}M.   ✕ 10^{-4}M.

STARCH: 400 mg/l

pH
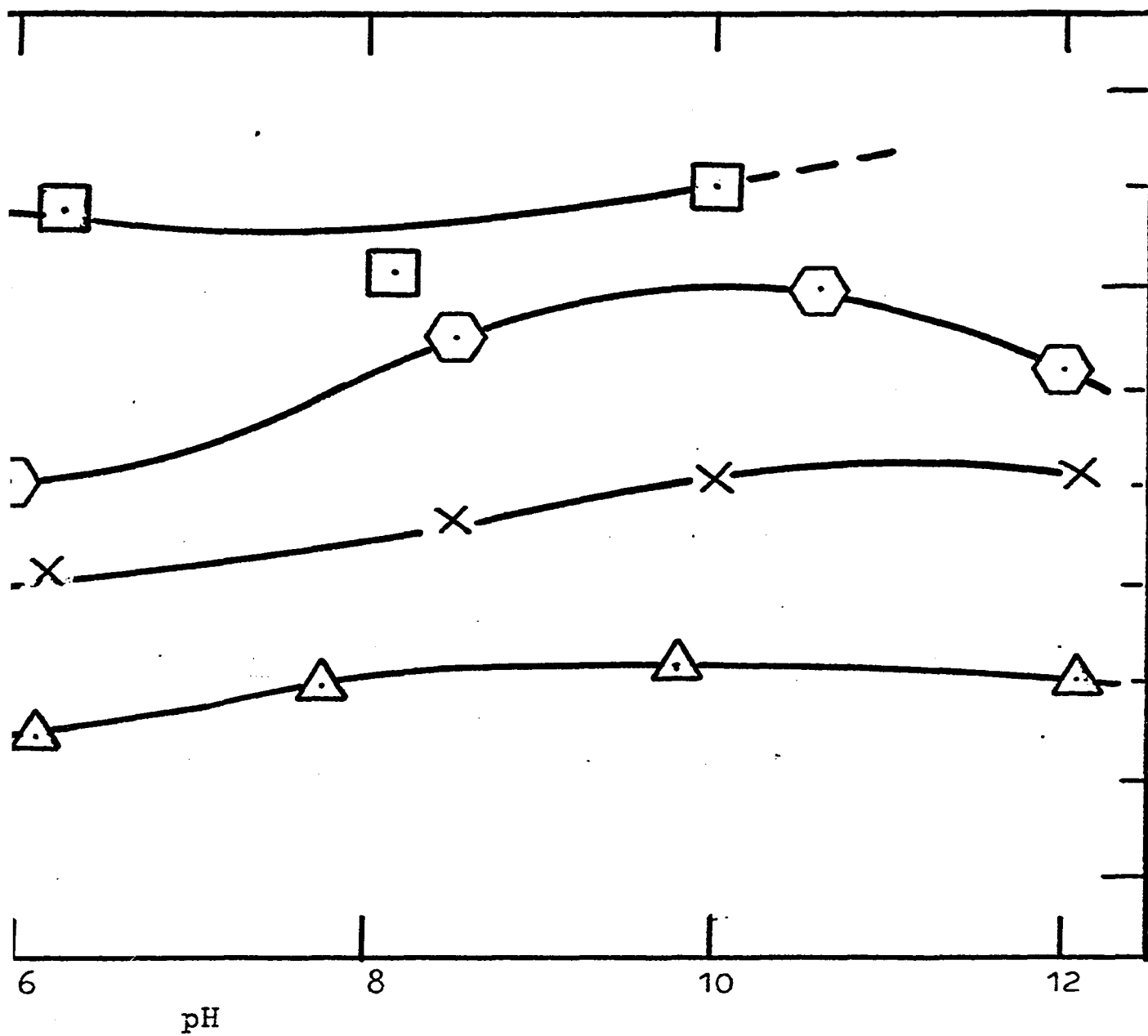
$\langle$ 10^{-4} M. $\langle\hexagon\rangle$ 10^{-3} M. $\square$ 10^{-2} M.

FIGURE 20

ADSORPTION OF AMINE AS A FUNCTION OF CONCENTRATION AND pH

STARCH: 1000 mg/l

STARCH: 1000 mg/1

pH
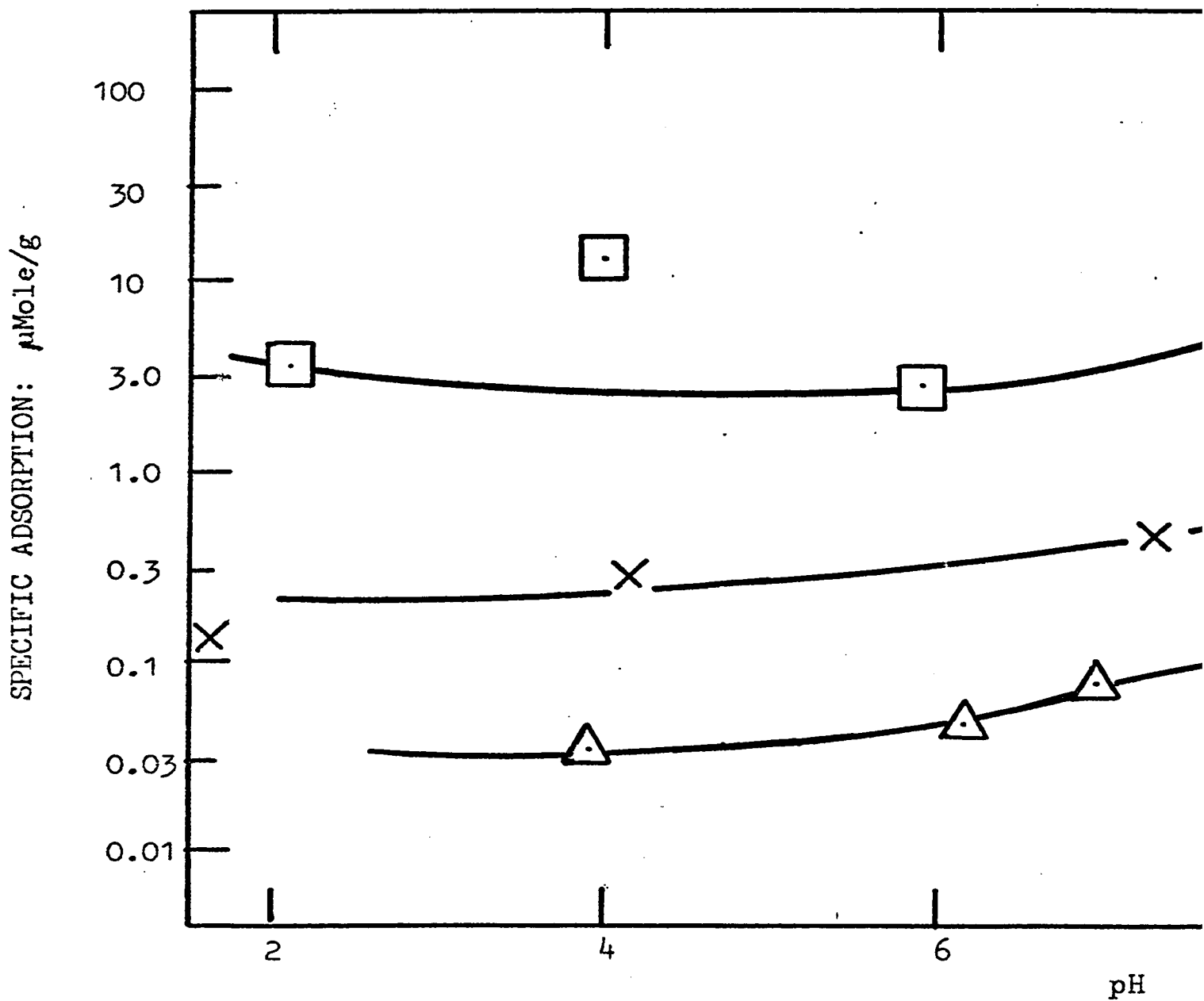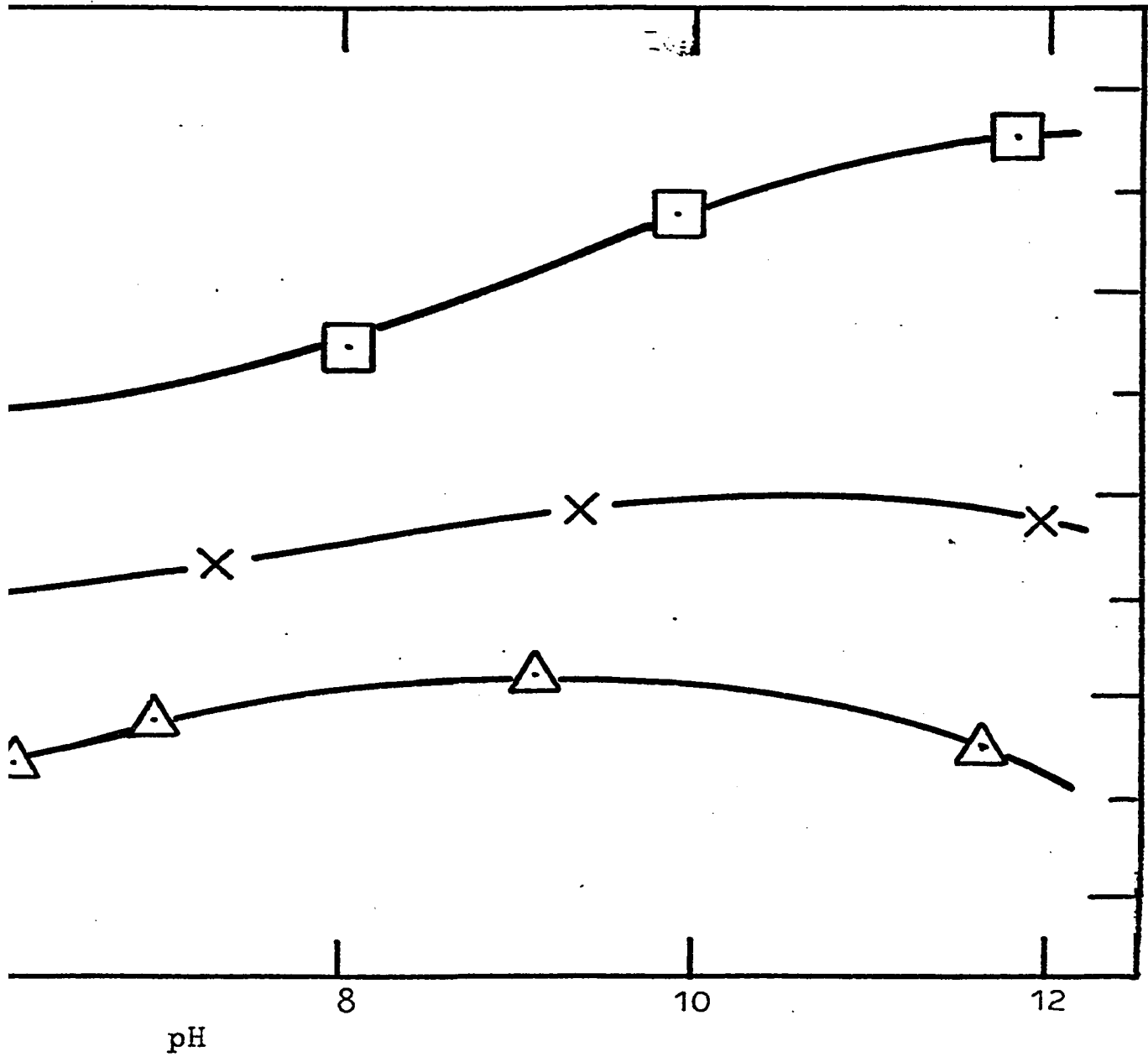
$\times$ 10^{-4}M. $\boxdot$ 10^{-2}M.

10^{-2} molar solution is anomalous in that an increase in adsorption is observed at pH < 5 and > 10, with little change in near-neutral solutions.

The effect of starch depends on pH. In the acid region amine adsorption increases with starch concentration, the effect being most marked at low amine concentrations and the rate of increase decreasing with increasing starch.

Little effect is observed in the pH region 7 - 9 but at higher pH the effect of starch is reversed. In strongly alkaline solution amine adsorption is found to decrease with starch concentration. The effect is most evident with solutions of high amine concentration and the rate of change increases with increasing starch.

The 10^{-2} molar amine solution is again anomalous, being little affected by starch except at a starch concentration of 1000 mg/l. At pH 5, the adsorption density of amine dropped from 30 to 3 µmole/g on increasing starch concentration from 400 to 1000 mg/l.

Starch adsorption was found to be low and of the same order as experimental fluctuations. The effect of pH, if any, was masked by this fluctuation. By averaging the results for each combination of concentrations (i.e. ignoring pH differences), the relationship between starch adsorption density and concentration was determined at each amine concentration (Figure 21). Similarly, the effect of amine concentration on starch adsorption was determined and is shown in Figure 22.

FIGURE 21

ADSORPTION OF STARCH AS A FUNCTION OF STARCH CONCENTRATION

ADSORPTION DENSITY, mg/g

STARCH CONCENTRATION
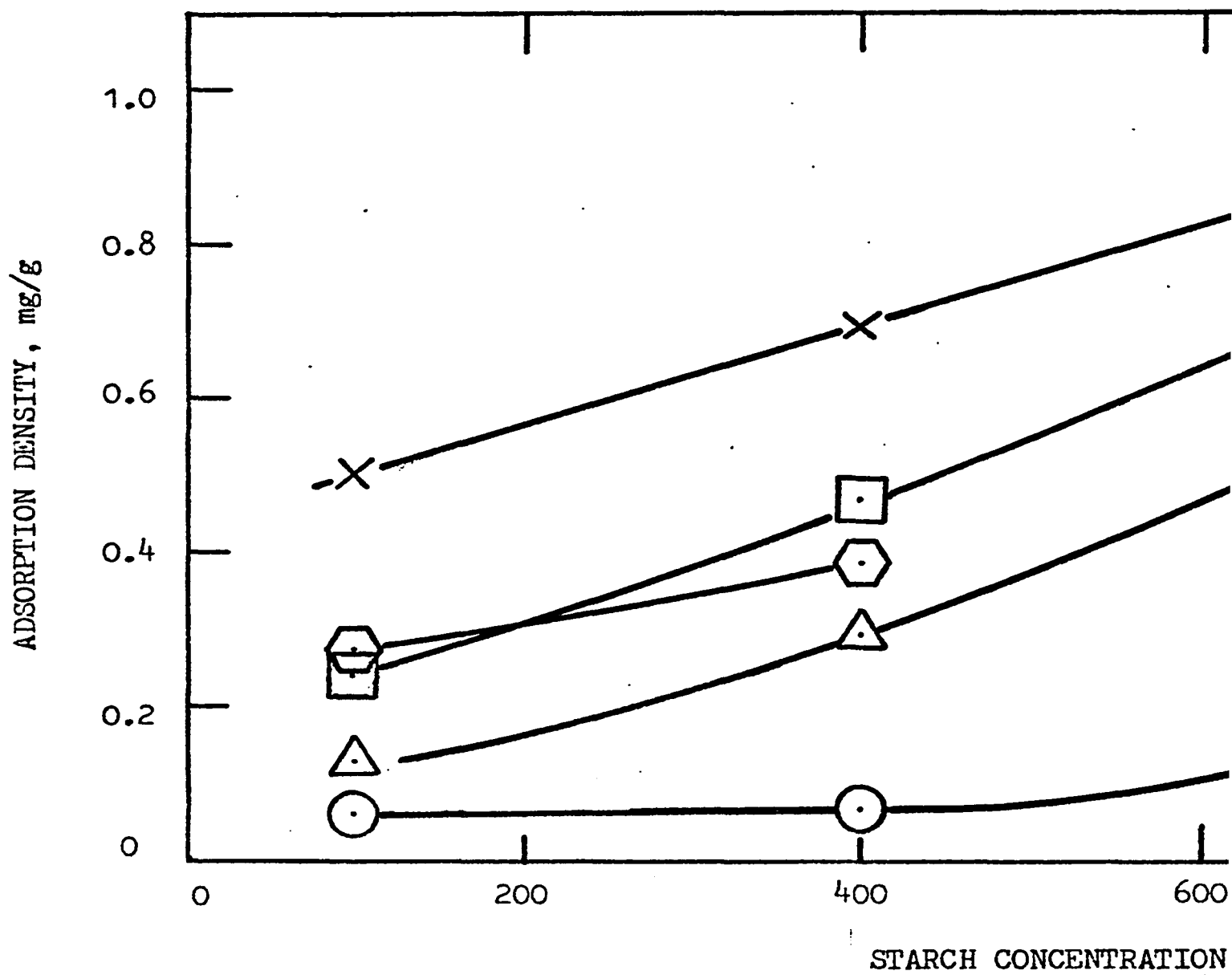
AMINE: ⊙ zero △ 10^{-5}M. ✕ 10^{-4}M.
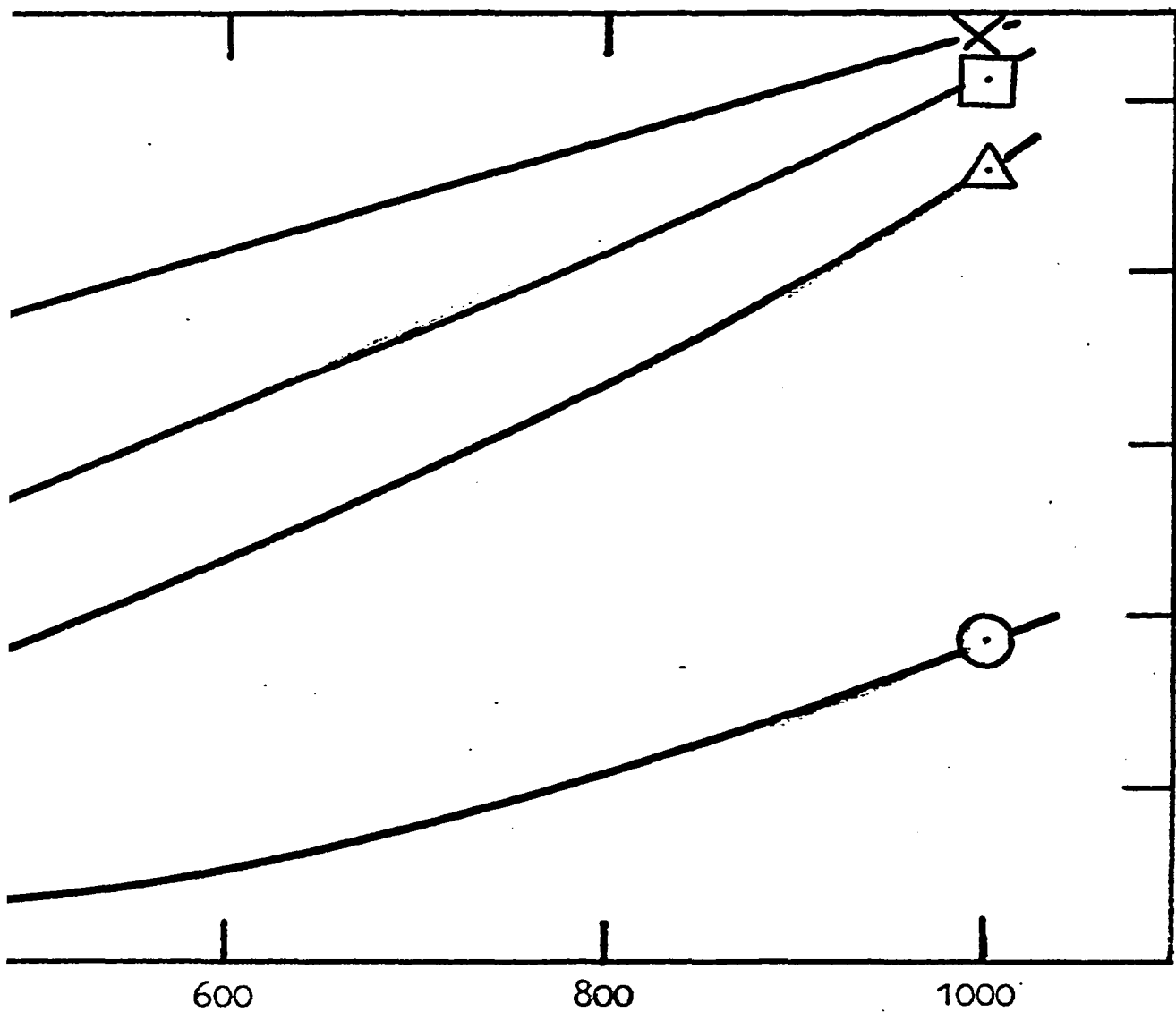
CONCENTRATION   mg/1

$\times$ 10^{-4}M.   ⬡· 10^{-3}M.   ☐· 10^{-2}M.

FIGURE 22

ADSORPTION OF STARCH AS A FUNCTION OF AMINE CONCENTRATION
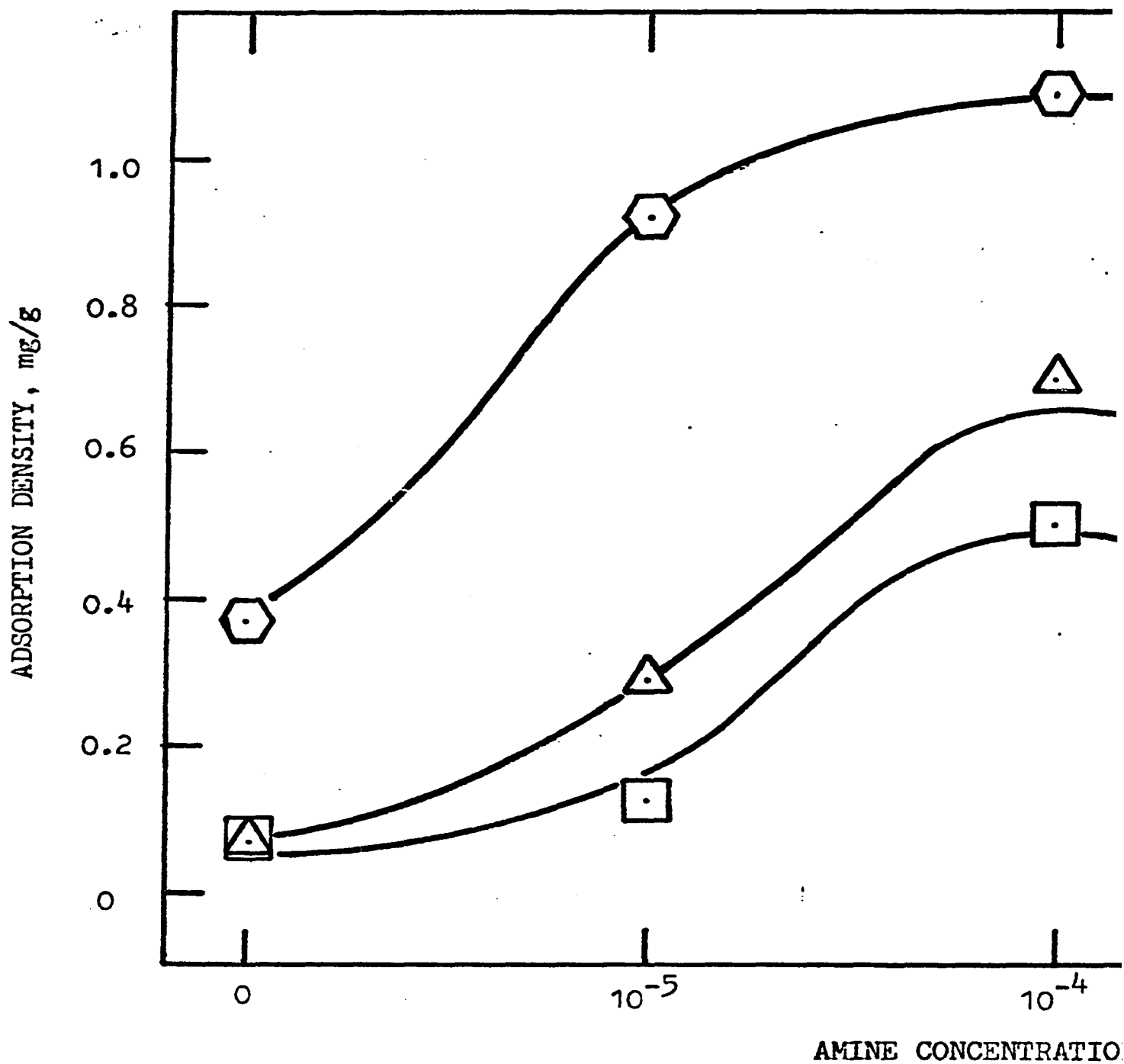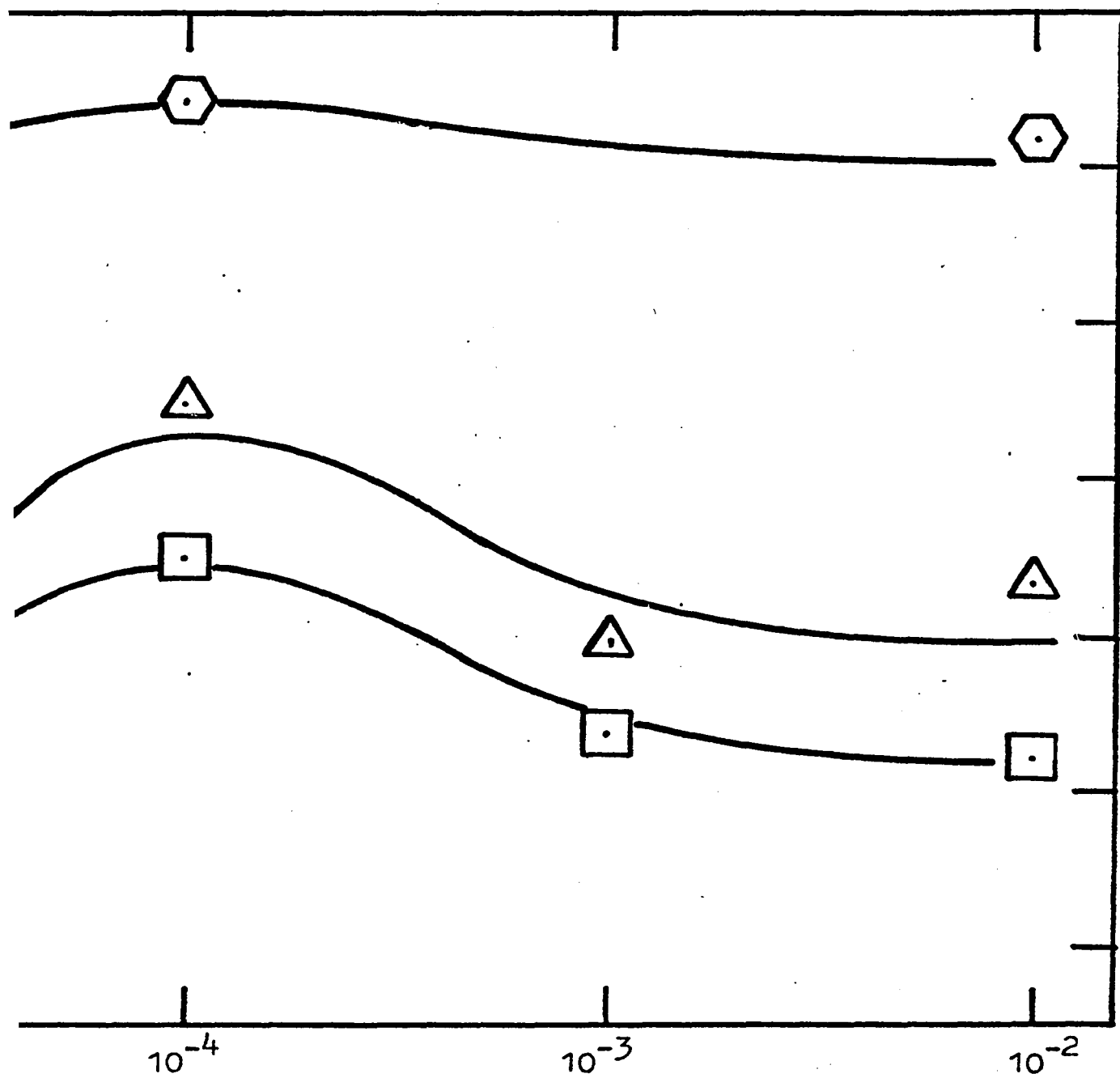
CONCENTRATION, Mole/l

△ 400 mg/l   ⬡ 1000 mg/l

(c) <u>Solubility</u>

As can be seen from the results, Table 14, starch gave no
apparent change in the pH at which precipitation was first observed.
The higher amine concentrations gave a readily detected precipitation
point but at 10^{-4}M. amine the beam was relatively difficult to detect.
No scattering was observed with the 10^{-5}M. amine solution. The observed
points, shown as $\odot$ in Figure 2, were at slightly lower pH than the
theoretical levels.

Subjectively, it was noted that the free amine suspension
increased in density at higher pH levels in the absence of starch. With
starch present a maximum density was observed at pH ~ 11, the density
decreasing at higher pH levels. The effect was most evident at high
starch/amine ratios.

Complete results are given in Tables 3 - 13 (Flotation and
Adsorption) and Table 14 (Solubility).

VII. DISCUSSION

It is necessary to consider the significance and possible mechanisms of the following observed phenomena:

(i)   The form of the adsorption curves of amine and starch.

(ii)   Mutual adsorption effects of amine and starch.

(iii)   The form of the flotation curves and the effect of starch.

(iv)   The low-pH float achieved with acetic acid.

(v)   The secondary flotation peak at low amine - starch - pH conditions.

(i) ADSORPTION

(a) Amine

Several mechanisms have been proposed to explain amine adsorption[80]. The coincidence between the pH at which a marked increase in adsorption occurs and the zero point of charge is probably fortuitous. Solution conditions are considered more important than surface potential in controlling adsorption[81, 82].

At pH levels below the z.p.c. (pH ~ 8), hematite is positively charged and possible adsorption mechanisms are:

1. Exchange of RNH_3^+ for H^+ from the inner layer or from the diffuse layer.

2. Formation of oxyamine compounds with OH^- in the diffuse layer, e.g. $OH^- + RNH_3^+ \rightleftharpoons OH_3NR^- + H^+$ ...23
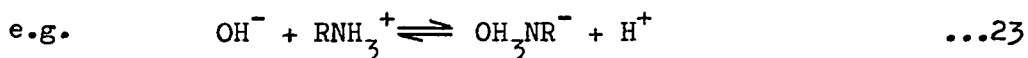
or,   3. Specific adsorption of un-ionized amine in the Stern layer.

At higher pH levels, the same reactions may occur, or:

4. RNH_3^+ may adsorb directly at the surface, thus reducing the net negative charge.

Reactions 1., 2. and 3. result in the liberation of H^+ into bulk solution but no corresponding consistent pH decrease was observed in practice (Tables 3 - 14). Reaction 3. is unlikely in acid solution due to the high degree of ionization (Figure 2) although any adsorbed RNH_2 will be replaced immediately to restore equilibrium. The rapid increase in adsorption initiated at pH ~ 7 may be attributed to the concentration of RNH_2 becoming significant (Figure 2).

The total charge in the double layer, σ_d, is given by the Gouy-Chapman equation[83]:

$$\sigma_d = - \sqrt{\frac{DkTn}{2\pi}} \cdot \sinh\left(\frac{ze\psi_o}{2kT}\right) \qquad ...24$$

The symbols are as defined on p. 7.

Morrow[84] showed that, by assuming OH^- and H^+ to be the potential determining ions and RNH_3^+ to be the adsorbing species, the equation at constant pH simplifies to

$$\sigma_d = K\sqrt{n} \qquad ...25$$

where K is a constant. Further, by assuming n is equal to the

concentration of the amine salt (C) and that the ions adsorb only in the diffuse layer,

$$\Gamma_{RNH_3^+} = K\sqrt{C} \quad . \qquad \qquad ...26$$

This relationship was verified experimentally for adsorption from dilute solutions onto quartz[85] but Morrow found Γ to vary approximately as $C^{0.6}$ for adsorption onto hematite and the gradient to increase sharply to 1.16 at amine concentrations greater than $10^{-3}M$.

These results can be explained by assuming a dual adsorption mechanism, the adsorption of RNH_3^+ into the diffuse layer being supplemented by RNH_2 adsorption or RNH_3^+ chemisorption at the solid surface. The last two mechanisms are indistinguishable and, in cases of low surface coverage and dilute solutions, will conform to the Langmuir adsorption conditions (p. 12). Hence

$$\Gamma_m = K'c_m \qquad \qquad ...27$$

where Γ_m is the adsorption density of chemisorbed ions and adsorbed molecules at the surface, K' is a constant and c_m is the concentration of free amine in solution. Therefore

$$\Gamma_{total} = K\sqrt{C} + K'c_m \qquad \qquad ...28$$

$$= K\sqrt{C} + K''C \qquad \qquad ...29$$

since c_m is related to C by the dissociation equation (Equation 12, p. 17).

The sharp increase in the gradient of the log Γ - log C plot

observed at the higher concentrations has been attributed to micelle formation. The phenomenon is the result of Van der Waals' forces between hydrocarbon chains which become significant at concentrations significantly below saturation. The resultant attraction gives rise to aggregations of molecules into spherical or plate-like groups in solution[86] or planar 'hemi-micelles' at a solid surface[61]. For dodecylamine at natural pH the critical micelle concentration in bulk solution is 0.015 M.[87]. This concentration is readily exceeded in the compacted double-layer even when the bulk solution concentration is appreciably lower[61].

In this study the experiments were not designed to yield adsorption isotherms. However, by interpolation from the Γ - pH curves four points on the isotherm can be derived for any chosen pH. This has been done for all starch concentrations at pH 2, 7 and 12 and the results plotted in Figures 23 - 25. Insufficient points are available for much reliance to be placed on the graphs. Nevertheless, several points of interest are evident. At pH 7 (Figure 24) the best fit Freundlich lines are strikingly similar to the results of Morrow. At low concentrations (<0.5 mM. amine) the gradient is 0.6 (i.e. $\Gamma = KC^{0.6}$) and no significant change is effected by starch addition. At higher concentrations the gradient increases to 1.2 in the absence of starch. The effect of starch is to reduce the gradient, 1000 mg/l restoring its value to 0.6 .

At pH 2 (Figure 23) no inflection is evident but the gradient over the entire concentration range decreases from 0.96 at zero starch to 0.7 with 1000 mg/l starch. Separation of free amine at pH 12 (Figure 25)

FIGURE 23

AMINE ADSORPTION AS A FUNCTION OF CONCENTRATION

pH 2

pH 2
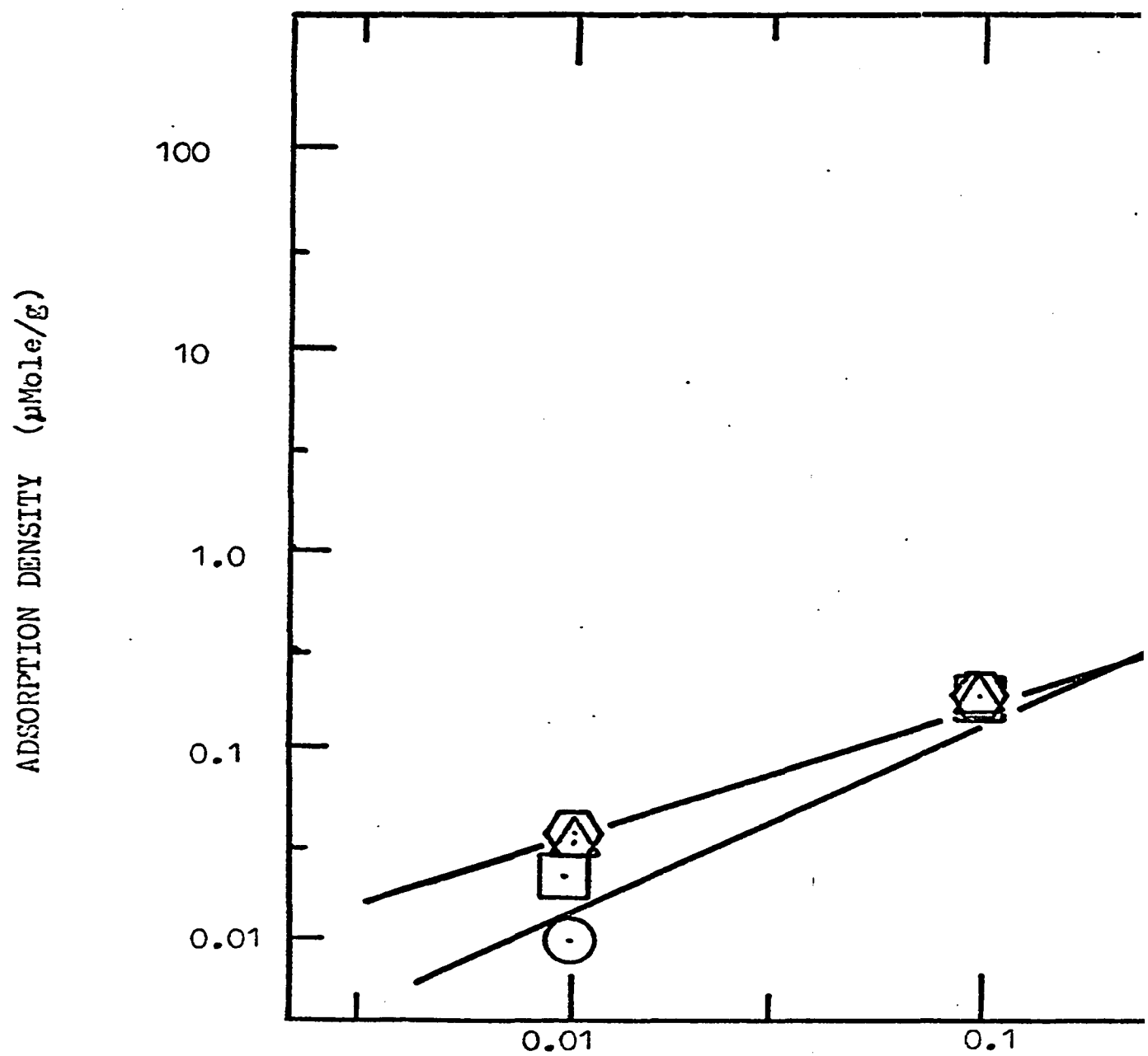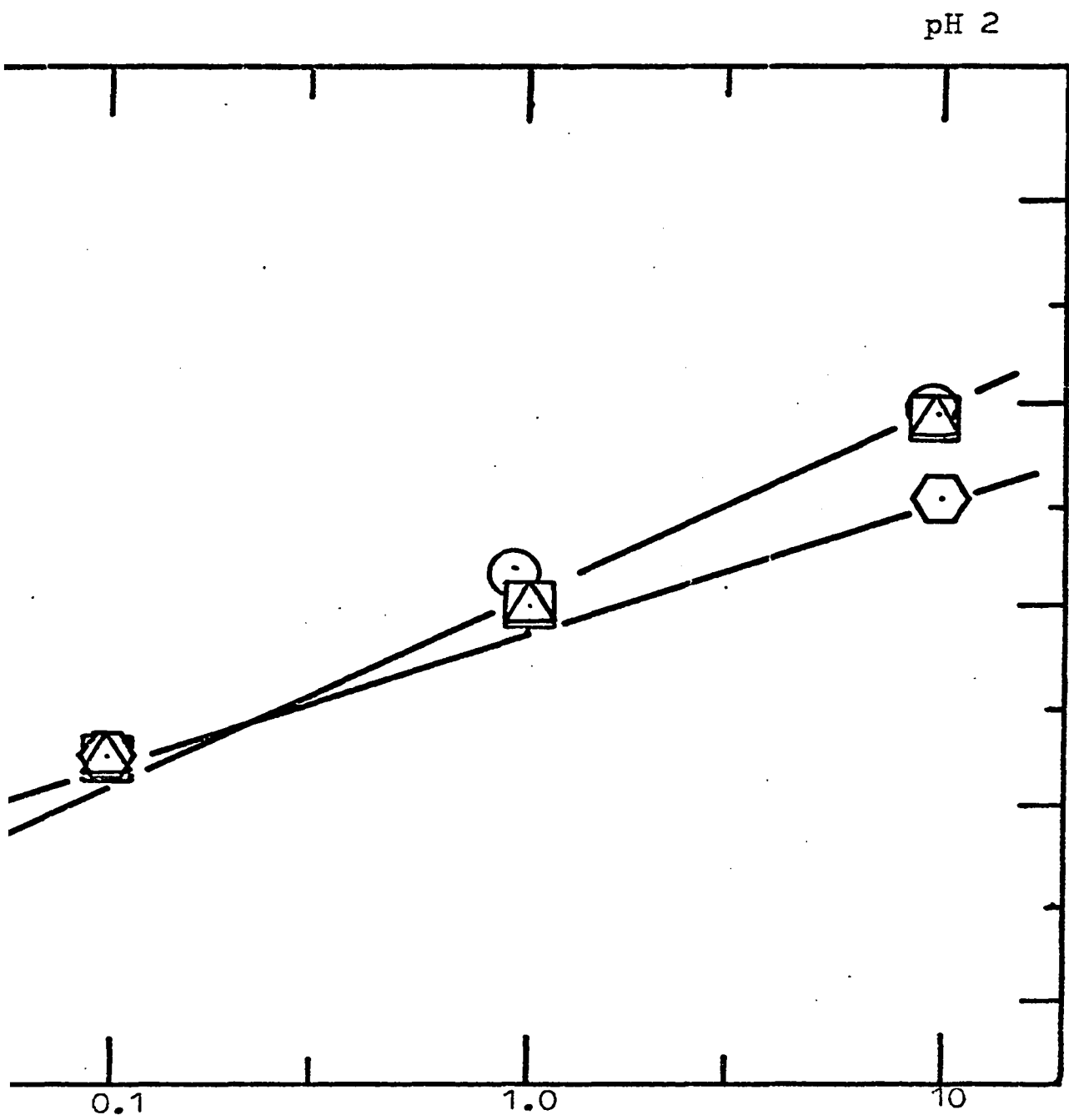
LIBRIUM CONCENTRATION, mMole/l

☐ · 100 mg/l   △ 400 mg/l   ⬡ · 1000 mg/l

FIGURE 24

AMINE ADSORPTION AS A FUNCTION OF CONCENTRATION

pH 7

pH 7

ERIUM CONCENTRATION, mMole/l

□⋅ 100 mg/l   △ 400 mg/l   ⬡⋅ 1000 mg/l

0.1   1.0   10
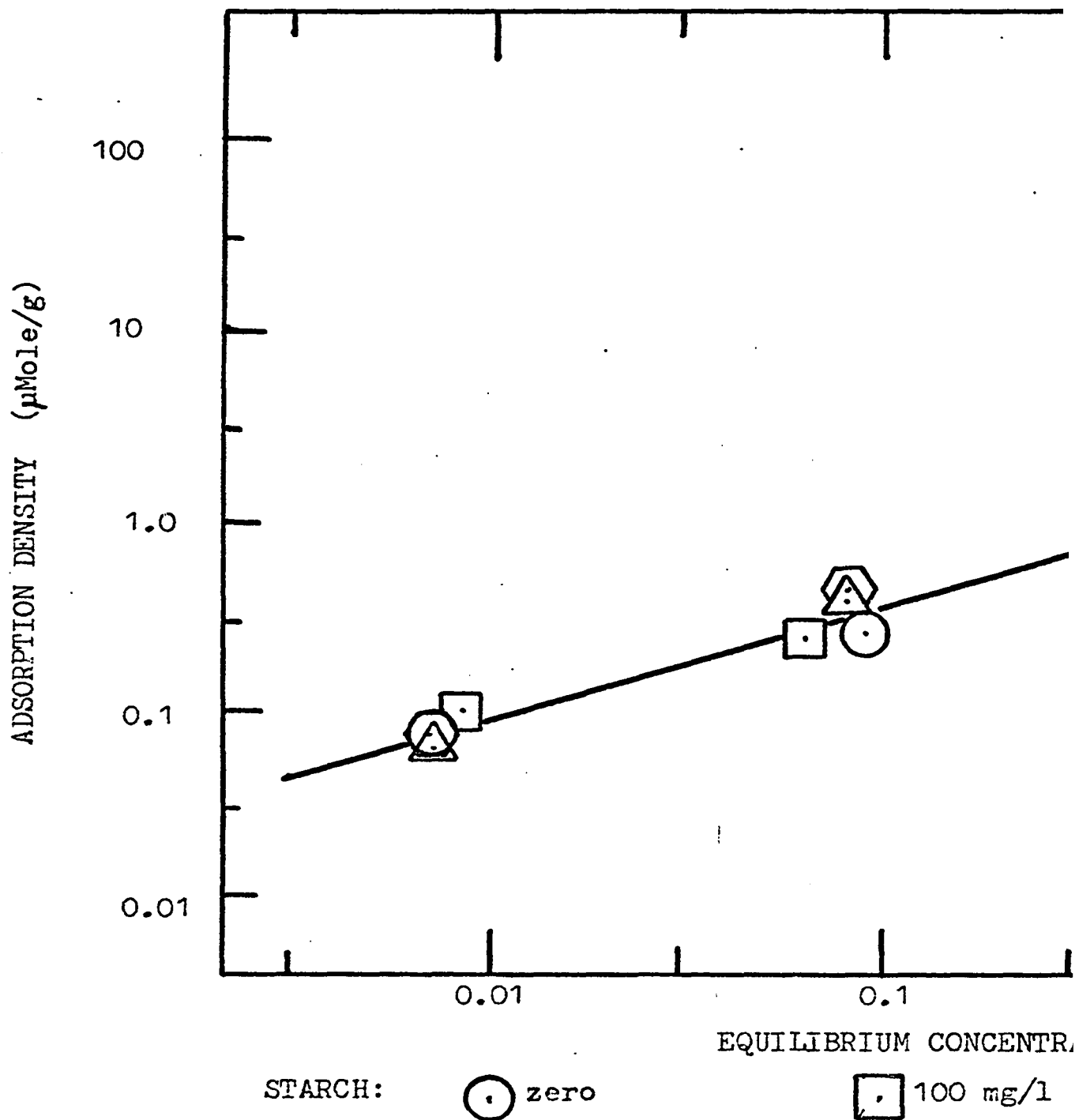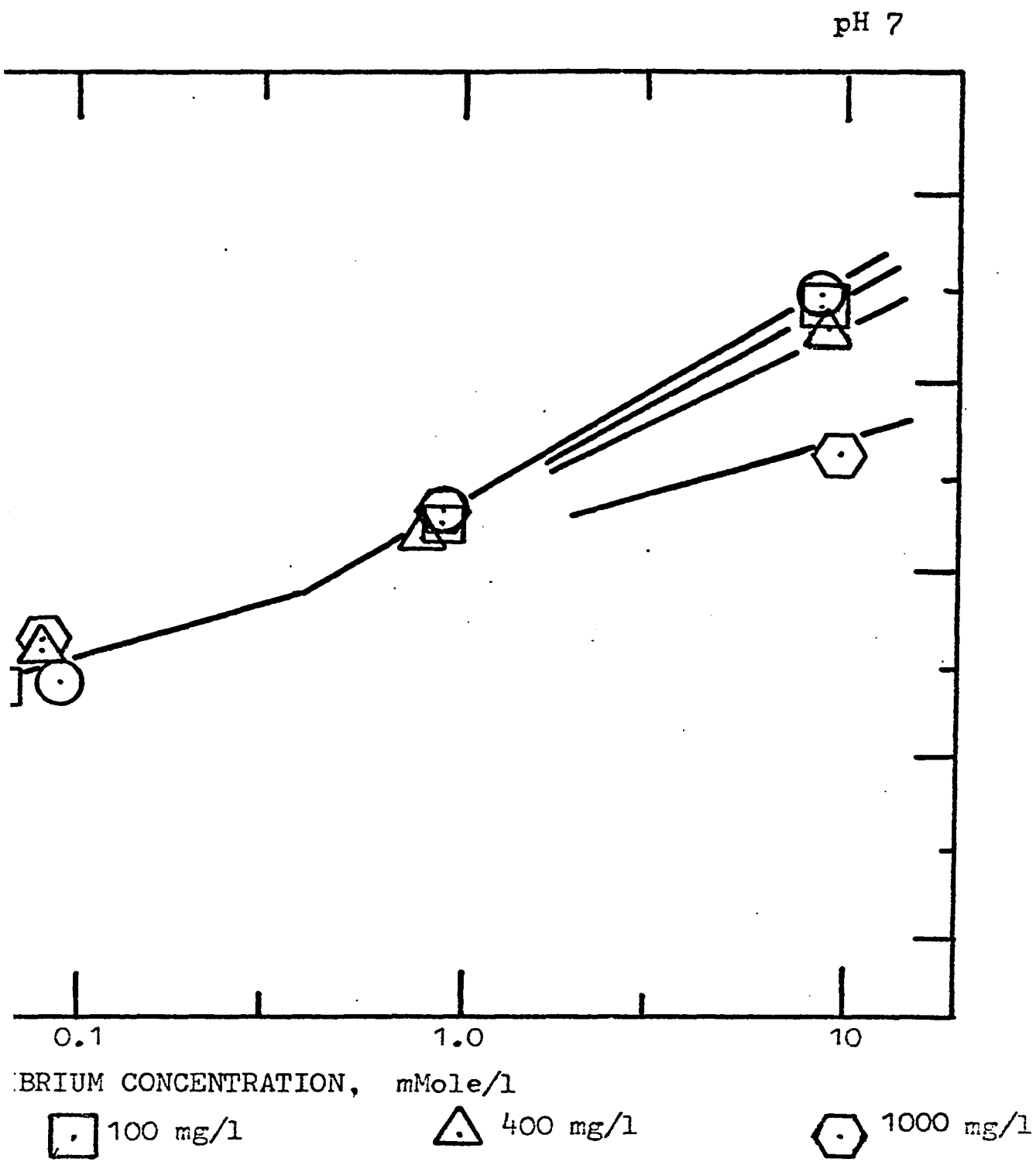
FIGURE   25

AMINE   ADSORPTION   AS   A   FUNCTION   OF   CONCENTRATION

pH 12
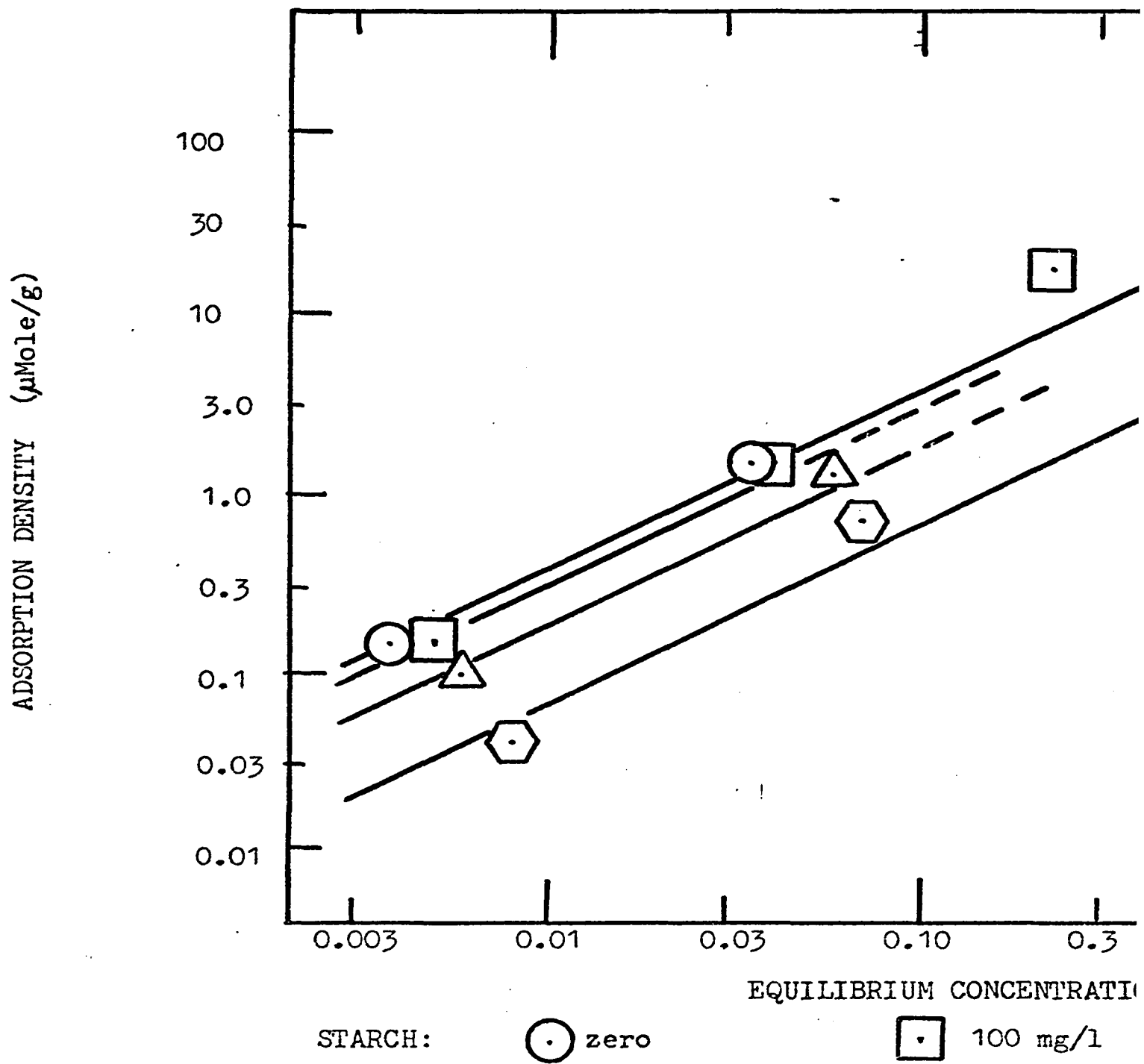
pH   12
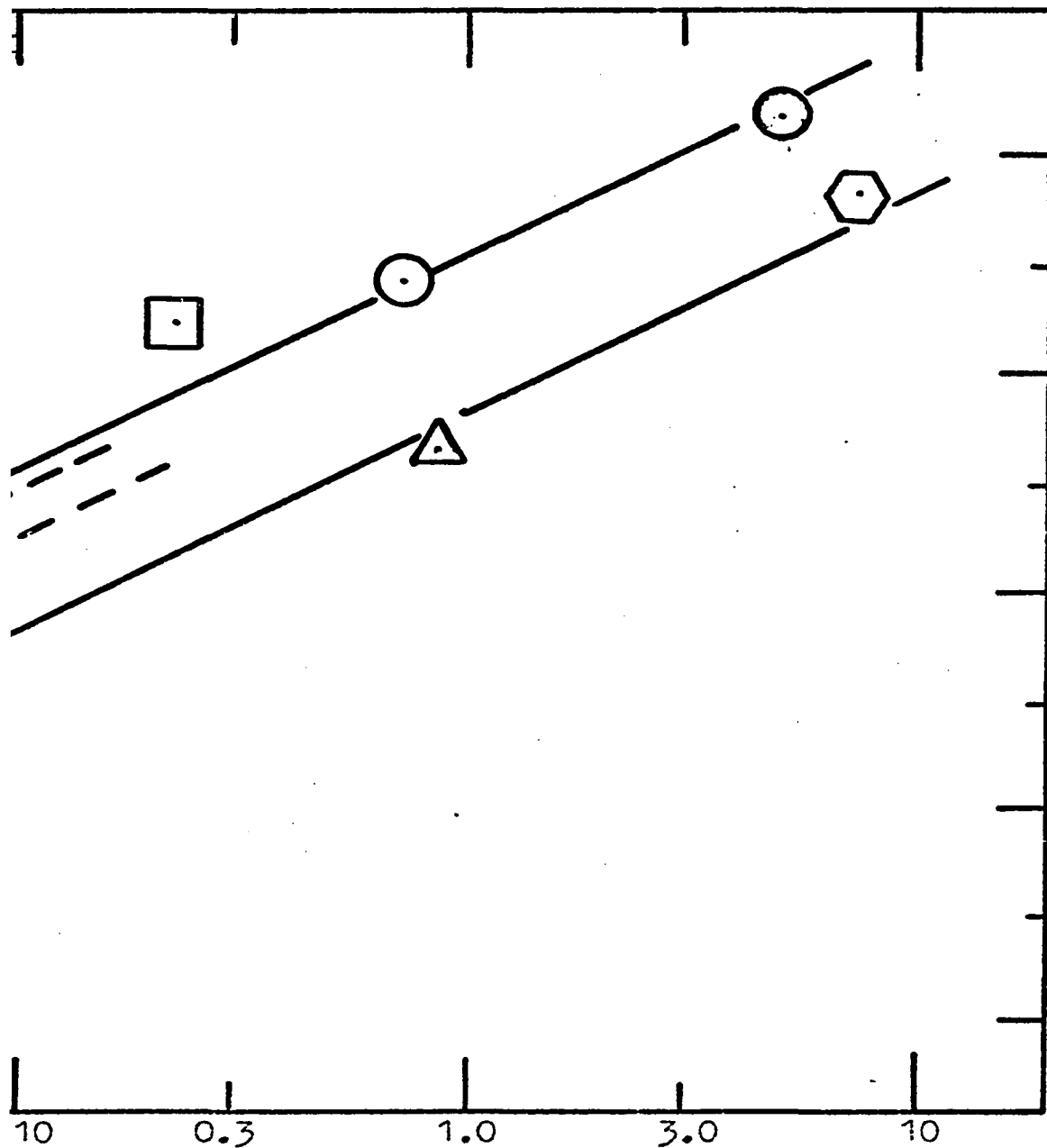
M CONCENTRATION,   mMole/l

⊡ 100 mg/l   △ 400 mg/l   ⬡ 1000 mg/l

gave rise to considerable scatter of results at the higher concentrations. However, the points suggest a gradient of one, i.e. $\Gamma = KC$. The extent of adsorption is shown to be decreased by starch addition.

(b) <u>Starch</u>

The adsorption data for starch were masked by experimental scatter. The pH-independent adsorption curves given in Figure 22 agree, qualitatively, with the results of Schultz and Cooke[43] and Iwasaki and Lai[45]. These workers also showed that Γ_{starch} decreases with increasing pH. Hydrogen bonding is the most likely adsorption mechanism. Bonding decreases with increasing pH as protons are stripped from the structure and the molecule gains a negative potential. The hydrogen bonding theory is supported by the fact that replacement of -OH starch groups by phosphate, sulphonate, xanthogenate or carboxyl groups reduces the depressant effect[88]. Hydrogen bonds may be envisaged between starch and both the surface 'hydroxide' layer of the mineral and water, thus making the mineral hydrophyllic. An increase of pH weakens hydrogen bonds and increases the negative charge on both starch and mineral, thus tending to decrease adsorption, as has been reported[43, 45]. Adsorption was seen to increase with concentration and the more extensive data of other workers[43, 45] indicate a Langmuir-type isotherm which suggests an approach to a monolayer. Starch has frequently been used as a flocculant[89, 90], the large size of the adsorbed monolayer greatly reducing electrostatic repulsion of hematite particles. The inability to screen adequately the much larger surface charge of silica in near-neutral

solutions has been utilized to effect a selective removal of quartz slimes from an ore containing hematite and quartz before flotation[89].

(c) <u>Simultaneous Amine-Starch Adsorption</u>

It is proposed that interaction between amine and starch gives rise to two species, (i) a surface active group composed of starch and aminium ion(s) and (ii) a soluble, non-adsorbing group composed of starch and un-ionized amine. Due to the relative proportions of RNH_2 and RNH_3^+, species (i) would be expected to predominate at lower pH and amine concentrations, and species (ii) at high pH and amine concentrations. (In the latter case starch is negatively charged as it readily loses protons and is therefore repelled by the similarly charged hematite surface.) These relationships conform with the observed adsorption phenomena: at low pH (where RNH_3^+ predominates almost exclusively),

(1) Γ_{amine} increases with starch concentration; and

(2) Γ_{starch} is at its highest level.

At high pH, where RNH_2 is the significant form of the amine,

(1) Γ_{amine} is decreased by the presence of starch; and

(2) Γ_{starch} is at its lowest level.

In near-neutral or moderately alkaline solution both RNH_3^+ and RNH_2 exist in significant quantities and no change of Γ_{amine} was observed at different starch levels. However, Γ_{starch} was found to decrease at high amine concentrations, conditions under which RNH_2 would become of increasing importance.

The anomalous behaviour of the adsorption from 10^{-2}M. amine

solution can also be explained by this proposal. Concentration in the double layer is envisaged as exceeding the RNH_2 solubility limit, accounting for the exceptionally high apparent adsorption at low or zero starch (Figures 17 - 19). High starch concentration could result in solvation of the precipitated coating (Figure 20).

From the theoretical treatment of the amine adsorption isotherm (p. 68), it can be seen that solvation of RNH_2 and enhanced adsorption of RNH_3^+ should reduce the gradient of the Freundlich plot. Figures 23 - 25 show that the addition of starch did give the expected gradient reduction.

Ample evidence for the complexing properties of starch has been published[91-93]. The classical example is the coloured complex formed with iodine which occupies the space within the starch helix of amylose[91]. Hydrogen bonding between starch and both polar and non-polar hydrocarbons has been reported[92] and the inhibition of the starch-iodine reaction by paraffin-chain surfactants has been used for quantitative analysis of the surfactant[93]. Ghigi[94, 95] has investigated the inter-action of cationic collectors and water soluble polymers and concluded that binding between the collector 'tail' and the polymer by Van der Waals' forces or hydrogen bonding gave a complex with intermediate properties. Thus the association of dodecylamine with polyvinylacetate was a less effective collector than the amine alone due to the hydrophyllic nature of the polymer[94]. Association of macromolecules has also been utilized to promote flotation[96].

Interaction between the non-polar portion of adsorbed ions and un-ionized molecules of the same species has been reported to enhance flotation[97].

(ii) FLOTATION

The complete interrelationships of amine concentration, starch concentration, pH and floatability are shown in Figure 26. The change effected by starch addition is clearly seen by comparison of Figures 27 and 28.

The low-flotation region surrounding the observed peak may be considered in four sections: high and low amine concentration and high and low pH.

Depression at low concentration can be attributed to insufficient collector adsorption to overcome the naturally hydrophyllic nature of the mineral. At high concentrations bubble 'armouring' provides a probable explanation for depression[98, 99].

The results at low and high pH can be explained in terms of the two sorption mechanisms described above. Thus at low pH, the RNH_3^+-starch complex will adsorb or form at the surface and the hydrophobic amine chain will be rendered ineffective by the screening effect, or simply the great water avidity, of the starch. At high pH, complexing will overcome the hydrophobicity of adsorbed RNH_2 as well as lowering the concentration of that agent at the surface. The failure to effect complete depression in moderately alkaline solution can only be explained if RNH_2-starch complexes

FIGURE 26

FLOATABILITY REGIONS

ZERO STARCH

% FIOAT

100
80
60
40
20

10⁻²
10⁻³
10⁻⁴
10⁻⁵
0

AMINE MOLARITY

pH   2   4   6   8   10   12

400 mg/1 STARCH

% FIOAT

100
80
60
40
20

10⁻²
10⁻³
10⁻⁴
10⁻⁵
0

AMINE MOLARITY

pH   2   4   6·   8   10   12

100 mg/1 STARCH

100

%
FLOAT

%
FLOAT

80

60

40

20

10^{-2}

10^{-3}

10^{-4}

10^{-5}

0

AMINE MOLARITY

pH 2   4   6   8   10   12

DO

30

60

40

20

0^{-2}

$^{-3}$

MOLARITY

1000 mg/1 STARCH

100

%
FLOAT

%
FLOAT

80

60

40

20

10^{-2}

10^{-3}

10^{-4}

10^{-5}

0

AMINE MOLARITY

pH 2   4   6   8   10   12

0

0

0

0

2
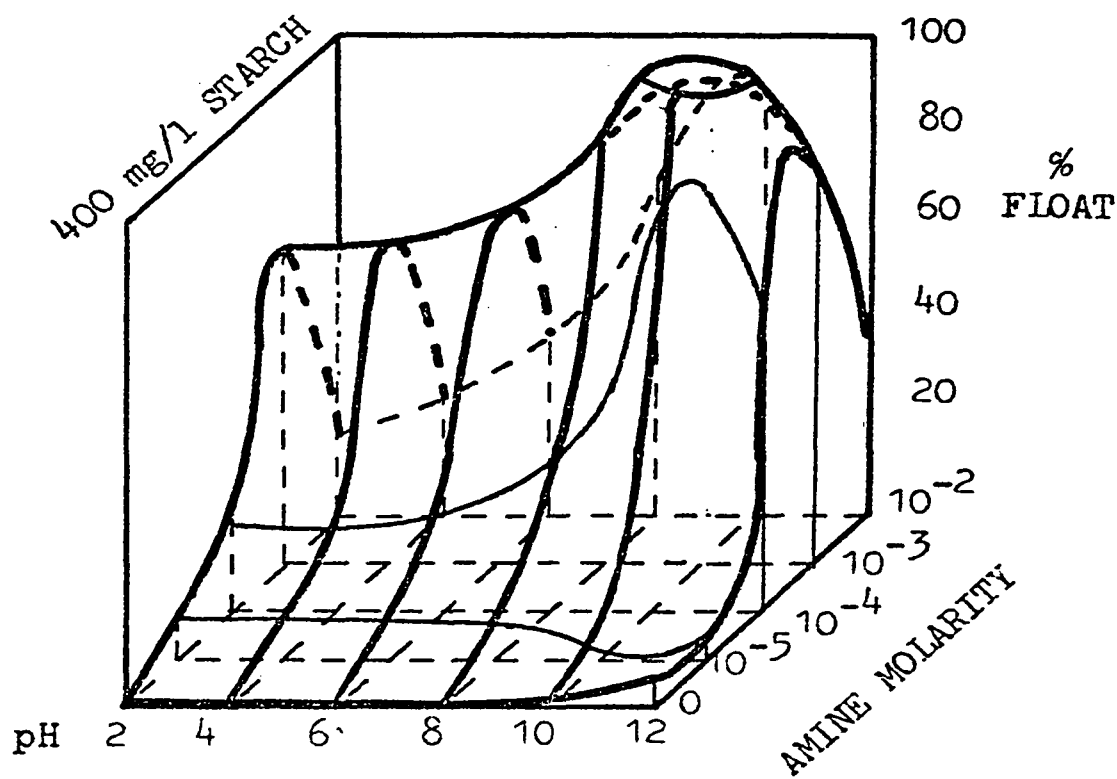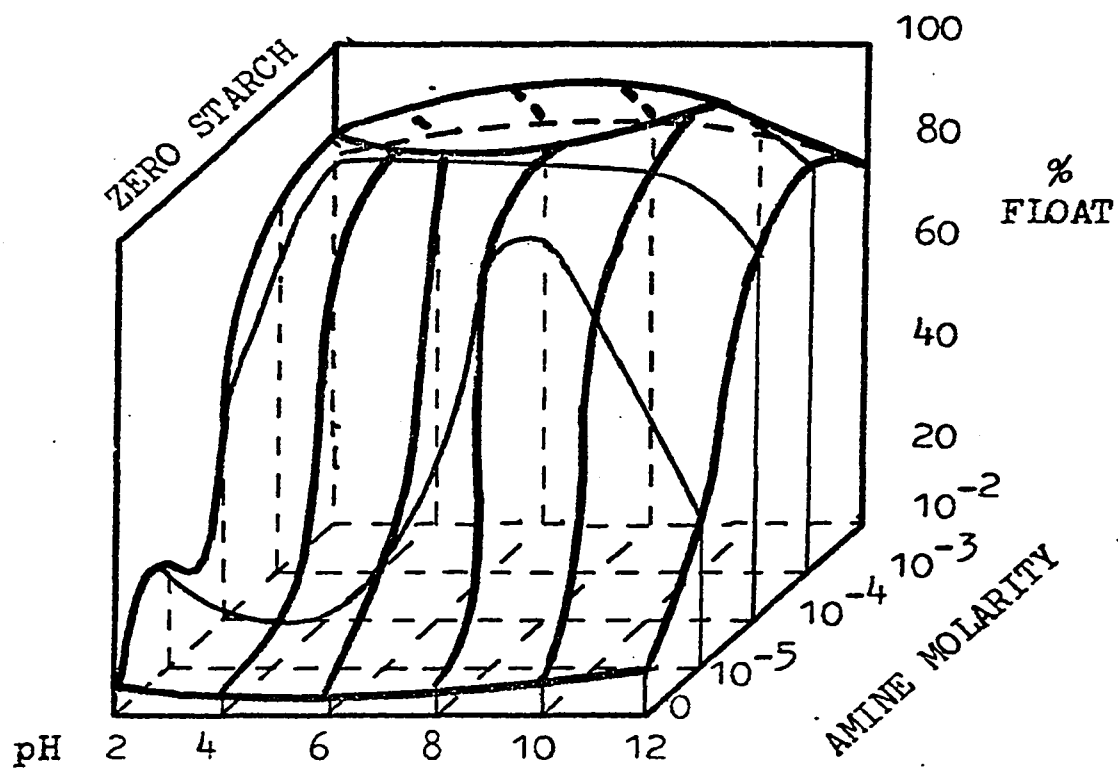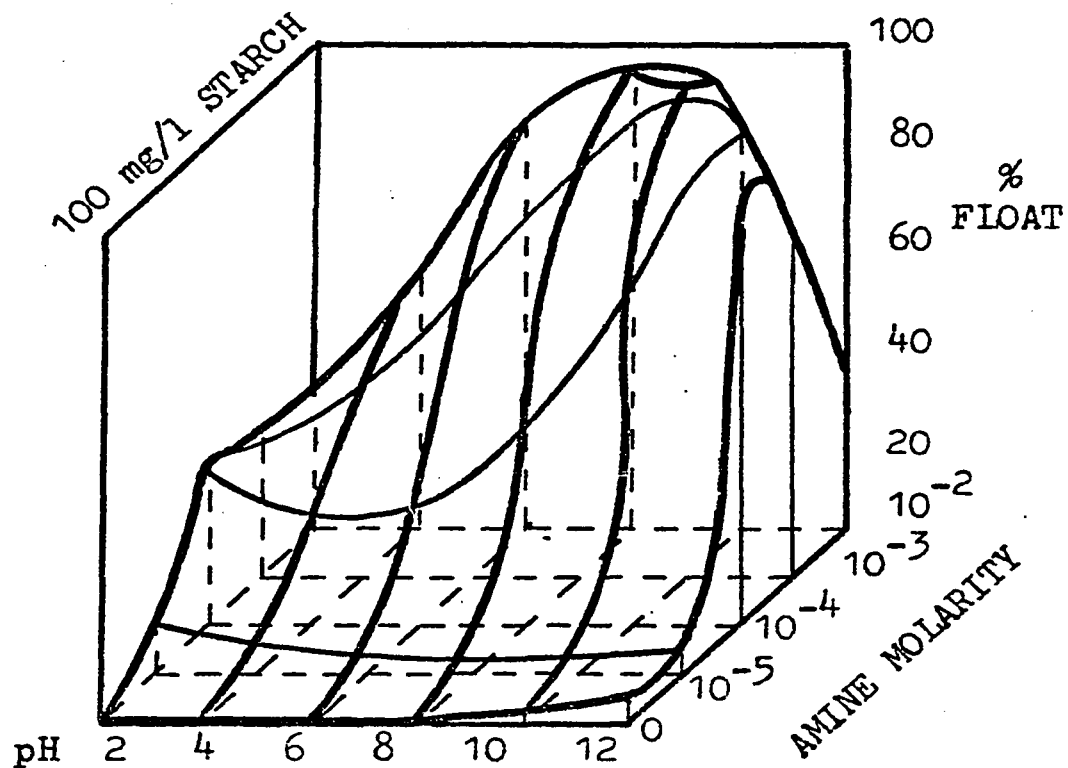
RITY
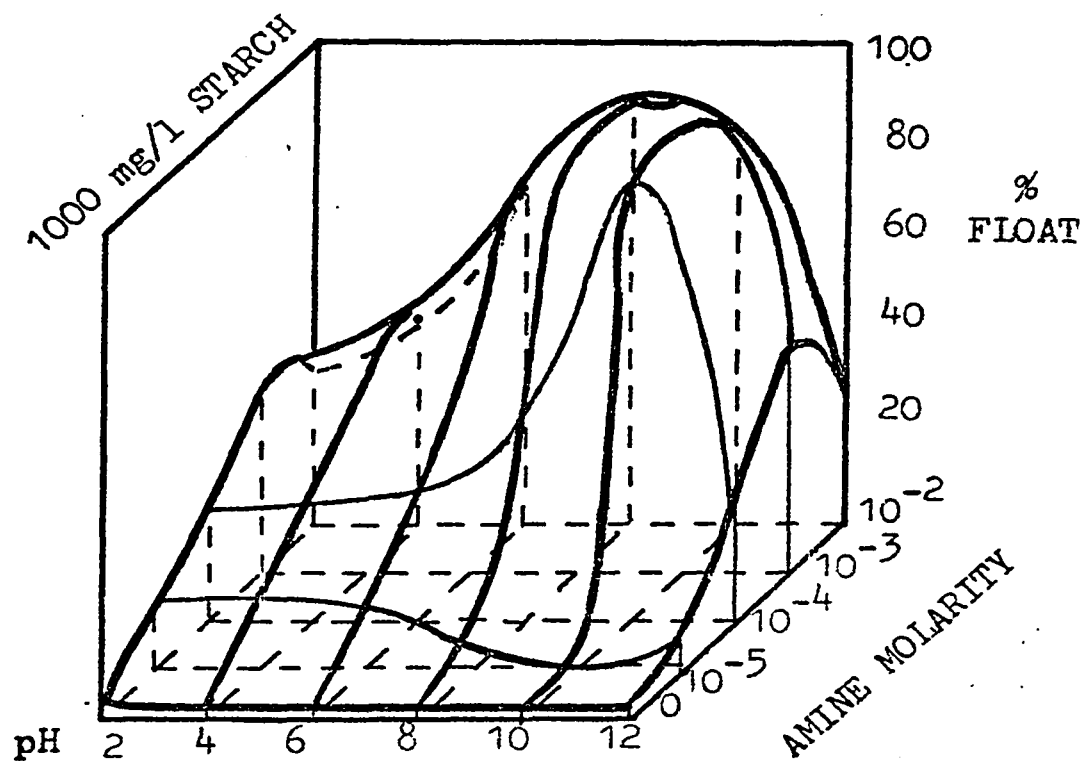
FIGURE   27

PERCENTAGE   FLOATABILITY   CONTOURS   AS   A   FUNCTION   OF

AMINE   CONCENTRATION   AND   pH

STARCH: zero

AMINE CONCENTRATION MOLE/1

10^{-2}

10^{-3}

10^{-4}

10^{-5}

80

90

100

40

20

10

1

3

5

7

p

NUMBERS ON CURVES INDICATE PE

pH
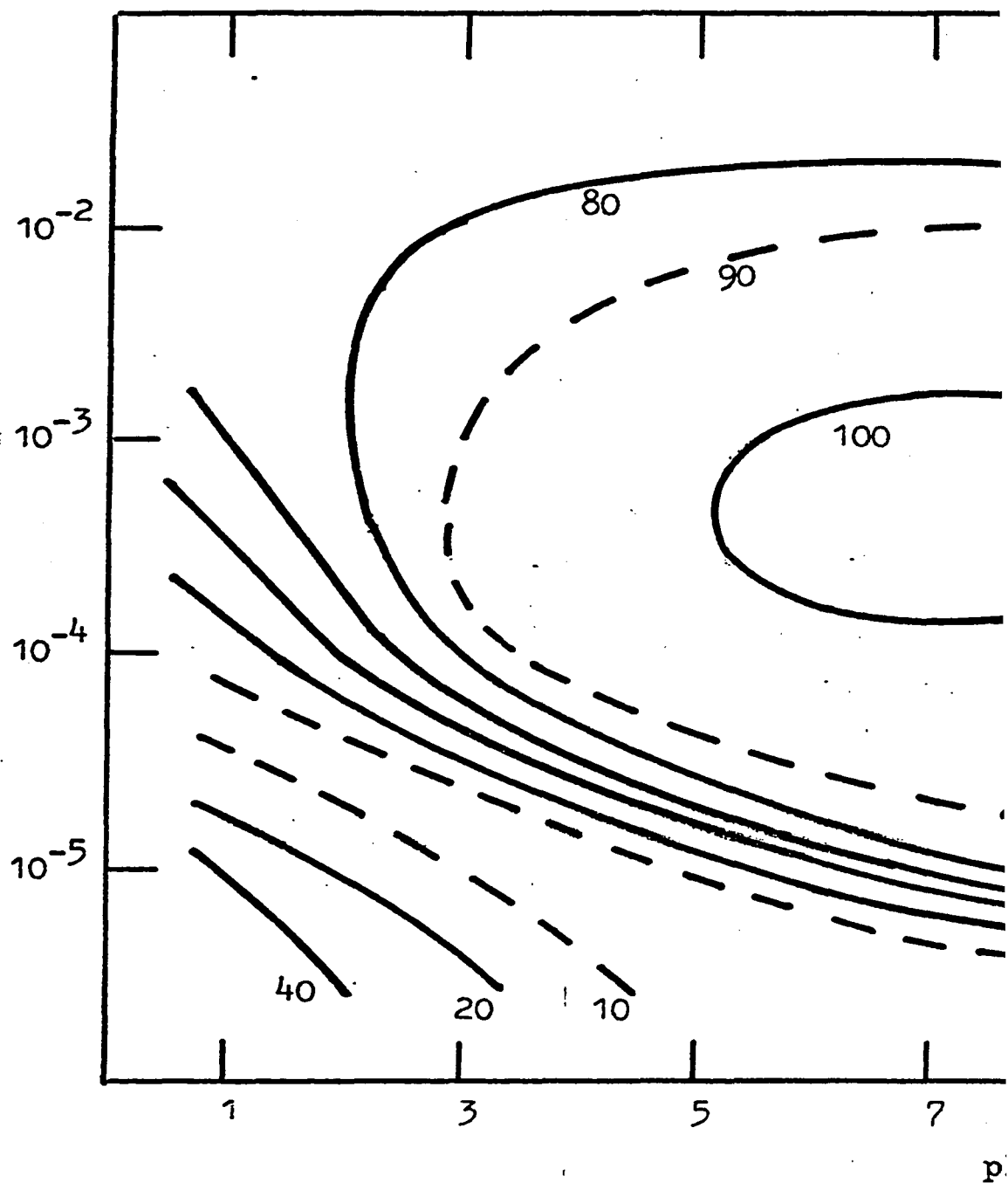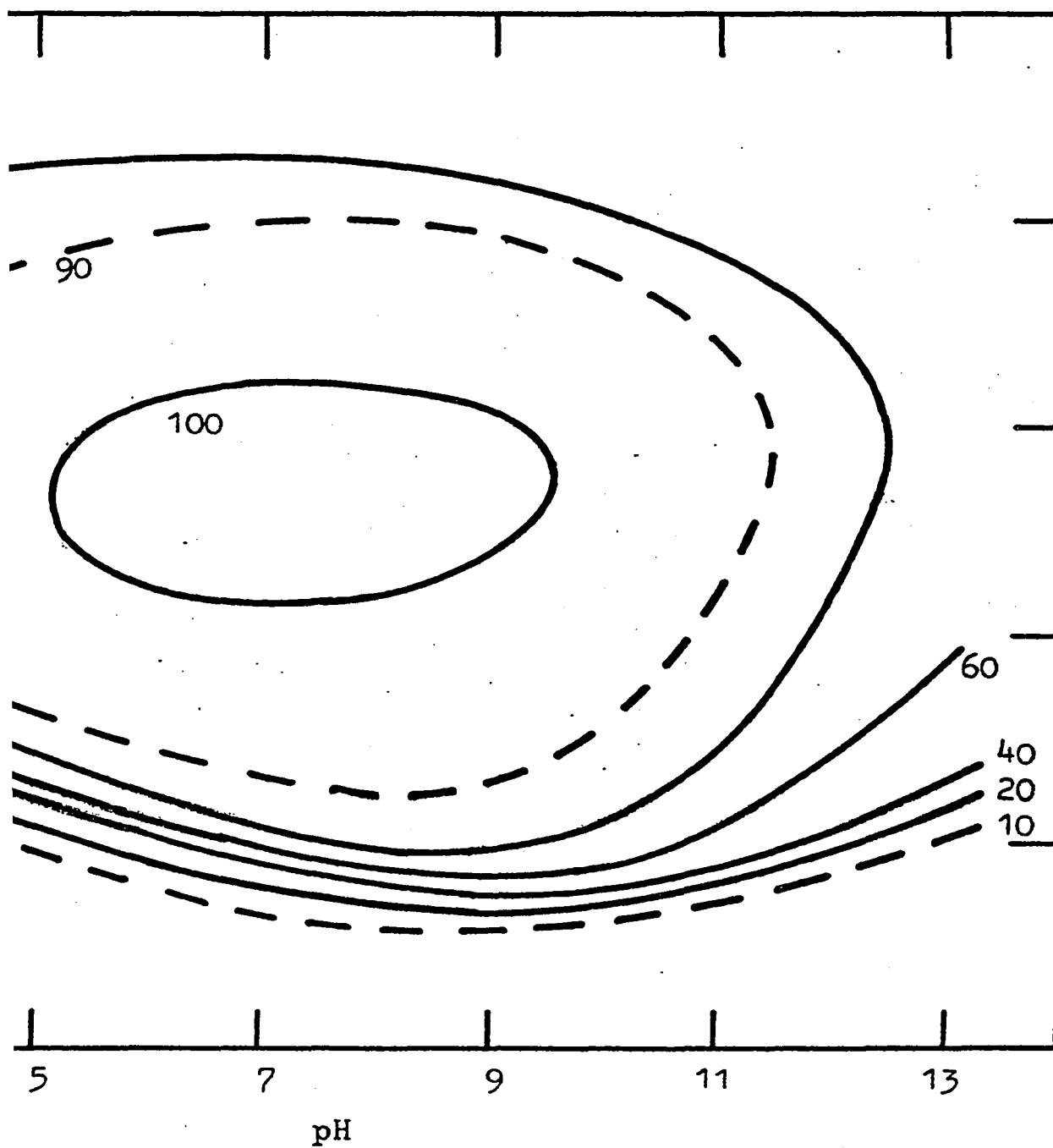
CURVES INDICATE PERCENTAGE FLOATABILITY

FIGURE 28

PERCENTAGE FLOATABILITY CONTOURS AS A FUNCTION OF

AMINE CONCENTRATION AND pH
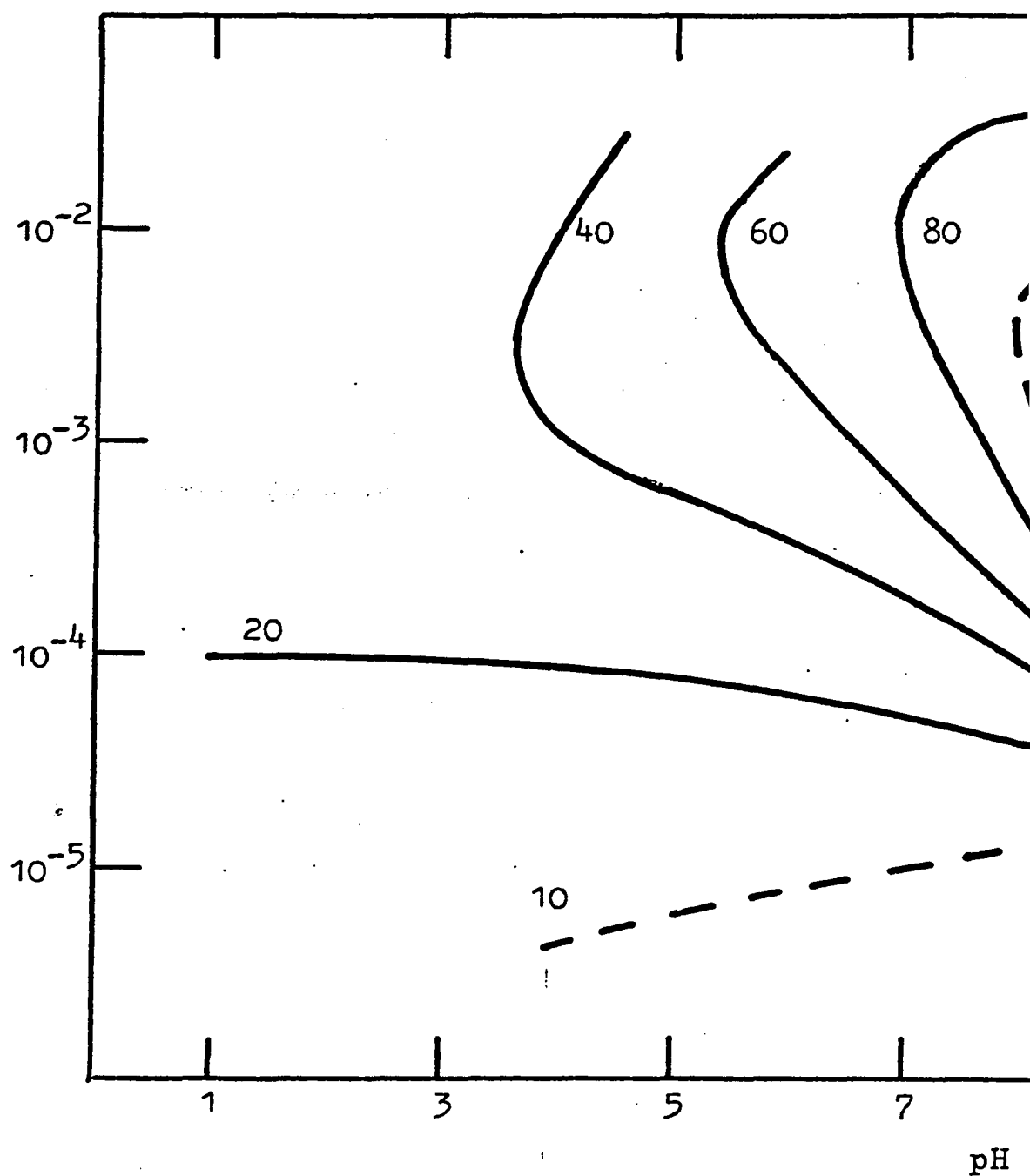
STARCH: 1000 mg/l

NUMBERS ON CURVES INDICATE PER

1000 mg/1 STARCH

pH
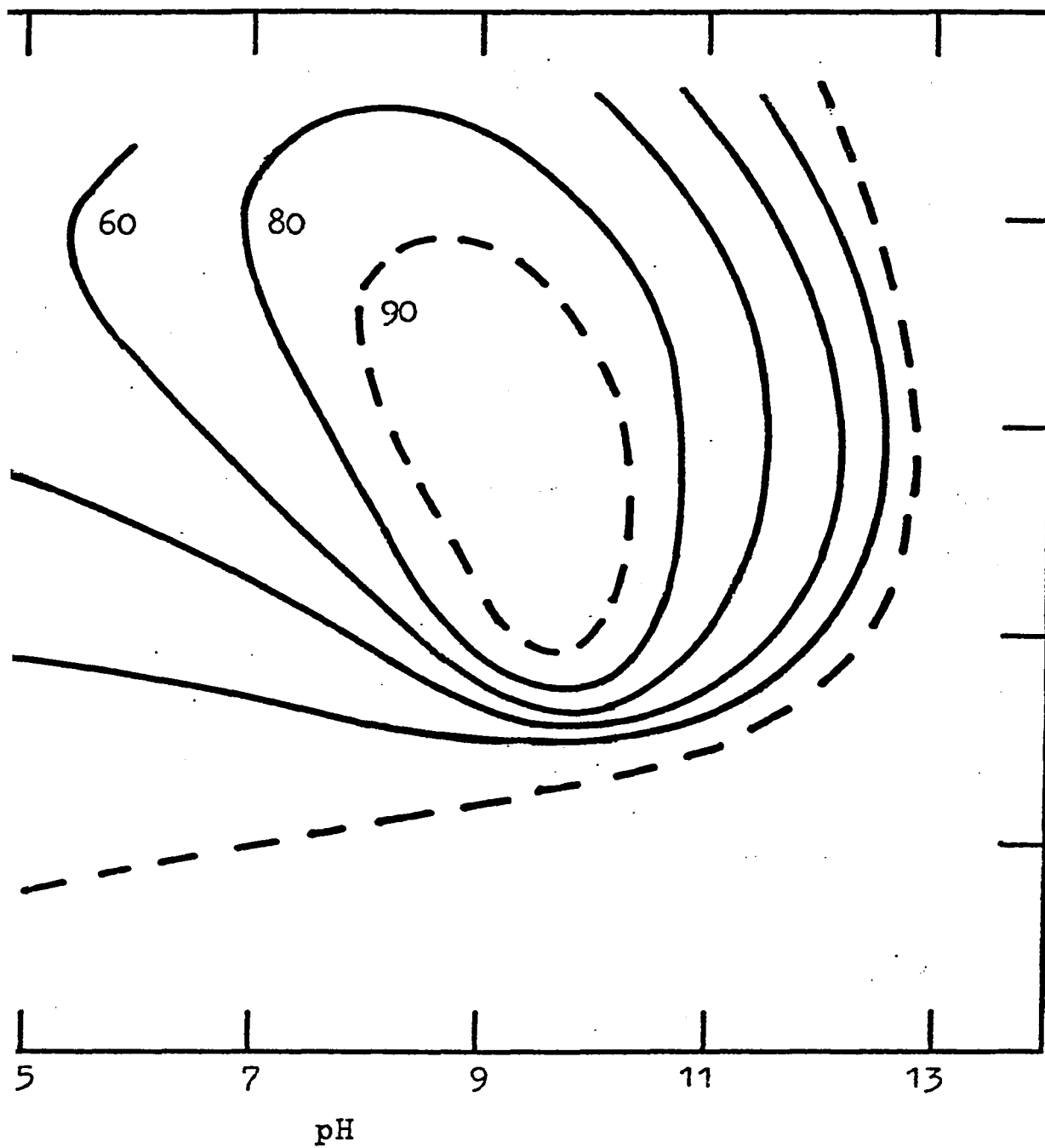
CURVES INDICATE PERCENTAGE FLOATABILITY

fail to form at pH < 10.

The significance of these results in industrial practice is difficult to evaluate as no comparative data has been obtained for adsorption onto the common gangue materials. Clearly, quartz (z.p.c. $\sim$ pH 3) will possess a higher (negative) surface potential than hematite (z.p.c. $\sim$ pH 8) in neutral or alkaline solution. The charge density, σ_d, and corresponding gegen-ion concentration at the surface will be correspondingly greater. Why this should result in different depressant action is not clear. An interesting feature of the industrial process is that typical operating conditions are very close to the maximum flotation peak found in this work. Thus, Major-Marothy[40] found optimum conditions to be pH $\sim$ 10, amine 0.2 - 0.3 lb/ldt feed and starch 0.8 - 1.2 lb/ldt. These values, assuming operation at 35% solids, correspond to approximately 3×10^{-4}M. amine and 200 mg/l starch. A recovery of approximately 70% was achieved under those conditions in this study. One possibly significant difference lies in the industrial practice of conditioning with depressant before contact with collector. In these experiments, the two reagents were added as one solution. It has been stated[72] that order of reagent addition makes no difference to the depressant effect but this aspect could usefully be studied further. Starch action in soap flotation of quartz from hematite has been shown to be enhanced by the presence of the Ca^{++} used for activation[46]. The effect of similar ions inevitably present in industrial circuits may also play an important part in cationic circuits.

(iii) ACETIC ACID AS A COLLECTOR

Shergold et al. reported a low-pH floatability region for the
hematite-dodecylamine system in 1968[100]. However they used $HClO_4$ acid
for pH modulation and required halide ions for activation. In this
study floatability was encountered without collector and in the apparent
absence of foreign ions other than from the acetic acid. It is therefore
logical to assume that the acid was acting as a collector. Electrostatic
equilibrium in acetic acid solution requires that:

$$[CH_3COO^-] + [OH^-] = [H^+] \qquad \ldots 30$$

Therefore, at pH 2

$$[CH_3COO^-] + 10^{-12} = 10^{-2} \qquad \ldots 31$$

Hence

$$[CH_3COO^-] = 10^{-2} - 10^{-12}$$

$$\simeq 10^{-2} \text{ mole/l} \qquad \ldots 32$$

As the zero point of charge for hematite is approximately pH 8 (p. 21),
the mineral possesses a high positive surface charge at pH 2. CH_3COO^-
can therefore be expected to adsorb strongly and it appears that the
single $-CH_3$ group of the acid gives rise to adequate hydrophobicity.

(iv) ACETYL RADICAL AS A COLLECTOR

The secondary flotation region in the presence of amine collector
also seems a result of CH_3COO^- adsorption as the activators previously
found necessary[100] were not present. The acetyl radical in this case

comes from the ionization of the amine salt. By calculation of $[CH_3COO^-]$ a comparison with acetic acid flotation can be made.

The derivation of $[RNH_3^+]$ was given earlier (Equations 10 - 20). Hence $[CH_3COO^-]$, numerically the same, may be determined. Calculation for 10^{-5} molar solution at pH 2 gives

$$[CH_3COO^-] = (1 - 2.4 \times 10^{-9}) \times 10^{-5} \qquad \ldots 33$$

That is, the amine acetate is effectively completely ionized and $[CH_3COO^-] \simeq 10^{-5}M$. From Equation 30 it can be seen that acetic acid has this acetyl radical concentration at pH 5. Floatabilities in the two solutions were found to be 11% and 19% respectively. The correlation is evidently poor, but it must be remembered that the surface potential (and, therefore, the adsorption of the anion) will be greater at the lower pH.

VIII. SUGGESTIONS FOR FURTHER WORK

(1)   To be of practical use the equivalent properties of the quartz-amine-starch system must be determined.

(2)   Similarly, the effect of reagent addition order and of possible modifiers such as Ca^{++} and other multivalent cations should be investigated.

(3)   There is a need for the measurement of such system properties as zeta potential, contact angles, etc. as such data are notably absent for solutions which include starch as a component.

(4)   Solution properties such as surface tension, conductivity, osmotic pressure, absorption spectra, etc. could usefully be studied to help elucidate the nature of dissolved species.

(5)   Measurements at different temperatures might yield information on bonding mechanisms and may indicate operating conditions giving better selectivity.

(6)   A study of alternative colloidal depressants could be made, although economic considerations would be a crucial factor.

(7)   The apparent collection action of the acetyl radical merits further investigation.

APPENDICES

A.1. HEMATITE ANALYSES

The cleaned hematite was identified by X-ray diffraction analysis and its purity determined by atomic absorption analysis.

(a) X-ray Diffraction

The sample was scanned in a Phillips Diffractometer at two different sensitivities in order to locate all detectable peaks. Results are compared with A.S.T.M. file card 13-534 (α-hematite) in Table 15.

Experimental conditions:

Radiation   Fe K_α (Mn filter)

Power   40 Kv x 12mA = 480 W

Scan speed 2θ = $\frac{1}{2}°$/minute.

All detected peaks were attributable to $\alpha\text{-Fe}_2O_3$.

(b) Atomic Absorption Analysis

Three weighed samples (each ~ 0.5 g) of the hematite were dissolved in 50 cc portions of hot 1% solution of stannous chloride in concentrated hydrochloric acid[101] and made up to 100 cc with water. Portions of these solutions were further diluted 1:100. Standard solutions and the three test solutions were introduced successively into the flame of a Unicam SP 90 Atomic Absorption Spectrophotometer. The

absorbance of a beam from an iron lamp (λ = 24.83μ m) passing through the flame was noted for each solution.

Experimental conditions:

Lamp current	18mA
Slit width	0.1 mm
Wavelength	24.83 μm
Gain	6
Damping	1

The calibration curve is shown in Figure 29 and results and calculation given in Table 16.

The sample was found to contain 69.7% iron.

FIGURE   29

CALIBRATION   CURVE   FOR   ATOMIC   ABSORPTION   ANAYLSIS   FOR   IRON

ABSORBANCE

0.5

0.4

0.368 →

0.3

0.287 →

0.231 →

0.2

0.1

26.4

36.1

0

0   10   20   30   40   50

p.p.m. I

.368 →

53.7

36.1

40   50   60   70   80   90   100
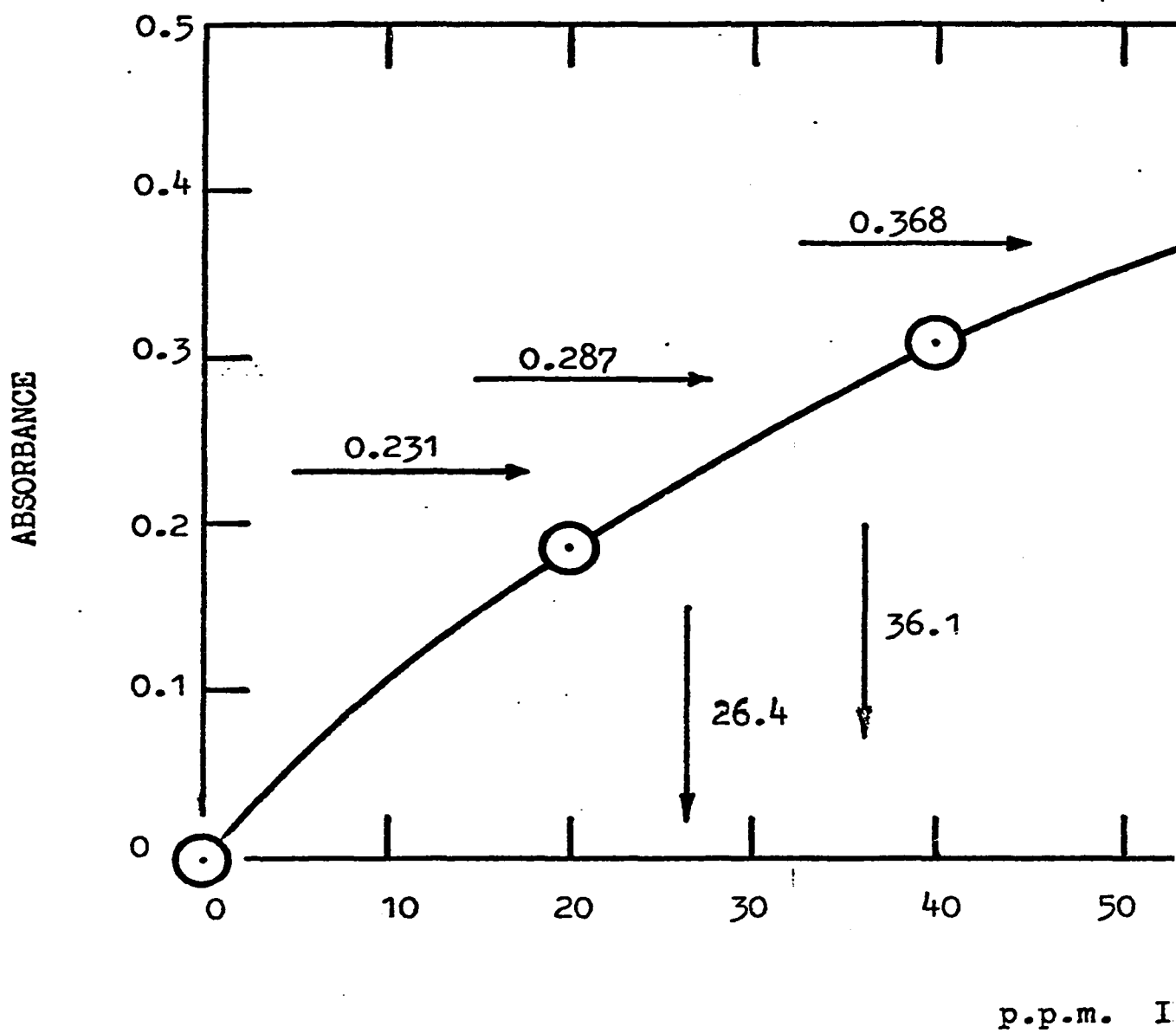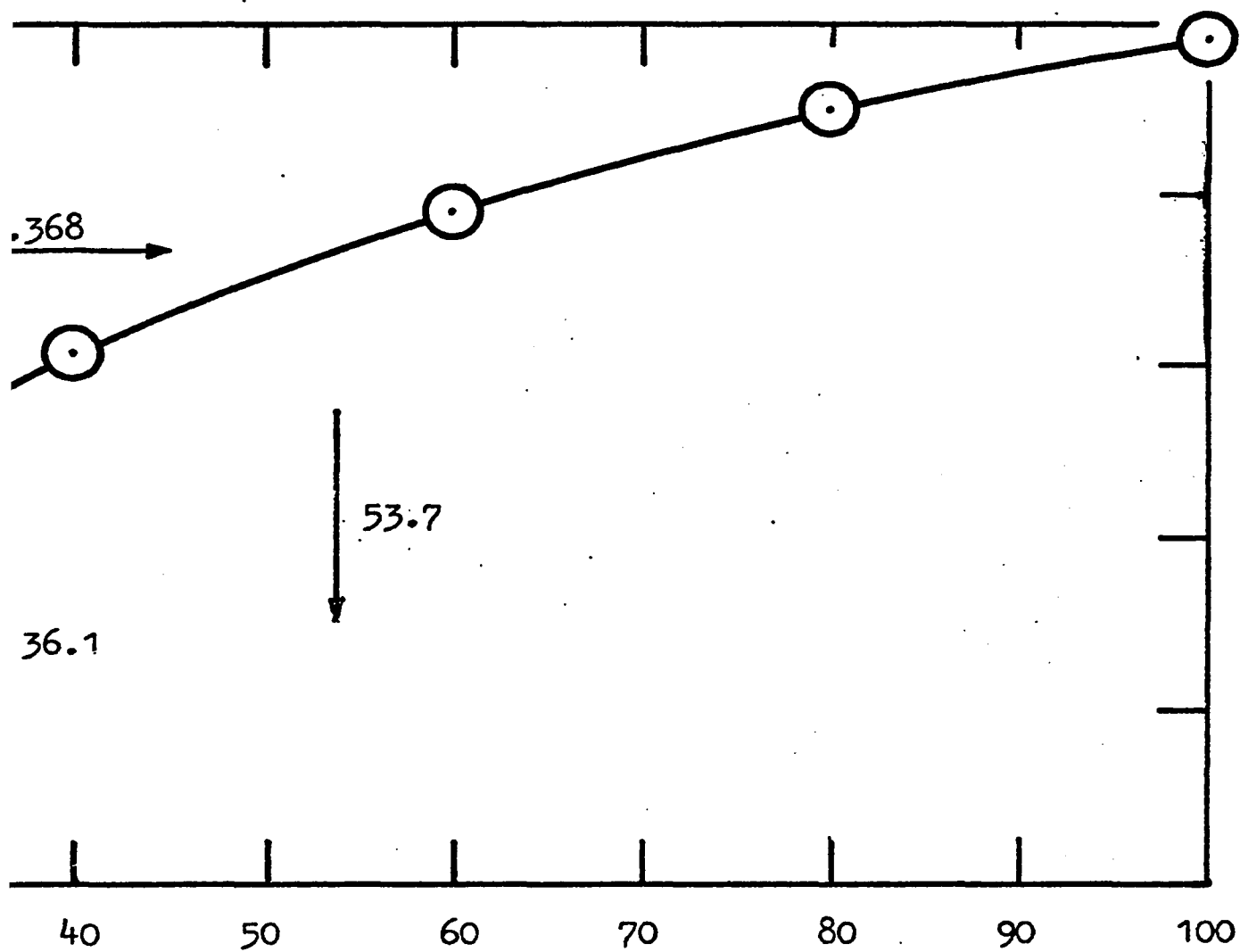
p.p.m.   IRON

A.2. RADIOISOTOPE TECHNOLOGY

(a) Introduction

The use of radioisotopes in adsorption studies dates back at least fifty years[102] but was severely limited at that time by the need to use natural isotopes and by the lack of suitable instrumentation. With the stimulation to nuclear technology of the war years came an increase in the availability and use of artificial isotopes more suitable for laboratory work. Foremost in the field of mineral processing at that time was the work of Gaudin et al.[103-105] at M.I.T. who developed an elegant analysis method for carbon-14 oxidation under vacuum and subsequent internal counting of the resultant carbon dioxide in a Geiger-Müller tube. It was not until the availability of commercial liquid scintillation counters within the last fifteen years, however, that the use of isotopes became commonplace, the ability to trace and determine small amounts of many different elements proving valuable in a wide variety of disciplines.

(b) Radioisotopes

For reasons not yet fully understood, there is only a very limited range of stable neutron/proton ratios for the nucleus of any particular element. Any excess or deficiency of neutrons outside that range results in an unstable nucleus which tends to decay spontaneously to a more stable form by a change in neutron and/or proton content.

Such radioactive decay events fall into a number of categories,

of which only Negative Beta Emission is of significance in the present

study. In this phenomenon an excess neutron content is decreased by

ejection of a 'negative beta particle' (i.e. an electron) from a neutron

which consequently becomes a proton:

$$n \rightarrow p^{+} + \beta^{-}$$

or, more fully:
$$^{A}_{Z}M \rightarrow ^{A}_{Z+1}N + e^{-}$$
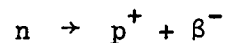
The atomic number of the element (i.e. the number of protons), Z, is

increased by one, a new element being formed but with no change in

atomic weight, A.

Two aspects of beta particle emission are of relevance in tracer

studies, namely the energy and frequency of emission. Both are found to

be characteristic of the particular isotope, providing a means of

discerning between two or more tracers present in a single sample. The

energies of emitted particles from any specific isotope are not at discrete

levels but are found to form a continuum of the shape shown in Figure

30[(106)] for Carbon-14 ($^{14}_{6}C$) and Tritium ($^{3}_{1}H$), the two isotopes used in

this study. Consequently it is not possible to discriminate between

isotopes by simple isolation and measurement of particular energy levels

and a multi-level count and subsequent calculation is required.

Emission rate is dependent upon the nature of the particular

isotope as the probability (p) of disintegration of an individual isotope

nucleus is a characteristic of that isotope and in no way influenced by

its physical or chemical environment. The probability is very small for the isotopes used but is directly proportional to the length of the selected time interval. Consequently over a long period the number of disintegrations is appreciable when compared with the total number of unstable nuclei, n. The parent population thus decays exponentially:

$$\frac{d\,n}{d\,t} = -K\,n \qquad \qquad \ldots 34$$

or, integrating,

$$n_t = n_o e^{-K\,t} \qquad \qquad \ldots 35$$

where n_o is the initial population, n_t is the population after time t and K is a constant characteristic of the isotope.

By defining the half-life of the isotope $(t_{\frac{1}{2}})$ as the time required for one half of the initial nuclei to decay, we may substitute $n_t = \frac{1}{2}n_o$, giving

$$\frac{1}{2} = e^{-K\,t_{\frac{1}{2}}} \qquad \qquad \ldots 36$$

or

$$t_{\frac{1}{2}} = (\log_e 2)/K \quad . \qquad \qquad \ldots 37$$

For the two isotopes of interest:-

$$t_{\frac{1}{2}} \,(^{14}_{6}C) = 5.73 \times 10^3 \text{ years} \qquad \qquad \ldots 38$$

and

$$t_{\frac{1}{2}} \,(^{3}_{1}H) = 12.26 \text{ years}^{(107)}. \qquad \qquad \ldots 39$$

The decay curve is shown in Figure 31, from which it can be seen that carbon-14 activity can be regarded as constant for periods of several years whereas (inset) a correction had to be applied to the tritium standard over the period of the study.

During the short (5 minute) counting periods the probability of disintegration of an individual nucleus is so small that the final population, $n - np$, is numerically indistinguishable from the initial population, n. The population, however, is very large in any practical situation. Therefore, as emission is completely random, the probability (P_x) of x radioactive events in such a population is given by the Poisson Law[108]:

$$P_x = \frac{e^{-(n\,p)} \cdot (n\,p)^x}{x!} \qquad \ldots 40$$

$$(x = 0, 1, 2, \ldots)$$

for which it can be shown[108] that the standard deviation (d) is equal to the square root of the mean (i.e. $d = (np)^{\frac{1}{2}}$) and the 'relative dispersion' (d/np) is equal to $(np)^{-\frac{1}{2}}$, thus decreasing with increasing sample activity (αn) and/or counting time (αp).

This relationship can be regarded as a special case of the more commonly encountered Normal (Gaussian) model, or more properly, as the distribution is not strictly continuous, of the Binomial (Bernoulli) model in which $d = (np(1-p))^{\frac{1}{2}}$. As p is assumed very small, $(1-p)$ approaches unity and the expression simplifies to that stated above.

FIGURE 30

BETA - RADIATION EMISSION SPECTRA

FOR CARBON - 14 AND TRITIUM

RELATIVE FREQUENCY OF OCCURENCE (ARBITRARY UNITS)

3
1

MAXIMUM EMISSION ENERGY:

^{14}C 0.158 MeV

^{3}H 0.018 MeV

0.0003   0.001   0.003

ENERGY OF EMISSI

$^{3}_{1}$H

$^{14}_{6}$C

0.01   0.03   0.1
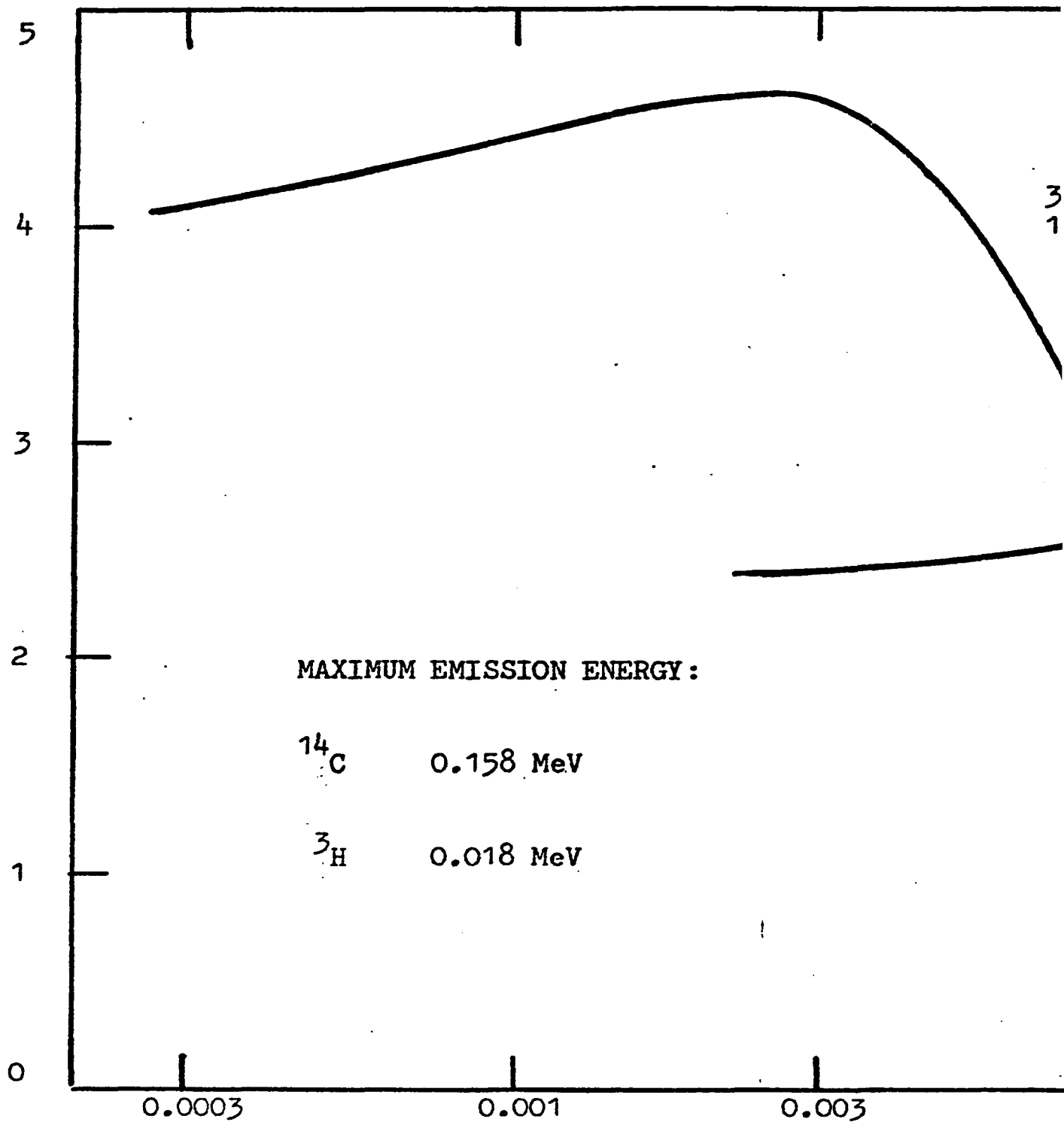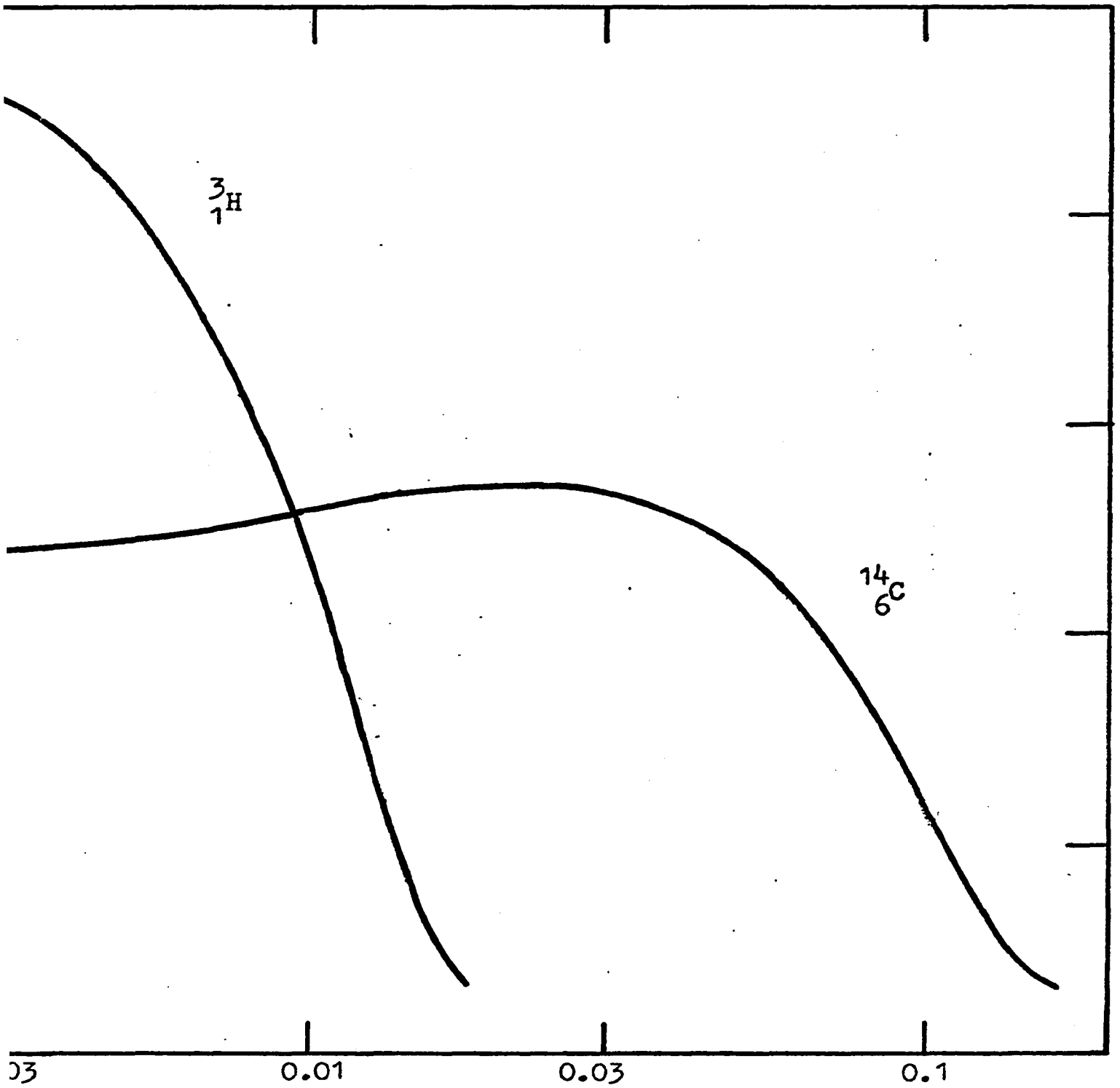
ERGY OF EMISSION (MeV)

FIGURE 31

RADIOACTIVE DECAY CURVES

FOR CARBON - 14 AND TRITIUM

TRITIUM (WEEKS)

SHORT-TERM DECAY

ACTIVITY %
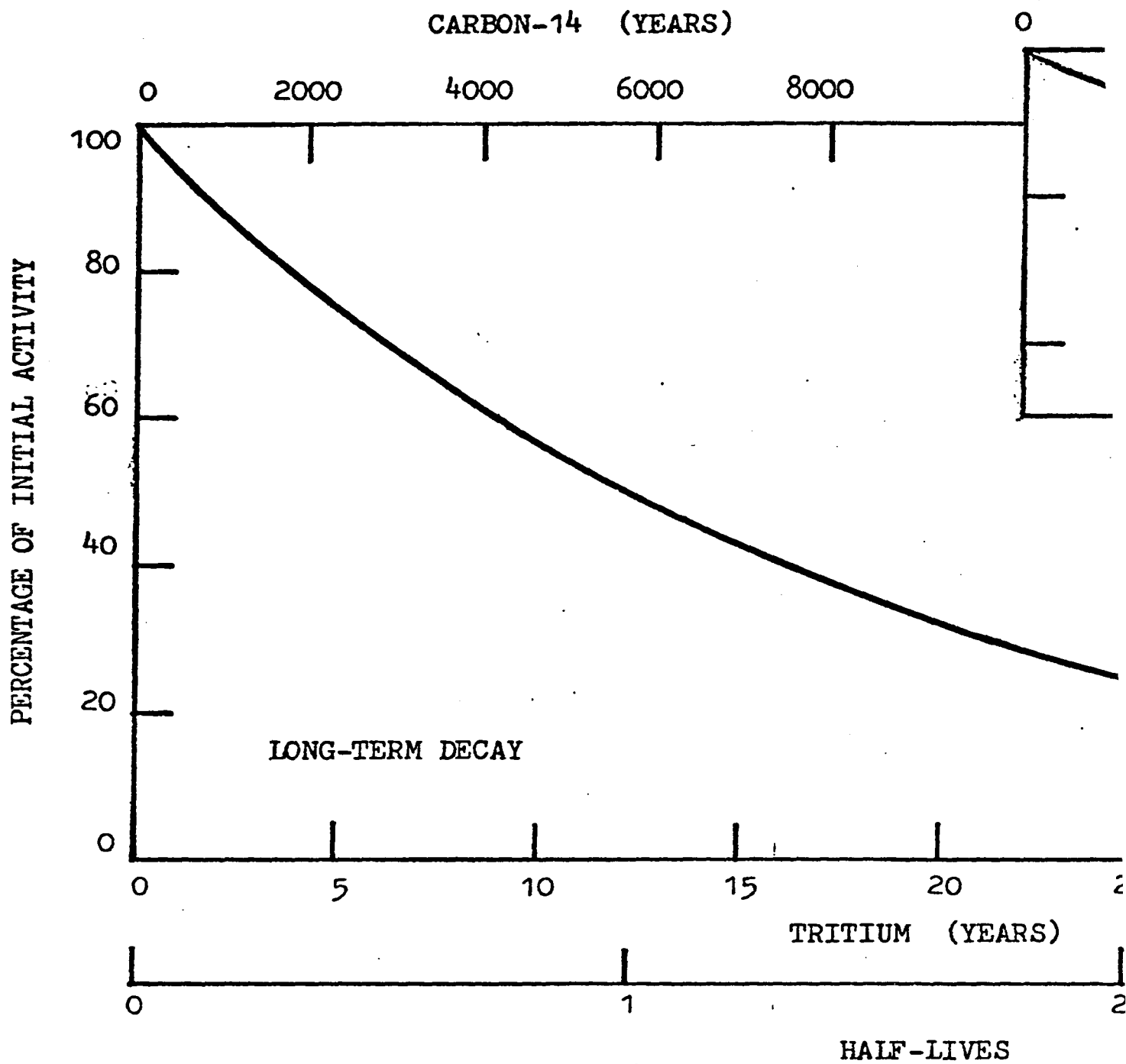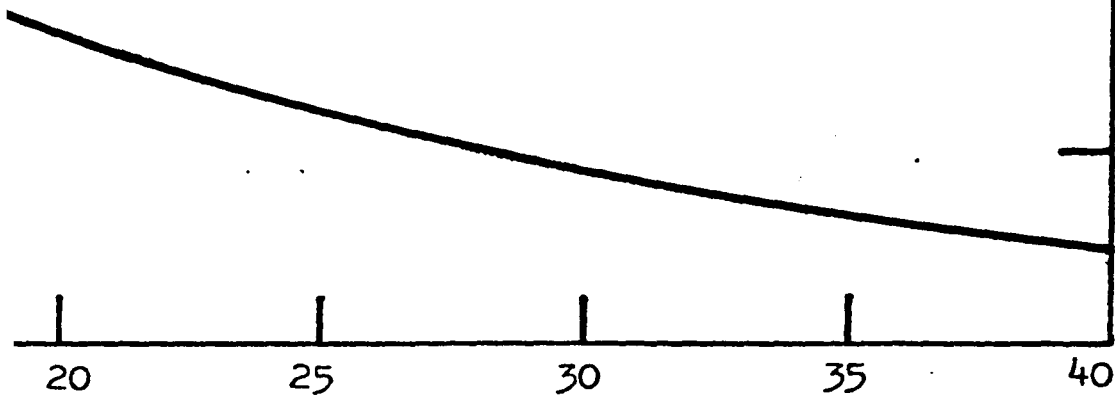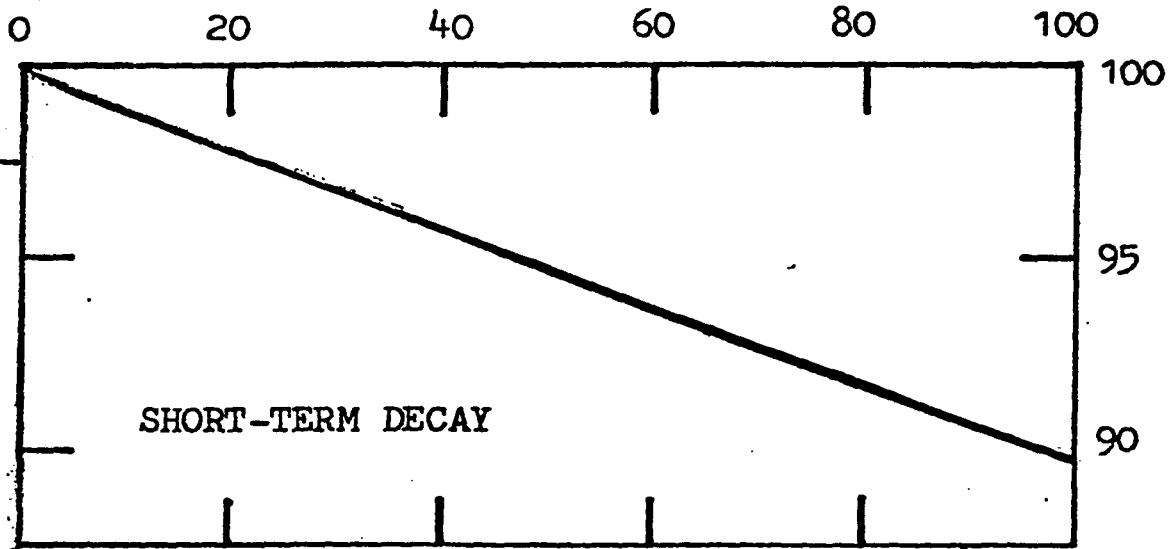
(YEARS)
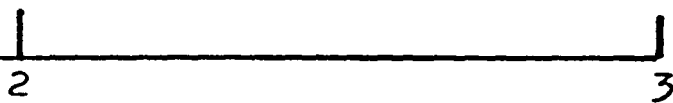
-LIVES

(c) Liquid Scintillation Counting

When a beta particle is ejected in the neutron-proton transformation it is immediately subject to steric and coulombic influences from its environment leading to interactions of various forms, the most useful of these being between the beta particle and an outer orbital electron of an atom of the environment. In this case, a transfer of energy is made to the orbital electron, which, if not actually stripped from the parent atom, will be raised to an excited state. Subsequent fall-back then results in the emission of a photon lying, for many substances ('scintillators'), in the visible or ultra-violet range. Such light flashes can be detected under suitable conditions and utilized as a measure of the total radioactivity. Systems using a liquid medium, in which both radioactive sample and scintillator are dissolved, are especially suitable for the measurement of low energy radiation such as that emitted from carbon-14 and tritium. No barrier or window is interposed between emitter and detector (scintillator) and 4π geometry is readily achieved - i.e. the emitter is totally surrounded by detector, thus improving efficiency.

(d) The Scintillation Counter

The Beckman model LSS 1517A scintillation counter holds up to two hundred 22 ml vials which are automatically fed in turn into the counting chamber. Counting is initiated in three selected energy ranges ('windows') and continues until a pre-set count or elapsed time is reached.

Counts in each window (expressed in terms of elapsed time and computed counts-per-minute) are recorded on a print-out. Each vial is counted a pre-set number of times before being replaced. The machine incorporates an external standard, used in the determination of counting efficiencies, and an automatic background-count subtract facility.

Light emissions from a vial are detected by two photomultiplier tubes, thermal or other stray emissions occuring in only one tube being rejected by a coincidence circuit. The photomultipliers are of a bialkali type which have a pseudo-logarithmic response mode, eliminating the need for extensive amplification stages. A single 'gain' control is used. Thermionic noise is low and, like the efficiency, independent of temperature between 15° and 40^oC, thus permitting operation at room temperature. The tubes have good response at lower wavelengths in contrast with earlier types. Thus, the use of simple scintillator solutions is made possible.

(e) Scintillator Solution

A large number of 'cocktails' (mixtures of solvent, fluors and other agents) have been developed during the past decade[109]. Dioxane based solutions are in general use in counting aqueous solutions due to the relatively high water content possible. A dioxane based solution usually contains a freezing point depressant (F.P. of dioxane = $+12^o$C), permitting low-temperature counting to reduce thermionic noise. A secondary fluor such as 'POPOP' (1. 4-bis-2-(phenylyoxazolyl)-benzene)

is usually also required to raise the wavelength of emitted light into the sensitivity range of the photomultiplier tubes. Due to the characteristics of the Beckman tubes neither of these precautions was necessary and the following solution was used:

> PPO (2, 5 diphenyloxazole) (fluor)   6 g/l
>
> Naphthalene (reduces water quenching)   100 g/l
>
> 1, 4 Dioxane   remainder.

Tests showed this mixture to form a homogenious solution with up to 25% water at room temperature. Sample volumes up to 3.3 cc may therefore be added to the standard 10 cc of scintillator solution.

QUENCHING AND COUNTING EFFICIENCY

Anything in the solution which reduces energy of emitted radiation is termed a quench agent. The result is an apparent shift of the emission spectrum to a lower energy region (Figure 32.a.). Many substances act as quenchers, notably water[73]. Both amine and starch were found to cause a small spectrum shift.

The practical effect of quenching is a change of counting efficiency in a chosen window. Several methods have been evolved to overcome this difficulty. Common approaches include the use of paper discs (low sensitivity), flattening the curve by extensive amplification (one isotope only), addition of internal standards (excessively tedious) and a channels-ratio method (one isotope only)[110].

In this study the automatic 'quench-ratio' facility of the machine

FIGURE 32

THE EFFECT AND MEASUREMENT OF QUENCHING

IN SCINTILLATOR SOLUTIONS
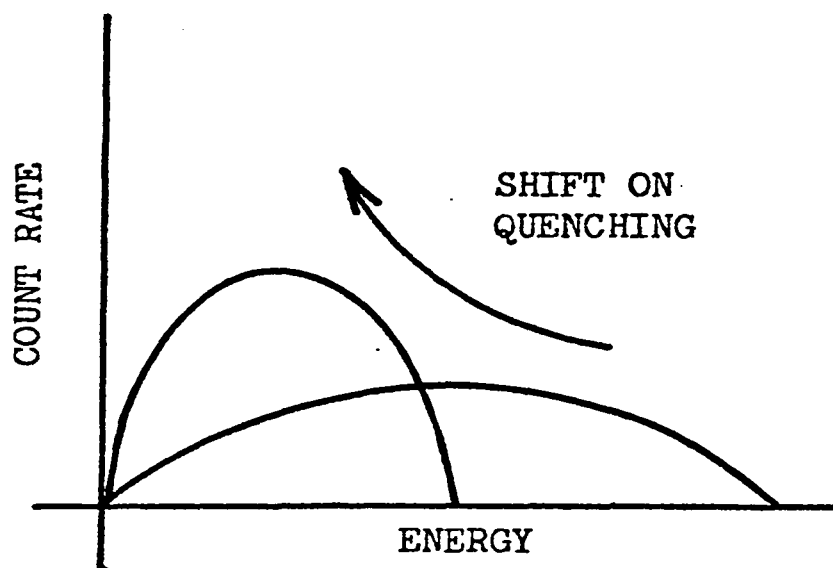
(a) EFFECT OF QUENCHING
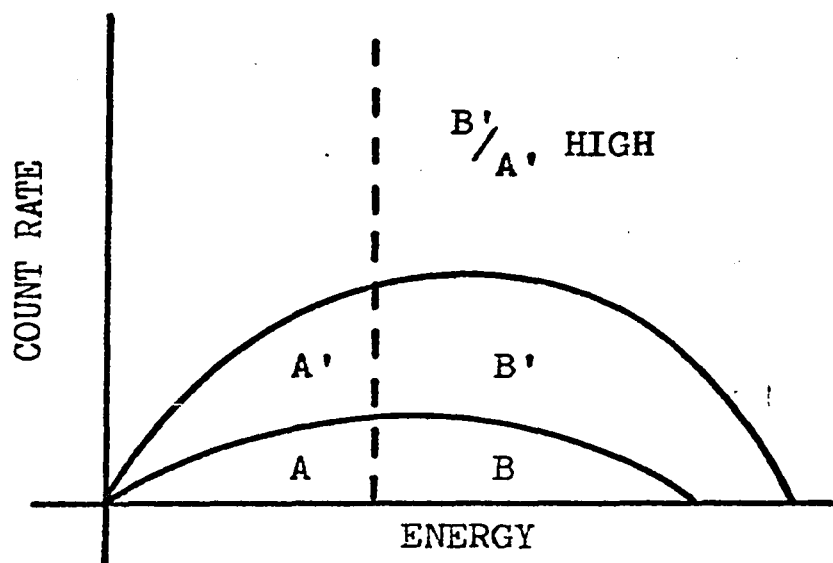
(c) SAMPLE + STANDARD, UNQUENCHED
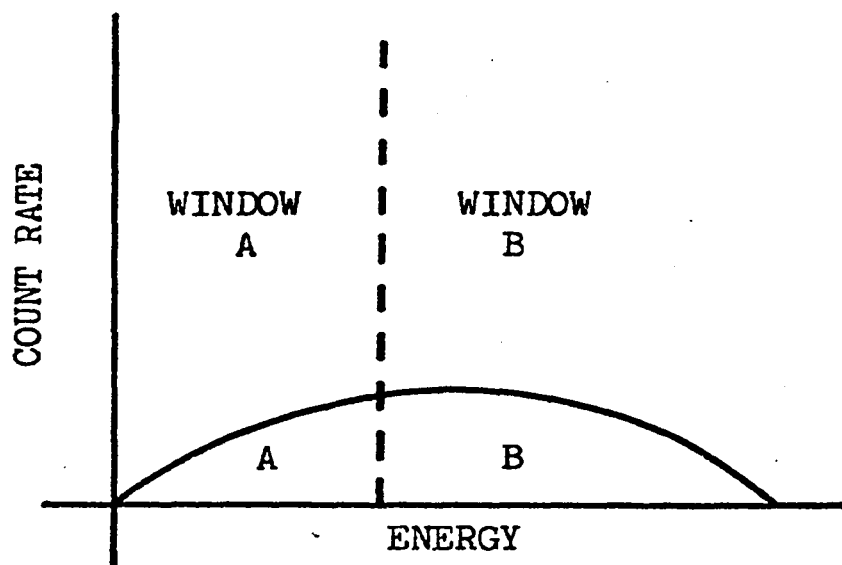
(b) COUNTING IN TWO WINDOWS
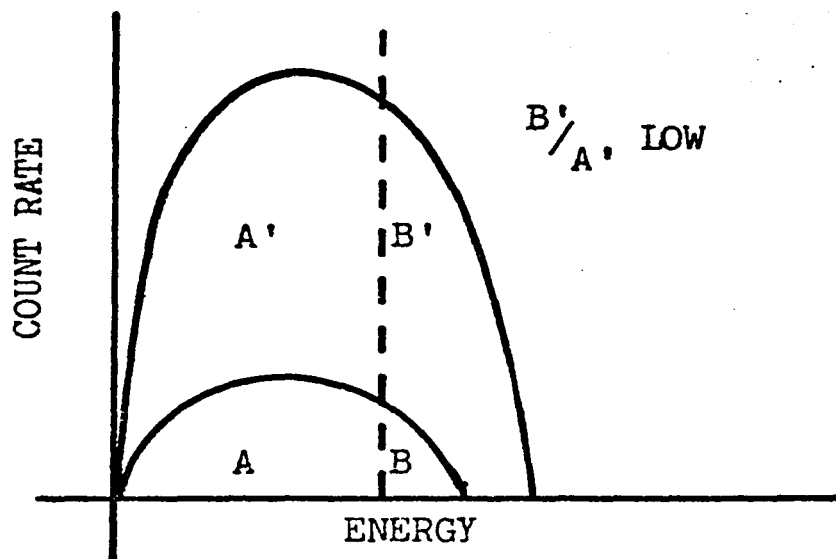
(d) SAMPLE + STANDARD, QUENCHED

was utilized. The degree of quenching is indicated by the ratio of counts

from a built-in standard in two different energy windows. The counts

result from the production of Compton electrons[111] by interaction of

the vial and its contents with gamma radiation from an adjacent ^{137}Cs

source. The unknown sample, which may contain any number of isotopes,

is first counted in two windows, A and B (Figure 32.b.). The ^{137}Cs source

is automatically positioned adjacent to the vial and counting repeated

(Figure 32.c.). The sum of counts from the sample and standard in each

window is A + A' and B + B'. By subtraction and division, the quench

ratio B'/A' is computed internally and printed out. A comparison of

Figure 32.c. and d. shows that quenching results in lower values of the

quench ratio which may be correlated with counting efficiencies in any

window.

TWO-ISOTOPE DETERMINATION

In order to determine the true activity (disintegrations per

minute, d.p.m.) of a sample containing a single isotope it is necessary

to determine the detected count rate (c.p.m.) and the counting efficiency

for the particular isotope and energy window used. Efficiency, expressed

as a percentage, is defined as the ratio c.p.m./d.p.m. and depends on

the emission spectrum of the isotope, the counting window limits and

the degree of quenching.

For two isotopes, simultaneous counts in two windows are required

and the efficiency of counting of each isotope in each window must be

known. Activities of the two isotopes can be determined by solution of

the simultaneous equations:-

$$A = (C \times E_A^C) + (H \times E_A^H) \qquad \ldots 41$$

and

$$B = (C \times E_B^C) + (H \times E_B^H) \qquad \ldots 42$$

where   A   =   Count rate in window A

      B   =   Count rate in window B

      C   =   Activity of isotope 'C' (e.g. $^{14}_{6}C$)

      H   =   Activity of isotope 'H' (e.g. $^{3}_{1}H$)

and E_A^C =   Counting efficiency for isotope 'C' in window A, etc.

Solving for the isotope activities:

$$C = \left\{ B - A \times \frac{E_B^H}{E_A^H} \right\} \bigg/ \left\{ E_B^C - E_A^C \times \frac{E_B^H}{E_A^H} \right\} \qquad \ldots 43$$

and

$$H = \left\{ B - A \times \frac{E_B^C}{E_A^C} \right\} \bigg/ \left\{ E_B^H - E_A^H \times \frac{E_B^C}{E_A^C} \right\} \qquad \ldots 44$$

EXPERIMENTAL PROCEDURE

On the Beckman LSS counter the energy limits to the windows are pre-selected by means of plug-in modules. As the appropriate modules for carbon-14 and tritium counting were not functioning when required, those intended for ^{32}P and ^{32}P with ^{3}H were used successfully. The

energy ranges covered were:

Window A - All detected counts.

Window B - Counts of higher energy than most tritium emissions.

Optimum counting conditions were considered to be those in which E_B^H was sufficiently large that Poisson variation would be small after counting for a convenient time period. It was assumed that this would be achieved if approximately 10% of the recorded tritium counts fell in window B. In order to obtain these conditions a vial with 1 cc tritiated water was prepared and the counts in channels A and B recorded at 'gain' (amplification) stages between 0 and 1000 (full scale). From the results (Figure 33) a gain setting of 700 was selected for all subsequent tests.

The background counts for fifty vials, each containing 10 cc scintillator solution only, were determined and the mean value in each window automatically subtracted from future counts in that window.

To determine the counting efficiencies as functions of quench ratio, two series of standards were prepared for both tritium and carbon-14. Each vial contained 0.5 cc of a standard activity solution (prepared as described in Chapter IV) and 0 to 2.75 cc of water in increments of 0.25 cc. The vials were counted three times and, for each vial, the mean efficiency of counting determined and recorded together with the corresponding mean quench ratio. An equation of the general form

$$E = a + bS + cS^2 + dS^3 \qquad \qquad \ldots 45$$

was computed for each of the four efficiency curves (E_A^C, E_B^C, E_A^H and E_B^H).

FIGURE 33

TRITIUM COUNTS IN WINDOW B AS A FUNCTION OF GAIN
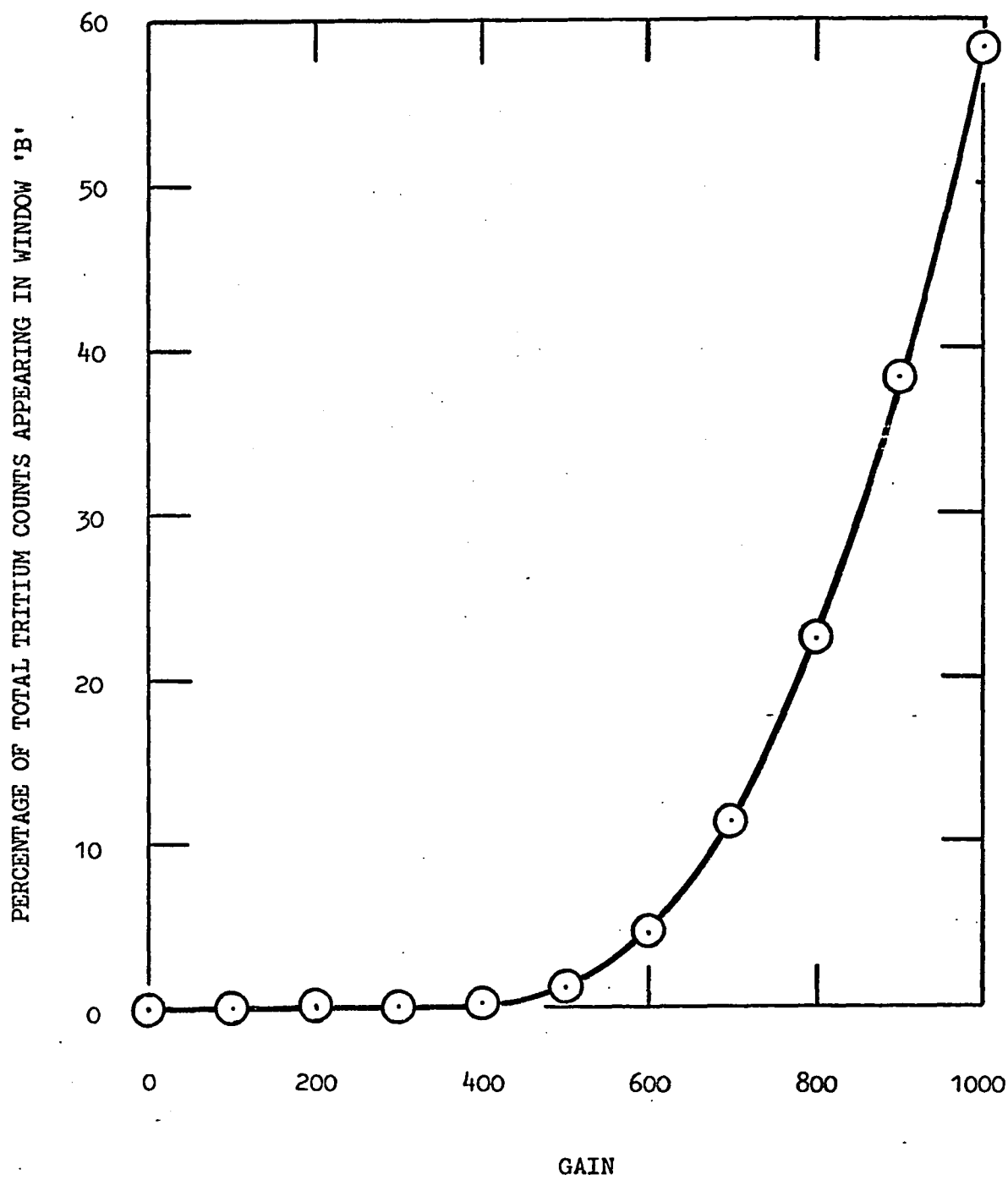
These equations were incorporated in a computer programme (Appendix 3) which was used to solve the simultaneous equations for mixed-isotope samples. All test solutions were sampled in triplicate and each sample counted three times for five minutes. A minimum of 5000 counts were recorded for each solution.

A.3. CALCULATIONS

(a) Efficiency Curves

Equations of the general form:

$$E = a + bS + cS^2 + dS^3 , \qquad \text{...46}$$

where E is the counting efficiency at quench ratio S, were fitted to the experimental standards counts. A least-squares fit was calculated. That is, an equation was derived to minimize the expression

$$\sum_{i=1}^{n} (E_i - a - bS_i - cS_i^2 - dS_i^3)^2 ,$$

where E_i and S_i are the experimentally determined count-efficiency and quench ratio for the ith quench standard and a, b, c and d are constants.

Partial differentiation with respect to a, b, c and d gives the required conditions:

$$\sum_{i=1}^{n} (E_i - a - bS_i - cS_i^2 - dS_i^3) = 0 \qquad \text{...47}$$

$$\sum_{i=1}^{n} S_i (E_i - a - bS_i - cS_i^2 - dS_i^3) = 0 \qquad \text{...48}$$

$$\sum_{i=1}^{n} S_i^2 (E_i - a - bS_i - cS_i^2 - dS_i^3) = 0 \qquad \text{...49}$$

and $\qquad \displaystyle\sum_{i=1}^{n} S_i^3 (E_i - a - bS_i - cS_i^2 - dS_i^3) = 0 \qquad \text{...50}$

Thus the normal equations are:

$$\Sigma(E_i) - na - b\Sigma(S_i) - c\Sigma(S_i^2) - d\Sigma(S_i^3) = 0 \qquad \text{...51}$$

$$\Sigma(S_i E_i) - a\Sigma(S_i) - b\Sigma(S_i^2) - c\Sigma(S_i^3) - d\Sigma(S_i^4) = 0 \qquad \text{...52}$$

$$\Sigma(S_i^2 E_i) - a\Sigma(S_i^2) - b\Sigma(S_i^3) - c\Sigma(S_i^4) - d\Sigma(S_i^5) = 0 \qquad \text{...53}$$

and

$$\Sigma(S_i^3 E_i) - a\Sigma(S_i^3) - b\Sigma(S_i^4) - c\Sigma(S_i^5) - d\Sigma(S_i^6) = 0 \qquad \text{...54}$$

$$i = 1, 2, ..., n$$

Four sets of standards were counted, each with eleven vials. Each vial was counted three times, thus yielding nine E - S combinations. The summations in the normal equations were therefore computed for n = 396 combinations. These values were inserted into the equations and, by simultaneous solution of the four equations, the values of a, b, c and d were determined. This operation was carried out for the four efficiency curves, ^{14}C and ^{3}H in windows A and B. The resultant counting efficiency equations were included in the computer program used to determine the quantities of ^{14}C and ^{3}H in a combined sample.

(b) Computations

A FORTRAN level G computer program was written to convert counts in windows A and B into separate carbon-14 and tritium activities. A second program was used to calculate the corresponding solution concentrations and adsorption densities on hematite.

(i)   Solving for ^{14}C and ^{3}H:

The program is shown in Figure 34. Essential features are:

Line 9. Read data: Counting vial no. and triplicate values of counts in windows A and B and quench ratio.

Lines 10 - 12. Calculation of mean A. B and S for the vial.

Lines 13 - 16. Calculation of the four counting efficiency values corresponding to the mean S.

Lines 17 - 18. Solving for tritium and carbon-14 content.

Lines 19 - 23. Summing results for triplicate vials and calculation of mean.

Line 99. Print-out vial no. (last in group of three) and mean tritium and carbon-14 values.

(ii)   Calculation of Solution Concentrations and Adsorption Densities:

The program is shown in Figure 35. Essential features are:

Line 9. Read-in series number, number of vials in series, initial concentrations of amine ('DAA') and starch and corresponding activities.

Line 12. Read individual vial volume, weight of hematite and final solution activities.

Line 13. Calculate volume of hematite.

Line 17. Calculate equilibrium concentration of amine ('COLL').

Line 21. Calculate equilibrium concentration of starch ('DEPR').

Lines 22 - 23. Calculate adsorption density of amine and starch on

hematite.

FIGURE 34

COMPUTER PROGRAM TO SOLVE FOR ^3H AND ^{14}C

IN A MIXED SAMPLE

```
Ø1      /LOAD FORTG
Ø2      /JOB GO
Ø3              CALL XGCON
Ø4              READ(5,1)N
Ø5        1     FORMAT(1ØG8Ø.Ø)
Ø6              DO 99 I=1,N
Ø7              C=Ø.Ø
Ø8              H=Ø.Ø
Ø9        2     READ(5,1)JAR,A1,A2,A3,B1,B2,B3,S1,S2,S
1Ø              CPMA=(A1+A2+A3)/3.
11              CPMB=(B1+B2+B3)/3.
12              S=(S1+S2+S3)/3.
13              EC14A=-8.7678+27.3414*S+43.3363*S**2-1
14              EC14B=-92.Ø966+28.3554*S+1Ø4.6128*S**2
15              EH3A=-59.9483+26.2297*S+3Ø.4923*S**2-1
16              EH3B=1.1713-1.Ø844*S-2.3Ø79*S**2+1.843
17              H3=1ØØ.Ø*(CPMB-(CPMA*EC14A))/(EH3B-(EH
18              C14=1ØØ.Ø*(CPMB -(CPMA*EH3B/EH3A))/(EC
19              C=C+C14
2Ø              H=H+H3
21              IF(MOD(JAR,3))2,98,2
22       98     C=C/3.
23              H=H/3.
24       99     WRITE(6,3)JAR,C,H
25        3     FORMAT(T5,I3,T13,F8.1,T23,F8.1)
26              STOP
27              END
28      /DATA
```

2,A3,B1,B2,B3,S1,S2,S3
.
.

3414*S+43.3363*S**2-17.9366*S**3
.3554*S+104.6128*S**2-39.7508*S**3
2297*S+30.4923*S**2-10.2909*S**3
4*S-2.3079*S**2+1.8431*S**3
PMA*EC14A))/(EH3B-(EH3A*EC14B/EC14A))
(CPMA*EH3B/EH3A))/(EC14B-(EC14A*EH3B/ EH3A))

8,2

F8.1,T23,F8.1)

FIGURE 35

COMPUTER PROGRAM FOR CALCULATION OF

SOLUTION CONCENTRATION AND ADSORPTION DENSITY

```
Ø1        /LOAD FORTG
Ø2        /JOB GO
Ø3                CALL XGCON
Ø4                WRITE (6,1)
Ø5        1       FORMAT('1',T6,'EQM CONC',T22,'SUR
Ø6                XT8,'DAA',T23,'CONC',T37,'STARCH
Ø7                X/L       MG/G'/)
Ø8                DO 99 J=1,2Ø
Ø9                READ(5,2)LOT,N,DAA,STARCH,H3GO,C1
1Ø                WRITE(6,4)LOT
11                DO 99 I=1,N
12                READ(5,2)V,W,H3END,C14END
13                V=V-W/5.25
14                IF(H3GO.NE.Ø.Ø)GO TO 22
15                COLL=Ø.Ø
16                GO TO 23
17        22      COLL=DAA*H3END/H3GO
18                IF(C14GO.NE.Ø.Ø)GO TO 23
19                DEPR=Ø.Ø
2Ø                GO TO 24
21        23      DEPR=STARCH*C14END/C14GO
22        24      ADSDAA=V*(DAA-COLL)/(W*1ØØØ.)
23                ADSSTA=V*(STARCH-DEPR)/(W*1ØØØ.)
24        99      WRITE(6,3)COLL,ADSDAA,DEPR,ADSSTA
25        2       FORMAT(6G8Ø.Ø)
26        3       FORMAT(T3,E12.5,4X,E12.5,T36,F7.1
27        4       FORMAT(//T1Ø,'**********  RUN NO'
28                STOP
29                END
3Ø        /DATA
```

```
}M CONC',T22,'SURFACE',T36,'EQM CONC      SURFACE'/
IC',T37,'STARCH      CONC'/T9,'M',T24,'M/G',T38,'MG


A,STARCH,H3GO,C14GO


ID,C14END

) TO 22


GO
0 TO 23


D/C14GO
L)/(W*1ØØØ.)
DEPR)/(W*1ØØØ.)
SDAA,DEPR,ADSSTA

X,E12.5,T36,F7.1,T48,F7.4)
*******  RUN NO',I4,'  **********'/)
```

A.4. TABLES

TABLE 1

CONCENTRATIONS OF $\left[RNH_2\right]_{soln.}$, $\left[RNH_3^+\right]_{soln.}$ AND $\left[RNH_2\right]_{ppt.}$

AS A FUNCTION OF pH AND TOTAL DODECYLAMINE CONCENTRATION

  (1) TOTAL CONCENTRATION: 10^{-5}M.

  (2) TOTAL CONCENTRATION: 10^{-4}M.

  (3) TOTAL CONCENTRATION: 10^{-3}M.

  (4) TOTAL CONCENTRATION: 10^{-2}M.

(1) TOTAL CONCENTRATION: 10^{-5}M.

pH	$[RNH_2]_{soln.}$	$[RNH_3^+]_{soln.}$	$[RNH_2]_{ppt.}$
6.0	2.40×10^{-10}	1.00×10^{-5}	--
6.5	7.59×10^{-10}	1.00×10^{-5}	--
7.0	2.40×10^{-9}	1.00×10^{-5}	--
7.5	7.59×10^{-9}	9.99×10^{-6}	--
8.0	2.39×10^{-8}	9.98×10^{-6}	--
8.5	7.54×10^{-8}	9.92×10^{-6}	--
9.0	2.34×10^{-7}	9.77×10^{-6}	--
9.5	7.06×10^{-7}	9.29×10^{-6}	--
10.0	1.94×10^{-6}	8.06×10^{-6}	--
10.5	4.32×10^{-6}	5.68×10^{-6}	--
11.0	7.06×10^{-6}	2.94×10^{-6}	--
11.5	8.84×10^{-6}	1.16×10^{-6}	--
12.0	9.60×10^{-6}	4.00×10^{-7}	--
12.5	9.87×10^{-6}	1.30×10^{-7}	--

(2) TOTAL CONCENTRATION: 10^{-4}M.

pH	$[RNH_2]_{soln.}$	$[RNH_3^+]_{soln.}$	$[RNH_2]_{ppt.}$
6.0	2.40×10^{-9}	1.00×10^{-4}	--
6.5	7.59×10^{-9}	1.00×10^{-4}	--
7.0	2.40×10^{-8}	1.00×10^{-4}	--
7.5	7.59×10^{-8}	9.99×10^{-5}	--
8.0	2.39×10^{-7}	9.98×10^{-5}	--
8.5	7.54×10^{-7}	9.92×10^{-5}	--
9.0	2.34×10^{-6}	9.77×10^{-5}	--
9.5	7.06×10^{-6}	9.29×10^{-5}	--
10.0	1.94×10^{-5}	8.06×10^{-5}	--
10.5	2.00×10^{-5}	2.63×10^{-5}	5.37×10^{-5}
11.0	2.00×10^{-5}	8.33×10^{-6}	7.17×10^{-5}
11.5	2.00×10^{-5}	2.63×10^{-6}	7.74×10^{-5}
12.0	2.00×10^{-5}	8.33×10^{-7}	7.92×10^{-5}
12.5	2.00×10^{-5}	2.63×10^{-7}	7.97×10^{-5}

(3) TOTAL CONCENTRATION: $10^{-3}M$.

pH	$[RNH_2]_{soln.}$	$[RNH_3^+]_{soln.}$	$[RNH_2]_{ppt.}$
6.0	2.40×10^{-8}	1.00×10^{-3}	--
6.5	7.59×10^{-8}	1.00×10^{-3}	--
7.0	2.40×10^{-7}	1.00×10^{-3}	--
7.5	7.59×10^{-7}	9.99×10^{-4}	--
8.0	2.39×10^{-6}	9.98×10^{-4}	--
8.5	7.54×10^{-6}	9.92×10^{-4}	--
9.0	2.00×10^{-5}	8.33×10^{-4}	1.47×10^{-4}
9.5	2.00×10^{-5}	2.63×10^{-4}	7.17×10^{-4}
10.0	2.00×10^{-5}	8.33×10^{-5}	8.97×10^{-4}
10.5	2.00×10^{-5}	2.63×10^{-5}	9.54×10^{-4}
11.0	2.00×10^{-5}	8.33×10^{-6}	9.72×10^{-4}
11.5	2.00×10^{-5}	2.63×10^{-6}	9.77×10^{-4}
12.0	2.00×10^{-5}	8.33×10^{-7}	9.79×10^{-4}
12.5	2.00×10^{-5}	2.63×10^{-7}	9.80×10^{-4}

(4) TOTAL CONCENTRATION: $10^{-2}M$.

pH	$[RNH_2]_{soln.}$	$[RNH_3^+]_{soln.}$	$[RNH_2]_{ppt.}$
6.0	2.40×10^{-7}	1.00×10^{-2}	--
6.5	7.59×10^{-7}	1.00×10^{-2}	--
7.0	2.40×10^{-6}	1.00×10^{-2}	--
7.5	7.59×10^{-6}	9.99×10^{-3}	--
8.0	2.00×10^{-5}	8.33×10^{-3}	1.65×10^{-3}
8.5	2.00×10^{-5}	2.63×10^{-3}	7.35×10^{-3}
9.0	2.00×10^{-5}	8.33×10^{-4}	9.15×10^{-3}
9.5	2.00×10^{-5}	2.63×10^{-4}	9.72×10^{-3}
10.0	2.00×10^{-5}	8.33×10^{-5}	9.90×10^{-3}
10.5	2.00×10^{-5}	2.63×10^{-5}	9.95×10^{-3}
11.0	2.00×10^{-5}	8.33×10^{-6}	9.97×10^{-3}
11.5	2.00×10^{-5}	2.63×10^{-6}	9.98×10^{-3}
12.0	2.00×10^{-5}	8.33×10^{-7}	9.98×10^{-3}
12.5	2.00×10^{-5}	2.63×10^{-7}	9.98×10^{-3}

TABLE 2.   DETERMINATION OF TIME TO EQUILIBRIUM

Adsorption Vial Volume (cc)	Sample Weight (g)	Adsorption Time (hours)	Final Amine Concentration (μmole/l)	Amine Adsorption Density (nmole/gm)
A. INITIAL CONCENTRATION: AMINE, 10^{-5}M; STARCH, zero				
47.36	1.9781	¼	9.08	18.3
47.11	1.8314	1	8.14	37.1
47.63	2.1783	2	6.50	70.0
46.97	1.9255	3	4.55	109.0
47.03	2.1203	5	4.83	103.0
48.09	1.8681	7	3.77	125.0
B. INITIAL CONCENTRATION: AMINE, 10^{-5}M; STARCH, 400 mg/l				
47.59	1.8949	¼	9.30	14.0
46.93	1.7998	1	8.37	32.5
46.83	1.9614	2	5.65	87.0
47.28	2.0082	3	4.95	101.0
48.42	1.9342	5	3.83	123.0
46.63	1.9832	7	4.52	110.0
C. INITIAL CONCENTRATION: AMINE, 10^{-4}M; STARCH, zero				
46.91	1.9653	¼	93.3	130.0
47.21	1.7995	1	65.5	710.0
47.24	2.0316	2	58.2	830.0
47.91	2.0478	3	47.7	1050.0
47.20	1.5183	5	40.1	1200.0
46.97	1.8191	7	52.5	950.0

TABLE 3. RESULTS SUMMARY, SERIES (1)

Adsorption Vial Volume (cc)	Sample Weight (g)	Initial pH	Final pH	% Floats	pH Modifier
47.36	1.85	2.0	2.05	72.0	CH_3COOH
47.11	1.89	4.2	4.25	19.1	CH_3COOH
47.63	1.83	5.7	5.70	11.5	CH_3COOH
46.97	1.90	8.2	8.10	5.5	NaOH
47.03	1.93	10.2	10.15	5.1	NaOH
48.09	2.01	11.8	11.80	7.0	NaOH
46.91	1.94	2.5	2.50	88.1	CH_3COOH
47.21	2.01	3.6	3.75	14.4	CH_3COOH
47.24	1.96	5.7	6.00	7.4	CH_3COOH
47.91	1.78	7.9	7.40	6.9	NaOH
47.20	1.92	9.8	9.80	6.7	NaOH
46.97	1.82	12.1	12.10	6.5	NaOH
46.90	1.94	2.1	2.15	35.1	CH_3COOH
46.66	1.83	2.6	2.65	57.6	CH_3COOH
47.28	1.91	2.9	3.05	28.0	CH_3COOH
46.79	2.11	5.1	5.20	9.6	CH_3COOH
47.59	1.93	1.4	1.40	4.0	HCl
46.93	1.79	2.0	1.95	3.1	HCl
46.83	2.00	3.1	3.15	3.5	HCl
47.28	1.81	4.3	4.30	5.2	HCl
48.42	1.91	5.5	5.60	5.0	HCl
46.63	1.98	5.2	5.40	5.1	HCl

TABLE 4. RESULTS SUMMARY, S

	Adsorption Vial Volume (cc)	Sample Weight (g)	Initial pH	Final pH	% Floats	Counting Vials
(21)	46.83	1.9722	1.9	2.00	1.1	106-108
	47.28	1.8987	4.2	4.35	1.6	109-111
	48.42	1.9858	6.2	6.46	1.5	112-114
	46.63	1.9864	9.3	9.00	2.1	115-117
	47.36	1.9478	10.1	10.05	2.1	118-120
	47.11	1.8634	12.5	12.25	6.0	121-123
(31)	46.83	1.8277	1.9	1.90	6.3	295-297
	47.28	1.9047	4.1	4.20	1.6	298-300
	48.42	1.9321	6.1	6.22	0.5	301-303
	46.63	1.9552	8.0	7.68	2.1	304-306
	47.36	2.0043	10.1	9.95	2.6	307-309
	47.11	1.7826	12.2	12.20	4.6	310-312

Initial Concentrations: (21)   Amine, zero; Starc

(31)   Amine, zero; Starc

JLTS SUMMARY, SERIES (21) AND (31)

ts	Counting Vials	Equilibrium Concentration		Adsorption Density on Hematite	
		Amine (Mole/l)	Starch (mg/l)	Amine (Mole/g)	Starch (mg/g)
1	106-108	--	413.8	--	-0.325
5	109-111	--	388.9	--	0.274
5	112-114	--	380.8	--	0.466
1	115-117	--	413.5	--	-0.315
1	118-120	--	398.8	--	0.028
0	121-123	--	389.2	--	0.271
3	295-297	--	1005.3	--	-0.134
6	298-300	--	944.2	--	1.375
5	301-303	--	984.3	--	0.391
1	304-306	--	1002.3	--	-0.055
6	307-309	--	1006.9	--	-0.162
6	310-312	--	969.0	--	0.814

e, zero;   Starch, 400 mg/l   (1/2 x Counting Vials 103-105)

e, zero;   Starch, 1000 mg/l   (1/2 x Counting Vials 292-294)

TABLE 5.   RESULTS SUMMARY, SEF

	Adsorption Vial Volume (cc)	Sample Weight (g)	Initial pH	Final pH	% Floats	Counting Vials	(
(2)	46.90	1.9476	2.2	2.25	15.1	85-87	9
	46.66	1.8413	4.2	4.60	8.6	88-90	9
	47.28	2.1387	5.9	5.95	31.0	91-93	8
	46.79	1.9552	6.6	6.28	40.3	94-96	8.
	47.59	2.1023	9.7	9.50	80.1	97-99	3.
	46.93	1.8861	11.7	11.70	36.6	100-102	3.
(12)	47.63	1.8963	2.0	1.90	10.0	208-210	9.
	46.97	1.8749	4.0	4.05	5.5	211-213	8.
	47.03	1.9185	6.2	6.18	5.5	214-216	7.
	48.09	1.9455	7.9	7.44	5.9	217-219	5.
	46.97	1.9198	10.0	9.80	4.9	220-222	4.
	47.95	1.8372	11.9	11.90	3.9	223-225	5.

Initial Concentrations: (2)   Amine, 10^{-5}M;   Starch, z

(12)   Amine, 10^{-5}M;   Starch, 1

SUMMARY, SERIES (2) AND (12)

Counting Vials	Equilibrium Concentration		Adsorption Density on Hematite	
	Amine (Mole/l)	Starch (mg/l)	Amine (Mole/g)	Starch (mg/g)
85-87	9.602×10^{-6}	--	9.505×10^{-9}	--
88-90	9.243×10^{-6}	--	1.903×10^{-8}	--
91-93	8.416×10^{-6}	--	3.471×10^{-8}	--
94-96	8.255×10^{-6}	--	4.142×10^{-8}	--
97-99	3.309×10^{-6}	--	1.520×10^{-7}	--
100-102	3.891×10^{-6}	--	1.509×10^{-7}	--
208-210	9.272×10^{-6}	95.2	1.814×10^{-8}	0.120
211-213	8.435×10^{-6}	86.1	3.890×10^{-8}	0.345
214-216	7.400×10^{-6}	96.6	6.321×10^{-8}	0.084
217-219	5.822×10^{-6}	96.9	1.025×10^{-7}	0.076
220-222	4.205×10^{-6}	98.6	1.407×10^{-7}	0.035
223-225	5.023×10^{-6}	96.0	1.290×10^{-7}	0.103

M; Starch, zero   (1/200 x Counting Vials 64-66)

M; Starch, 100 mg/l   (1/2 x Counting Vials 205-207)

TABLE 6. RESULTS SUMMARY, SERIE:

	Adsorption Vial Volume (cc)	Sample Weight (g)	Initial pH	Final pH	% Floats	Counting Vials	Ai (M(
(22)	46.83	1.8682	2.0	1.85	8.2	187–189	1.(
	47.28	1.7720	4.0	4.10	8.6	190–192	8.:
	48.42	1.9212	6.2	6.10	10.7	193–195	7.!
	46.63	1.9744	8.3	7.74	9.0	196–198	5.!
	47.36	1.8762	10.0	9.80	3.2	199–201	5.:
	47.11	1.9360	12.1	12.10	6.4	202–204	5.!
(32)	47.63	1.8987	2.1	1.90	13.3	340–342	1.(
	46.97	1.7795	3.9	3.90	13.6	343–345	8.:
	47.32	1.9813	6.1	6.18	12.5	346–348	8.(
	48.09	1.9572	7.6	6.95	9.9	349–351	6.!
	46.97	1.8198	9.7	9.10	1.7	352–354	4.:
	47.95	1.7401	11.9	11.60	2.4	355–357	8.(

Initial Concentrations: (22)   Amine, 10^{-5}M;   Starch, l

(32)   Amine, 10^{-5}M;   Starch, ·

UMMARY, SERIES (22) AND (32)

ounting Vials	Equilibrium Concentration		Adsorption Density on Hematite	
	Amine (Mole/l)	Starch (mg/l)	Amine (Mole/g)	Starch (mg/g)
87-189	1.042×10^{-5}	381.7	negative	0.455
90-192	8.738×10^{-6}	382.8	3.343×10^{-8}	0.455
93-195	7.944×10^{-6}	389.9	5.142×10^{-8}	0.252
96-198	5.826×10^{-6}	396.2	9.777×10^{-8}	0.090
99-201	5.238×10^{-6}	392.3	1.193×10^{-7}	0.193
02-204	5.859×10^{-6}	386.8	9.997×10^{-8}	0.319
40-342	1.038×10^{-5}	1055.7	negative	-1.386
43-345	8.787×10^{-6}	959.0	3.178×10^{-8}	1.075
46-348	8.059×10^{-6}	943.9	4.598×10^{-8}	1.329
49-351	6.997×10^{-6}	942.3	7.321×10^{-8}	1.408
52-354	4.768×10^{-6}	972.8	1.340×10^{-7}	0.698
55-357	8.048×10^{-6}	912.6	5.343×10^{-8}	2.391

^{5}M; Starch, 400 mg/l (1/2 x Counting Vials 184-186)

^{5}M; Starch, 1000 mg/l (1/2 x Counting Vials 337-339)

TABLE 7.   RESULTS SUMMARY, SE<u></u>

	Adsorption Vial Volume (cc)	Sample Weight (g)	Initial pH	Final pH	% Floats	Counting Vials
(3)	46.91	1.8499	2.1	2.00	44.1	67-69
	47.21	1.7899	4.0	4.30	98.9	70-72
	47.24	1.9146	6.0	6.18	96.9	73-75
	47.91	2.0208	6.9	6.68	95.4	76-78
	47.20	1.9432	9.9	9.40	94.6	79-81
	46.97	1.8923	11.9	11.90	76.1	82-84
(13)	46.90	1.9214	2.0	2.00	33.1	232-234
	46.66	1.8960	4.3	4.30	22.9	235-237
	47.28	1.9424	6.5	6.35	30.0	238-240
	46.79	1.8653	7.3	7.05	28.3	241-243
	47.59	1.8710	10.0	9.80	65.5	244-246
	46.93	1.8300	12.2	12.20	73.5	247-249

Initial Concentrations: (3)   Amine, 10^{-5}M; Starch

(13)   Amine, 10^{-4}M; Starch

s	Counting Vials	Equilibrium Concentration		Adsorption Density on Hematite	
		Amine (Mole/l)	Starch (mg/l)	Amine (Mole/g)	Starch (mg/g)
	67-69	9.514×10^{-5}	--	1.226×10^{-7}	--
	70-72	9.918×10^{-5}	--	2.145×10^{-8}	--
	73-75	9.339×10^{-5}	--	1.618×10^{-7}	--
	76-78	9.321×10^{-5}	--	1.596×10^{-7}	--
	79-81	4.642×10^{-5}	--	1.291×10^{-6}	--
	82-84	3.377×10^{-5}	--	1.631×10^{-6}	--
	232-234	9.969×10^{-5}	65.2	7.463×10^{-9}	0.843
	235-237	9.385×10^{-5}	80.5	1.503×10^{-7}	0.476
	238-240	8.678×10^{-5}	88.0	3.192×10^{-7}	0.291
	241-243	8.437×10^{-5}	84.7	3.890×10^{-7}	0.382
	244-246	3.791×10^{-5}	77.5	1.568×10^{-6}	0.568
	247-249	4.345×10^{-5}	81.9	1.440×10^{-6}	0.460

, 10^{-5}M;   Starch, zero   (1/200 x Counting Vials 64-66)

, 10^{-4}M;   Starch, 100 mg/l   (1/2 x Counting Vials 229-231)

TABLE 8. RESULTS SUMMARY, SER]

	Adsorption Vial Volume (cc)	Sample Weight (g)	Initial pH	Final pH	% Floats	Counting Vials	(
(23)	46.91	1.8763	1.9	1.90	15.9	253-255	(
	47.21	1.8503	4.1	4.10	19.3	256-258	(
	47.24	1.8040	6.1	6.16	22.7	259-261	(
	47.91	1.8636	8.5	7.98	27.5	262-264	(
	47.20	2.0707	10.0	9.90	87.2	265-267	(
	46.97	1.7782	12.1	12.10	60.0	268-270	(
(33)	46.91	1.8254	1.7	1.60	22.3	361-363	(
	47.21	1.8861	4.1	4.15	22.9	364-366	(
	47.24	1.9784	6.1	6.14	30.5	367-369	(
	47.91	2.0022	8.1	7.28	29.5	370-372	(
	47.20	1.8947	9.6	9.35	90.8	373-375	(
	46.97	1.8165	11.9	11.90	29.7	376-378	(

Initial Concentrations: (23) Amine, 10^{-4}M; Starch,

(33) Amine, 10^{-4}M; Starch,

| Counting Vials | Equilibrium Concentration | | Adsorption Density on Hematite | |
	Amine (Mole/l)	Starch (mg/l)	Amine (Mole/g)	Starch (mg/g)
253-255	9.238×10^{-5}	371.4	1.892×10^{-7}	0.710
256-258	8.879×10^{-5}	352.6	2.839×10^{-7}	1.199
259-261	8.549×10^{-5}	369.4	3.771×10^{-7}	0.796
262-264	7.544×10^{-5}	379.0	6.267×10^{-7}	0.535
265-267	5.364×10^{-5}	380.6	1.048×10^{-6}	0.438
268-270	5.778×10^{-5}	381.3	1.107×10^{-6}	0.489
361-363	9.464×10^{-5}	969.5	1.366×10^{-7}	0.777
364-366	8.842×10^{-5}	928.2	2.878×10^{-7}	1.783
367-369	8.727×10^{-5}	966.9	3.013×10^{-7}	0.783
370-372	8.167×10^{-5}	945.2	4.352×10^{-7}	1.303
373-375	6.707×10^{-5}	999.1	8.140×10^{-7}	0.021
376-378	7.195×10^{-5}	928.0	7.201×10^{-7}	1.849

0^{-4}M; Starch, 400 mg/l (1/2 x Counting Vials 250-252)

0^{-4}M; Starch, 1000 mg/l (1/2 x Counting Vials 358-360)

TABLE 9. RESULTS SUMMARY, SERI

	Adsorption Vial Volume (cc)	Sample Weight (g)	Initial pH	Final pH	% Floats	Counting Vials	(
(4)	47.36	1.9365	1.8	1.80	77.0	46–48	9
	47.11	2.0613	3.9	3.95	98.0	49–51	9
	47.63	1.7959	5.8	5.85	98.1	52–54	9
	46.97	2.0874	7.1	6.62	96.5	55–57	9
	47.03	1.8513	10.0	9.85	99.5	58–60	5
	48.09	1.9181	11.9	11.90	84.6	61–63	7
(14)	46.90	1.8901	2.1	2.00	27.8	382–384	1
	46.66	1.8759	4.0	4.00	43.5	385–387	9
	47.28	1.8397	5.9	6.18	66.5	388–390	9
	46.79	1.9785	8.6	7.75	82.4	391–393	8
	47.59	1.9280	10.0	9.90	93.5	394–396	5
	46.93	1.9831	11.8	11.75	77.8	397–399	2

Initial Concentrations: (4) Amine, 10^{-3}M; Starch,

(14) Amine, 10^{-3}M; Starch,

| Counting Vials | Equilibrium Concentration | | Adsorption Density on Hematite | |
	Amine (Mole/l)	Starch (mg/l)	Amine (Mole/g)	Starch (mg/g)
46–48	9.301×10^{-4}	--	1.696×10^{-6}	--
49–51	9.915×10^{-4}	--	1.922×10^{-7}	--
52–54	9.636×10^{-4}	--	9.592×10^{-7}	--
55–57	9.363×10^{-4}	--	1.422×10^{-6}	--
58–60	5.316×10^{-4}	--	1.181×10^{-5}	--
61–63	7.196×10^{-5}	--	2.309×10^{-5}	--
382–384	1.005×10^{-3}	88.8	negative	0.276
385–387	9.596×10^{-4}	87.0	9.965×10^{-7}	0.320
388–390	9.293×10^{-4}	89.1	1.804×10^{-6}	0.278
391–393	8.923×10^{-4}	87.7	2.527×10^{-6}	0.288
394–396	5.566×10^{-4}	91.1	1.086×10^{-5}	0.218
397–399	2.285×10^{-4}	88.9	1.811×10^{-5}	0.260

10^{-3}M;   Starch, zero   (1/2 x Counting Vials 43–45)

10^{-3}M;   Starch, 100 mg/l   (1/2 x Counting Vials 379–381)

TABLE 10. RESULTS SUMMARY, SERIES

	Adsorption Vial Volume (cc)	Sample Weight (g)	Initial pH	Final pH	% Floats	Counting Vials	Am: (Mo:
(24)	46.83	1.9540	2.3	2.00	64.6	274-276	9.9:
	47.28	1.7957	4.4	4.10	70.5	277-279	9.6!
	48.42	2.0366	6.1	5.93	70.6	280-282	9.5(
	46.63	1.9304	9.0	8.50	99.0	283-285	7.6:
	47.36	1.9135	10.6	10.60	85.3	286-288	6.3(
	47.11	1.7915	12.0	12.10	80.7	289-291	8.5:
(34)	46.90	1.9627	2.0	1.95	37.8	316-318	7.74
	46.66	1.9601	4.1	4.20	41.2	319-321	9.0:
	47.28	1.9965	6.1	6.12	46.5	322-324	5.5:
	46.79	1.8758	7.9	7.42	75.1	325-327	6.81
	47.59	2.0437	9.9	9.75	98.0	328-330	9.77
	46.93	1.8256	11.8	11.60	59.1	331-333	1.24

Initial Concentrations: (24) Amine, $10^{-3}M$; Starch, 40

(34) Amine, $10^{-3}M$; Starch, 10

S SUMMARY, SERIES (24) AND (34)

Counting Vials	Equilibrium Concentration		Adsorption Density on Hematite	
	Amine (Mole/l)	Starch (mg/l)	Amine (Mole/g)	Starch (mg/g)
274-276	9.938×10^{-4}	386.5	1.471×10^{-7}	0.322
277-279	9.654×10^{-4}	384.8	9.040×10^{-7}	0.398
280-282	9.562×10^{-4}	378.1	1.032×10^{-6}	0.516
283-285	7.636×10^{-4}	380.6	5.664×10^{-6}	0.464
286-288	6.308×10^{-4}	392.0	9.068×10^{-6}	0.198
289-291	8.513×10^{-4}	383.3	3.883×10^{-6}	0.435
316-318	7.747×10^{-4}	1070.2	5.341×10^{-6}	-1.664
319-321	9.078×10^{-4}	983.9	2.177×10^{-6}	0.381
322-324	5.531×10^{-4}	988.1	1.050×10^{-5}	0.280
325-327	6.818×10^{-4}	998.0	7.877×10^{-6}	0.050
328-330	9.778×10^{-4}	1003.5	5.130×10^{-7}	-0.082
331-333	1.243×10^{-3}	1007.7	negative	-0.198

0^{-3}M; Starch, 400 mg/l   (1/2 x Counting Vials 271-273)

0^{-3}M; Starch, 1000 mg/l   (1/2 x Counting Vials 313-315)

TABLE 11. RESULTS SUMMARY, SERIES

	Adsorption Vial Volume (cc)	Sample Weight (g)	Initial pH	Final pH	% Floats	Counting Vials	Am (Mo
(5)	47.28	1.8842	1.9	1.80	--	4-6	9.6
	46.79	1.9085	3.7	3.60	--	7-9	9.2
	47.59	1.8948	5.3	5.30	--	10-12	9.1
	46.93	1.8657	8.3	8.10	--	13-15	8.7
	46.83	1.9716	9.9	9.90	--	16-18	8.4
	47.28	2.0105	11.8	11.80	--	19-21	5.3
(5')	46.91	1.95	2.0	2.05	80.0	--	
	47.21	1.89	3.9	3.85	82.1	--	
	47.24	1.98	5.9	5.70	83.7	--	
	47.91	2.04	8.3	8.12	92.1	--	
	47.20	2.03	10.1	9.70	82.6	--	
	46.97	1.90	11.7	11.70	74.0	--	

Note   Flotation cell broken for first series.   Second series

Initial Concentration: (5) Amine, 10^{-2}M;   Star

SUMMARY, SERIES (5) AND (5')

Counting Vials	Equilibrium Concentration		Adsorption Density on Hematite	
	Amine (Mole/l)	Starch (mg/l)	Amine (Mole/g)	Starch (mg/g)
4-6	9.692×10^{-3}	--	7.670×10^{-6}	--
7-9	9.211×10^{-3}	--	1.919×10^{-5}	--
10-12	9.110×10^{-3}	--	2.218×10^{-5}	--
13-15	8.723×10^{-3}	--	3.189×10^{-5}	--
16-18	8.455×10^{-3}	--	3.640×10^{-5}	--
19-21	5.348×10^{-3}	--	1.085×10^{-4}	--
--	--	--	--	--
--	--	--	--	--
--	--	--	--	--
--	--	--	--	--
--	--	--	--	--
--	--	--	--	--

Second series run to obtain flotation curve only.

ie, 10^{-2}M; Starch, zero   (1/2 x Counting Vials 1-3)

TABLE 12. RESULTS SUMMARY, SEF

	Adsorption Vial Volume (cc)	Sample Weight (g)	Initial pH	Final pH	% Floats	Counting Vials	
(11)	47.63	1.9394	2.0	2.00	0.5	124-126	
	46.97	1.9702	4.2	4.40	0.5	127-129	
	47.03	1.8733	6.2	6.38	0.5	130-132	
	48.09	1.9733	7.6	7.38	0.5	133-135	
	46.97	1.9318	9.9	9.80	1.1	136-138	
	47.95	1.9636	11.8	11.85	5.1	139-141	
(15)	46.83	1.8616	2.1	1.90	26.2	442-444	ς
	47.28	1.9195	4.1	4.15	56.4	445-447	1
	48.42	1.9435	6.3	6.42	89.4	448-450	ε
	46.63	1.9340	8.2	8.30	91.2	451-453	ε
	47.36	1.8675	10.1	10.00	85.6	454-456	ε
	47.11	1.9069	11.9	11.75	42.0	Note (i)	

Note (i): Not sampled. Phase separation of precipita

Initial Concentrations: (11) Amine, zero; Starch,

(15) Amine, 10^{-2}M; Starch,

ıts	Counting Vials	Equilibrium Concentration		Adsorption Density on Hematite	
		Amine (Mole/1)	Starch (mg/1)	Amine (Mole/g)	Starch (mg/g)
5	124–126	--	98.3	--	0.041
5	127–129	--	97.6	--	0.057
5	130–132	--	95.4	--	0.114
5	133–135	--	100.3	--	-0.008
1	136–138	--	97.1	--	0.070
1	139–141	--	95.9	--	0.100
2	442–444	9.617×10^{-3}	73.9	9.569×10^{-6}	0.652
4	445–447	1.001×10^{-2}	84.9	negative	0.369
4	448–450	8.924×10^{-3}	91.6	2.661×10^{-5}	0.208
2	451–453	8.747×10^{-3}	104.8	2.997×10^{-5}	-0.116
5	454–456	8.405×10^{-3}	95.4	4.015×10^{-5}	0.115
)	Note (i)	--	--	--	--

ıtion of precipitated amine.

, zero; Starch, 100 mg/l   (1/8 x Counting Vials 103–105)

, 10^{-2}M; Starch, 100 mg/l   (1/2 x Counting Vials 439–441)

TABLE 13. RESULTS SUMMARY, SE]

	Adsorption Vial Volume (cc)	Sample Weight (g)	Initial pH	Final pH	% Floats	Counting Vials
(25)	46.83	1.8558	1.9	1.75	16.0	403–405
	47.28	1.9760	3.9	4.00	30.1	406–408
	48.42	1.9068	6.1	6.27	38.7	409–411
	46.63	1.8667	8.2	8.16	76.7	412–414
	47.36	2.0127	9.9	10.00	86.1	415–417
	47.11	2.0702	11.8	11.70	42.8	Note (i)
(35)	46.90	1.8763	2.1	2.10	30.4	421–423
	46.66	2.0508	4.0	3.95	39.5	424–426
	47.28	1.8837	5.8	5.91	68.7	427–429
	46.79	1.8556	8.0	8.04	87.5	430–432
	47.59	1.9190	9.8	9.90	80.6	433–435
	46.93	2.0723	11.8	11.80	30.0	436–438

Note (i): Not sampled. Phase separation of precipit:

Initial Concentrations: (25) Amine, 10^{-2}M; Starch,

(35) Amine, 10^{-2}M; Starch,

Counting Vials	Equilibrium Concentration		Adsorption Density on Hematite	
	Amine (Mole/l)	Starch (mg/l)	Amine (Mole/g)	Starch (mg/g)
403–405	9.620×10^{-3}	351.5	9.510×10^{-6}	1.215
406–408	1.006×10^{-2}	376.4	negative	0.560
409–411	8.964×10^{-3}	358.9	2.610×10^{-5}	1.037
412–414	9.488×10^{-3}	415.7	1.269×10^{-5}	-0.389
415–417	8.653×10^{-3}	403.1	3.143×10^{-5}	-0.073
Note (i)	--	--	--	--
421–423	9.857×10^{-3}	1006.4	3.551×10^{-6}	-0.159
424–426	9.424×10^{-3}	905.4	1.299×10^{-5}	2.135
427–429	9.891×10^{-3}	993.9	2.725×10^{-6}	0.153
430–432	9.794×10^{-3}	1007.4	5.155×10^{-6}	-0.186
433–435	9.074×10^{-3}	918.8	2.277×10^{-5}	1.998
436–438	7.694×10^{-3}	901.1	5.179×10^{-5}	2.221

on of precipitated amine.

10^{-2}M;   Starch, 400 mg/l   (1/2 x Counting Vials 400–402)

10^{-2}M;   Starch, 1000 mg/l   (1/2 x Counting Vials 418–420)

TABLE 14. SOLUBILITY OF AMINE-STARCH MIXTURES

Amine Concentration (Mole/l)	Starch Concentration (mg/l)	Limit of Solubility (pH)		
		1st	2nd	MEAN
10^{-2}	0	7.6	7.6	7.6
10^{-2}	100	7.6	7.5	7.55
10^{-2}	400	7.7	7.6	7.65
10^{-2}	1000	7.8	7.8	7.8
				7.65 *
10^{-3}	0	8.8	8.6	8.7
10^{-3}	100	8.6	8.6	8.6
10^{-3}	400	8.7	8.7	8.7
10^{-3}	1000	8.8	8.8	8.8
				8.7 *
10^{-4}	0	9.8	9.6	9.7
10^{-4}	100	9.8	9.9	9.85
10^{-4}	400	9.8	9.9	9.85
10^{-4}	1000	9.8	9.8	9.8
				9.8 *
10^{-5}		- precipitate not detectable -		

* Plotted in Figure 2.

TABLE 15. X-RAY DIFFRACTION RESULTS

Observed	d Spacing ('A')		Difference	Peak Intensity I/I_o	
2θ	Calc.	ASTM 13-534	('A')	Observed	ASTM 13-534
30.4	3.694	3.66	0.034	20	25
42.0	2.703	2.69	0.013	100	100
45.2	2.521	2.51	0.011	60	50
--	--	2.285	--	0	2
52.0	2.210	2.201	0.009	30	30
55.5	2.080	2.070	0.010	1	2
63.3	1.846	1.838	0.008	50	40
69.7	1.695	1.690	0.005	60	60
72.3	1.642	1.634	0.008	5	4
74.5	1.600	1.596	0.004	20	16
81.3	1.487	1.484	0.003	35	35
83.5	1.455	1.452	0.003	35	35
91.7	1.350	1.349	0.001	5	4
95.2 *	1.312	1.310	0.002	25	20
100.6	1.259	1.258	0.001	10	8
104.2	1.228	1.226	0.002	1	2
105.9	1.214	1.213	0.001	5	4
108.9	1.191	1.189	0.002	10	8
112.3	1.166	1.162	0.004	10	10
116.2	1.141	1.141	0.000	10	12
122.8	1.103	1.102	0.001	15	14
128.2	1.077	1.076	0.001	1	2
133.2	1.056	1.055	0.001	15	18
136.5	1.043	1.042	0.001	1	2
137.6	1.039	1.038	0.001	1	2
156.8	0.9889	0.9890	0.0001	10	10

**

* All higher angles the weighted mean of peaks from α_1 and α_2 resolved

peaks: $2\theta_\alpha = 2\theta_{\alpha_1} + (2\theta_{\alpha_2} - 2\theta_{\alpha_1}) / 3$

** Higher listed peaks beyond equipment range.

TABLE 16. ATOMIC ABSORPTION ANALYSIS

(a) STANDARDS

CONCENTRATION p.p.m. IRON	ABSORBANCE
20	0.187
40	0.308
60	0.391
80	0.450
100	0.490

(b) SAMPLES

	WEIGHT g	ABSORBANCE	CONCENTRATION p.p.m. IRON
(i)	0.7733	0.368	53.7
(ii)	0.5174	0.287	36.1
(iii)	0.3790	0.232	26.5

(c) CALCULATION

Dilution Factor: 10,000.

Therefore % Fe in sample (i)   =   53.7 x 10,000/0.7733

                                =   69.7%

Similarly for sample (ii), % Fe =   69.8%

    and for sample (iii), % Fe =   69.5%

Mean value: 69.7% Fe

BIBLIOGRAPHY

1. Cofield, G.E. and D.F. MacKnight; Mining Review, 52, No. 10, March 1963.

2. Elliot, R.A.; in 'The Milling of Canadian Ores', 6th Commonwealth Min. and Met. Congress, 399, Canada 1955.

3. Morning, J.L.; Iron Ore, in 'Minerals Year Book Vol. I-II, Metals, Minerals and Fuels', U.S. Dept. of the Interior, Bureau of Mines, Washington, 1969, 571.

4. Knoerr, A.W.; Iron Ore and Steel, Eng. and Min. J., 171, No. 3, 144 (1970).

5. Schneider, V.B.; Iron Ore, Preprint 22 for the 'Canadian Minerals Yearbook 1968', Dept. of Energy, Mines and Resources, Ottawa, 1969.

6. Jones, W.R.; 'Minerals in Industry', Edn. 4, Penguin Books Ltd., U.K., 1963, 138.

7. Jones, G.H. and W.J.D. Stone; 'Wet Magnetic Separator for Feebly Magnetic Minerals', I.M.P.C., London, 1960, 717.

8. Barthelemy, R.E. and R.G. Mora; 'Electrical High Tension Minerals Beneficiation: Principles and Technical Aspects', I.M.P.C., London, 1960, 757.

9. Eketorp, S.; Magnetic Roasting of Hematite in 'Progress in Mineral Dressing', Trans. I.M.D.C., Stockholm, 1957, (Almqvist and Wiksell, Stockholm 1968), 285.

10. Hertzog, M.E. and M.L. Backer; I.M.P.C. (Cannes), Pergamon, 1963.

11. McKim, A.M. and J. Ambler; Ore Dressing - Scully Mine, Paper 94, 71st A.G.M., C.I.M., Montreal, 1969.

12. Taciuk, W. and A. Sobering; Operation of the Iron Ore Company of Canada's Pelletizing Plant, Bull. C.I.M., 62, No. 687, 722 (1969).

13. Beaumont, F.V.; The Fina Metal Process and its Development, Paper 46, A.G.M., C.I.M., Montreal, 1969.

14. Glembotskii, V.A.; 'Flotation', Primary Sources, 1963, 22.

15. Derjaguin, B.V., B.V. Karasiev and Z.M. Zorin; On the Special State of Liquids in Surface Layers, in 'Structure and Physical Properties of Substances in Liquid State' (Papers), Kiev University, 1954.

16. Helmholtz, H.L.F. von; Studien ueber elektrische Grenzschichten, Ann. Physik, 7, No. 4, 337 (1879).

17. Gouy, M; Sur la Constitution de la Charge Electrique à la Surface d'un Electrolyte, J. Phys., 9, No. 4, 457, (1910).

18. Chapman, D.L.; A Contribution to the Theory of Electrocapillarity, Phil. Mag. 25, No. 6, 475, (1913).

19. Stern, O.; The Theory of the Electrolytic Double Layer, Z. Elektro-chemie 30, 508, (1924).

20. Grahame, D.C.; The Electrical Double Layer and the Theory of Electrocapillarity, Chem. Revs. 41, 441, (1947).

21. Osipow, L.I.; 'Surface Chemistry, Theory and Industrial Application', Reinhold, N.Y., 1962, 70.

22. Gaudin, A.M.; 'Flotation', Edn. 2, McGraw-Hill, N.Y., 1957, 101.

23. Douglas, H.W. and R.A. Walker; The Electrokinetic Behaviour of Iceland Spar Against Aqueous Electrolyte Solutions. Trans. Faraday Soc., 46, 559, (1950).

24. O'Connor, D.J., N. Street and A.S.B. Buchanan; Charge Densities and Surface Conductancies at Solid-Solution Interfaces, Austral. J. Chem. 7, 245, (1954).

25. Bikerman, J.J.; 'Surface Chemistry, Theory and Applications', Edn. 2. Academic Press, N.Y., 1958.

26. Smith. G.W. and T. Salman; Zero-Point-of-Charge of Hematite and Zirconia, Cdn. Met. Quart. 5, No. 2, 93, (1966).

27. Smith, G.W.; The Adsorption of Dehydroabietylamine Acetate on Mineral Oxides, Ph.D. thesis, McGill, 1967, 17.

28. Parks, G.A. and P.L. de Bruyn; The Zero Point of Charge of Oxides, J. Phys. Chem. 66, 967, (1962).

29. Glemser, O. and G. Rieck; Zur Bindung des Wassers in den Systemen Al_2O_3/H_2O, SiO_2/H_2O und Fe_2O_3/H_2O, Z. für Anorg. und Allgem. Chemie, 297, 175, (1958).

30. Sutherland, K.L. and I.W. Wark; 'Principles of Flotation', Aust. I.M.M., Melbourne, 1955, 41.

31. Klassen, V.I. and V.A. Mokrousov;   'An Introduction to the Theory of Flotation', Butterworths, London, 1963, 159.

32. Joy, A.S. and A.J. Robinson;   'Flotation - Recent Progress in Surface Science', 2, Academic Press, N.Y., 1964, 172.

33. Bragg, Sir L. and G.F. Claringbull;   The Crystalline State, Vol. IV, 'Crystal Structures of Minerals', G. Bell and Sons, London, 1965, 22.

34. Langmuir, I.;   The Adsorption of Gases on Planar Surfaces of Glass, Mica and Platinum, J. Am. Chem. Soc. 40, 1361, (1918).

35. Moore, W.J.;   'Physical Chemistry', Longmans, London, 1957, 514.

36. Reference 22, p. 82.

37. Brunauer, S., P.H. Emmett and E. Teller;   Adsorption of Gases in Multimolecular Layers, J. Am. Chem. Soc. 60, 309, (1938).

38. Freundlich, H.;   'Kapillarchemie', Leipzig, 1909; and 'Colloid and Capillary Chemistry', Methuen, London, 1926.

39. Sipps, R.;   On the Structure of a Catalyst Surface, J. Chem. Phys. 16, 490, (1948).

40. Major-Marothy, G.;   Flotation Experiments with Earthy Iron Ores, Bull. C.I.M. 60, 1060, (1967).

41. Cooke, S.R.B., N.F. Schultz and E.W. Lindroos;   The Effect of Certain Starches on Quartz and Hematite Suspensions, Trans. A.I.M.E., 193, 697, (1952).

42. Chang, C.S., S.R.B. Cooke and R.O. Huch;   Starches and Starch Products as Depressants in Amine Flotation of Iron Ore, Trans. A.I.M.E. 196, 1282, (1953).

43. Schultz, N.F. and S.R.B. Cooke;   Froth Flotation of Iron Ores - Adsorption of Starch Products and Laurylamine Acetate, Ind. and Eng. Chem. 45, 2767, (1953).

44. Chang, C.S.;   Substituted Starches in Amine Flotation of Iron Ore, Trans. A.I.M.E. 199, 922, (1954).

45. Iwasaki, I. and R.W. Lai;   Starches and Starch Products as Depressants in Soap Flotation of Activated Silica from Iron Ores, Trans. A.I.M.E. 232, 364, (1965).

46. Iwasaki, I.;   Interaction of Starch and Calcium in Soap Flotation of Activated Silica from Iron Ores, Trans. A.I.M.E. 232, 384, (1965).

47. Kellogg, H.H. and H. Vásquez-Rosas; Amine Flotation of Sphalerite-Galena Ores, Trans. A.I.M.E. 169, 476, (1946).

48. Hoerr, C.W., M.R. McCorkle and A.W. Ralston; Studies on High Molecular Weight Aliphatic Amines and their Salts. X. Ionization Constants of 17 and Symmetrical 27 Amines in Aqueous Solution, J. Am. Chem. Soc. 65, 328, (1943).

49. Moore, W.J.; 'Physical Chemistry', Edn. 3, Prentice-Hall, N.J., 1962, 365.

50. Brown, D.J.; Unpublished Results, Dept. Metallurgy, M.I.T., quoted in de Bruyn, P.L.; Flotation of Quartz by Cationic Collectors, Trans. A.I.M.E. 202, 292, (1955).

51. Williams, J.M.; The Chemical Evidence for the Structure of Starch, in 'Starch and its Derivatives', J.A. Radley, Ed., Chapman and Hall, London, 1968, 125.

52. Cram, D.J. and D.G. Hammond; 'Organic Chemistry', McGraw-Hill, N.Y., 1959, 582.

53. Reference 51, p. 120.

54. Rundle, R.E. and D. French; J. Am. Chem. Soc. 65, 1707, (1943).

55. Bear, R.S.; Complex Formation between Starch and Organic Molecules, J. Am. Chem. Soc. 66, 2122, (1944).

56. Reference 33, p. 96.

57. Parks, G.A.; 'A Study of the Surface of Ferric Oxides in Aqueous Systems', Ph.D. thesis, M.I.T., 1959.

58. Parks, G.A. and P.L. de Bruyn; The Zero-Point-of-Charge of Oxides, J. Phys. Chem. 66, 967, (1962).

59. Parks, G.A.; The Isoelectric Points of Solid Oxides, Solid Hydroxides and Aqueous Hydroxo Complex Systems, Chem. Rev. 65, 177, (1965).

60. Reference 27, p. 102.

61. Gaudin, A.M. and D.W. Fuerstenau; Quartz Flotation with Cationic Collectors, Trans. A.I.M.E. 202, 958, (1955).

62. Taggart, A.F.; 'Handbook of Mineral Dressing', Wiley, N.Y., 1945, 8-02.

63. Stokes, G.G.; Trans. Cambridge Phil. Soc. 9, Part II, 51, (1851).

64. Iwasaki, I., R.B. Strathmore and Y.S. Kim; Surface Properties and
        Flotation Characteristics of Magnetite, Trans. A.I.M.E. 223,
        113, (1962).

65. Oko, M.U.; 'Adsorption of Fatty Acid Soaps on Hematite', M. Eng.
        thesis, McGill, 1965.

66. Reference 27, p. 39.

67. Timmermans, J.; 'Physico-Chemical Constants of Pure Organic Compounds',
        Edn. 2, Elsevier, 1965.

68. Harwood, J.H. and A.W. Ralston; The Synthesis of Lauric Acid and
        Dodecylamine Containing Carbon-14, J. Org. Chem. 12, 740,
        (1947).

69. Daniels, F.; 'Experimental Physics and Chemistry', Edn. 6, McGraw-
        Hill, Toronto, 1962, 501.

70. Scott, D.W., A.C. Richardson and N. Arbiter; Amine Flotation of
        Gangue from Magnetite Concentrates, Trans. A.I.M.E. 169,
        469, (1946).

71. Schuhmann, R. and B. Prakash; Effect of Barium Chloride and other
        Activators on Soap Flotation of Quartz, Trans. A.I.M.E. 187,
        591, (1950).

72. Grainger-Allen, T.J.N.; Bubble Generation in Froth Flotation
        Machines, Trans. I.M.M., 79, C15, (1970).

73. Paterson, J.G.; The Effect of Sodium Cyanide on the Adsorption of
        Sodium Isopropyl Xanthate on Synthetic Chalcocite, M. Eng.
        thesis, McGill, 1966.

74. Yoon, R.H.; Current research in Dept. Metallurgical Engineering,
        McGill, to be published as a Master's thesis.

75. Fuerstenau, M.C.; An Improved Micro-Flotation Technique, Eng. and
        Min. J. 165, No. 11, 108, (1964).

76. Fuerstenau, D.W., P.H. Metzger and G.D. Steel; How to use this
        Modified Hallimond Tube for Better Flotation Testing, Eng.
        and Min. J. 158, No. 2, 69, (1957).

77. Morrow, J.G.; Adsorption of Dodecyl Ammonium Acetate on Hematite
        and Sphalerite, Doctoral thesis, M.I.T., 1952.

78. Reference 27, p. 48.

79. Kruyt, H.R. and H.S. van Klooster; 'Colloids', Edn. 2, Wiley, N.Y.,
        1930, 129.

80. Reference 22, p. 264.

81. Reference 47.

82. Reference 27, p. 161.

83. Vewey, E.J.W. and J.T.G. Overbeek; 'Theory of the Stability of Hydrophobic Colloids', Elsevier, 1948.

84. Morrow, J.G.; Adsorption of Dodecylammonium Acetate on Hematite and Sphalerite, Ph.D. thesis, M.I.T., 1952, 50.

85. Bloecher, F.W.; 'Concerning the Adsorption of Dodecylamine', M.Sc. thesis, M.I.T., 1949.

86. Reference 31, p. 251.

87. Ralston, A.W., G.W. Hoerr and E.T. Hoffman; Studies on High Molecular Weight Aliphatic Amines and their Salts. IV. Electrical Conductivities of Aqueous Solutions of the Hydrochlorides and Acetates of Dodecyl- and Octadecyl-Amines, J. Am. Chem. Soc. 64, 97, (1942).

88. Reference 14, p. 594.

89. Frommer, D.W.; Preparation of Nonmagnetic Taconites for Flotation by Selective Flocculation, 8th I.M.P.C., Leningrad, 1968, pre-print D-9 (Institute Mekhanobr., Leningrad, 1968).

90. Iwasaki, I., W.J. Carlson and S.M. Parmerter; The Use of Starches and Starch Derivatives as Depressants and Flocculants in Iron Ore Beneficiation, Trans. A.I.M.E. 244, 88, (1969).

91. Holló, J. and J. Szeitli; The Reaction of Starch with Iodine, in 'Starch and its Derivatives', J.A. Radley, Ed., Chapman and Hall, London, Edn. 4, 1968, 203.

92. Shinoda, K., T. Nakagawa, B.-I. Tamamushi and T. Isemura; 'Colloidal Surfactants, Some Physico-Chemical Properties', Academic Press, N.Y., 1963, 158.

93. Takagi, T. and T. Isemura; Interaction of Surface Active Agents with Amylose, Bull. Chem. Soc. Japan 33, 437, (1960).

94. Ghigi, G. and C. Botrè; Polymer Complexes as New Collectors and their Use in Magnetite Flotation, Trans. I.M.M. 75, C240, (1966).

95. Ghigi, G.; Flotation of Quartz with Some Polymer Complex Collectors, Trans. I.M.M. 77, C212, (1968).

96. Fuerstenau, D.W. and B.J. Yamada; Neutral Molecules in Flotation Collection, Trans. A.I.M.E. 223, 50, (1962).

97. Somasundaran, P. and D.W. Fuerstenau; On Insipient Flotation Conditions, Trans. A.I.M.E. 241, 102, (1968).

98. Reference 31, p. 261.

99. Reference 22, p. 257.

100. Shergold, H.L., A.P. Prosser and O. Mellgren; New Region of Floatability in the Hematite-Dodecylamine System, Trans. I.M.M. 77, C166, (1968).

101. Kodama, K.; 'Methods of Quantitative Inorganic Analysis', Interscience, N.Y., 1963, 253.

102. Paneth, F.; 'Radio Elements as Indicators', McGraw-Hill, 1928.

103. Gaudin, A.M. and P.L. de Bruyn; Radioactive Tracers in Minerals Engineering Problems and Particularly in Flotation; Can. Min. Met. Bull., 42, 331, (1949).

104. Gaudin, A.M. and P.L. de Bruyn; Research Studies in Minerals Engineering using Radionuclides, Scientific Monthly, LXX, 365 (1950).

105. Gaudin, A.M.; Radioactivity in Mineral Dressing, Bull. I.M.M. No. 552, Nov. 1952, 29.

106. Marshall, J.H.; How to Figure Shapes of Beta Ray Spectra, Nucleonics, 13, No. 8, 34 (1955).

107. Weast, R.C., Ed.; 'Handbook of Chemistry and Physics', Edn. 50, Chem. Rubber Co., Cleveland, 1969, B267 and B268.

108. Burr, I.W.; 'Engineering Statistics and Quality Control', McGraw-Hill, N.Y., 1953, 204.

109. Hayes, F.N.; Solutes and Solvents for Liquid Scintillation Counting, Tech. Bull. No. 1, Packard Instr. Co., April 1963.

110. Wang, C.H. and D.L. Wills; 'Radiotracer Methodology in Biological Science', Prentice-Hall, N.J., 1965.

111. Tolansky, S. 'Introduction to Atomic Physics', Longmans, London, 1959, 168.